Smart Maintenance, Analysis and Remediation of Transport Infrastructure

Work Package 2 *Assessment & Models*

Deliverable 2.2

Statistical Analysis Technique

Project funded by the EU 7th Framework Programme under call SST.2011.5.2-6 Cost-effective improvement of rail transport infrastructure. Grant agreement no: 285683

Project Information

Project Duration:

01/09/2011 – 31/08/2014

Project Coordinator:

Dr. Kenneth Gavin (kenneth.gavin@ucd.ie)

School of Civil, Structural and Environmental Engineering

University College Dublin

Newstead Building

Belfield

Dublin 4

Ireland

Document information

Version	Date	Action	Partner
01	29/04/2014	Final Report	RODIS

Title: SMARTRAIL – Development of a General Rail Transport Infrastructure Safety Framework

Authors: The SMARTRAIL Consortium

Reviewer: Kenneth Gavin (UCD)

Table of Contents

1. Introduction

Europe needs a safe and cost effective transport network to encourage movement of goods and people within the EU and towards major markets in the East. This is central to European transport, economic and environmental policy. Many parts of Europe's rail network were constructed in the mid 19th century long before the advent of modern construction standards. Historic levels of low investment, poor maintenance strategies and the deleterious effects of climate change has resulted in critical elements of the rail network such as bridges, tunnels and earthworks being at a significant risk of failure. The consequences of failures of major infrastructure elements is severe and can include loss of life, significant replacement costs (typically measured in millions of Euro's) and line closures which can often last for months. The SMART Rail project brings together experts in the areas of highway and railway infrastructure research, SME's and railway authorities who are responsible for the safety of national infrastructure. The goal of the project is to reduce replacement costs and delay, and provide environmentally friendly maintenance solutions for ageing infrastructure networks. This will be achieved through the development of state of the art methods to analyse and monitor the existing infrastructure and make realistic scientific assessments of safety. These engineering assessments of current state will be used to design remediation strategies to prolong the life of existing infrastructure in a cost-effective manner with minimal environmental impact.

This report details Task 2.1 of the SMART Rail project – Development of a general rail transport infrastructure safety framework. A probability based framework is developed for optimised whole life management of infrastructural elements/networks. Structural Reliability has been used widely in the nuclear industry and for offshore oil platforms. In this task, a reliability framework is developed for railway infrastructure. It encompasses not just rail structures (bridges) but all aspects of rail infrastructure such as tracks susceptible to settlement (derailment risk) and the stability of slopes that might result in landslides onto railway lines. By employing a probabilistic basis to the assessment of safety, stochastic processes can be incorporated into the whole life management/future proofing strategy for the infrastructure in a mathematically robust and statistically acceptable sense. The flow chart presented in Figure 1.1 illustrates a brief overview of the reliability based classification procedure.

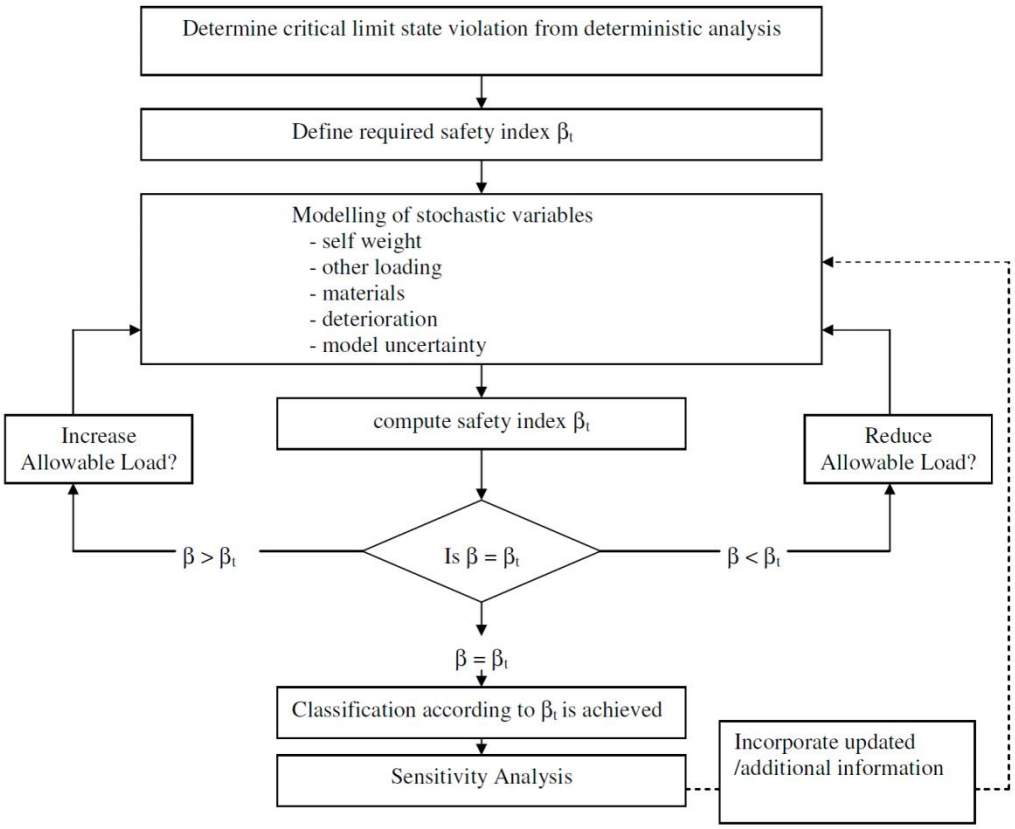

Figure 1.1: Outline of reliability based assessment

A comprehensive reliability framework is suitable for sophisticated users and for the management of network infrastructure at a regional or national level. However, engineers at a local level in some railway authorities may prefer a simpler approach for everyday use such as a Load and Resistance Factor Design (LFRD) approach. LFRD is used for everyday design by Structural Engineers – the factored effect of load is compared to the factored resistance to determine if the structure is safe. Task 2.1 also shows the development of simpler approaches to infrastructure assessment which are benchmarked against the comprehensive safety framework described under the reliability based classification procedure.

Examples of the application of the reliability analysis framework discussed herein are given in appendices A-C.

2. Assessment Procedure

2.1. Introduction

The safety and serviceability of existing railway infrastructure may need to be evaluated for a variety of reasons, for example, due to:

- changes of use or increase of loads (e.g. increased axle load limits or when there is a necessity to carry an exceptionally heavy load that is normally not permitted),
- effects of deterioration (e.g. corrosion, fatigue, climate change),
- an extension of the design working life
- damage as a result of extreme loading events or accidental actions and/or
- concern about design/construction errors or the quality of building materials and workmanship.

A change in use or increase in allowable loads is considered to be the main reason for safety and serviceability assessments. An element of infrastructure (e.g. a bridge) designed according to out-dated design codes may have to be checked against new codes and new traffic load requirements, for example, in the case where it is going to be reused within a new railway link.

The changes in structural resistance due to the effects of deterioration are structure and site specific. The main deterioration processes concerning structural strength are corrosion and fatigue. Typical indications of deterioration include; spalling, cracking, and degraded surface conditions. Furthermore, impact, earthquake or extreme wind can also result in structural damage. The remaining load carrying capacity needs to be analysed after such events.

The design of new infrastructure and/or the assessment of existing infrastructure requires different approaches and thought processes. When carrying out an assessment an engineer must answer the question: 'is the infrastructural element still sufficiently safe?' (SB-LRA, 2007). This is quite different to the questions faced by engineers during the design process of new infrastructure. Therefore the questions cannot be answered using the same methods i.e. using traditional safety checking procedures from design codes. It is implicit then that, the procedures for assessment differ from those for design. For an assessment the most suitable method will depend on the objectives of the assessment and the required capacity.

A wide range of different assessment procedures exist with varying levels of sophistication and effort. Assessment should begin with the least complex methodology and then proceed in stages of

increasing sophistication, aiming at greater precision in the result, where required, at each higher level. Advanced methods, i.e. those of the greatest level of sophistication, may only be needed when simpler methods lead to results suggesting rehabilitation or decommissioning. Of the advanced methods available, and outlined in this report, the highest level considered entails the application of reliability based methods (Melchers (1999), O'Connor et al. (2009)).

This chapter details the concepts and procedures which are possible to employ in the safety and serviceability assessment of existing railway infrastructure. At first the types of assessment are defined and the classification and criteria for assessment are then specified. Subsequently the different levels of assessment recommended for the safety assessment of existing railway infrastructure are presented. Detailed information and guidance is also provided regarding possible refinement of a safety assessment. This includes information on data acquisition, different types of structural analysis and various safety formats for different levels of assessment.

2.2. Types of assessment

The required level of detail and type of assessment will vary as shown in Figure 2.1. The decision on the type and detail will depend on the reasons for performing the assessment. The Guideline for Load and Resistance Assessment of Existing European Railway Bridges (SB-LRA, 2007) produced during the Sustainable Bridges Project provides details of varying assessment levels.

Line assessment

Many railway lines in Europe are classified according to the UIC 700 (UIC, 2004). The classification links the capacity of the line to the allowable axle load and line load of the goods wagons. When an upgrade of a line is required, this will entail a capacity assessment of the existing infrastructure along the line (e.g. a number of railway bridges). A line assessment would therefore typically initiate a primary sorting in order to identify the potentially critical bridges. Such primary sorting could be carried out by a simple comparison between the original design load and the classification load considering different simple static systems and span lengths. For the identified 'critical bridges', where the classification load is more unfavourable compared to the original design load, the assessment is then carried out at an individual bridge level.

Bridge assessment

Typical load, capacity and resistance assessment is carried out at bridge level. There are two types of analysis. Either the bridge is analysed for the critical elements and the ultimate capacity is found

equal to the lowest capacity of the bridge elements or the bridge is analysed as a system including the possible redundancy by treating the bridge as a "system".

Element assessment

Element assessment can either be part of a bridge assessment or be a standalone investigation. The latter can be relevant if, for example, an element is damaged or deteriorated.

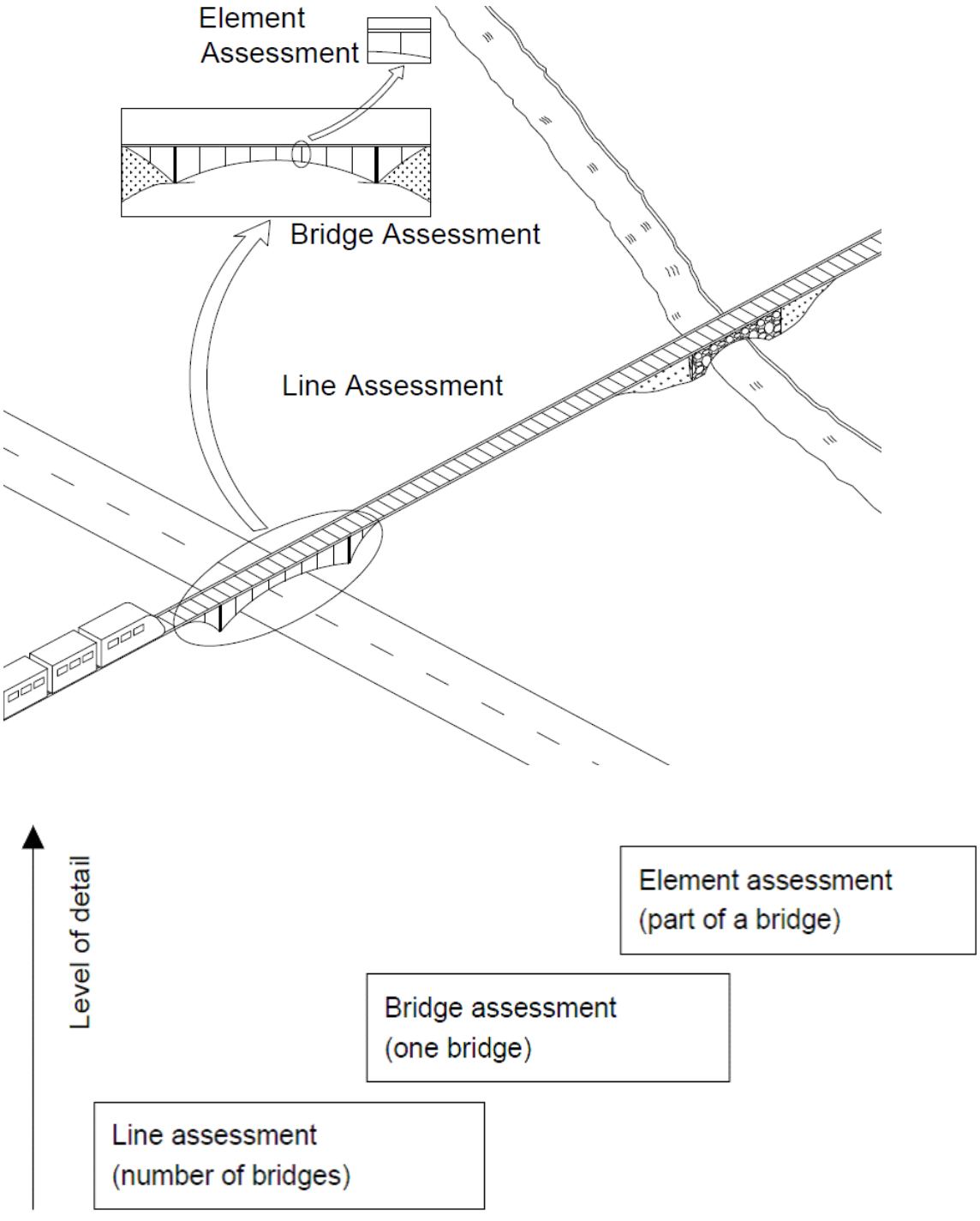

Figure 2.1: Types of assessment

2.3. Criteria for assessment

The assessment process must always begin with the clear specification of the assessment objective. This first step is crucial to identify the most important limit states. Having identified the significant limit states, the associated structural variables to be investigated and the assessment procedure can be selected. There are many different assessment procedures, with varying complexity. The choice of the appropriate procedure depends highly on the specified requirements of the assessment.

Railway infrastructure is typically assessed taking into account the following criteria:

- Ultimate Limit State, ULS
- Serviceability Limit State, SLS
- Fatigue Limit State, FLS
- Durability Limit State, DLS

The ultimate limit states concern the cases where the safety of persons and/or the safety of the infrastructure is considered, for example, loss of equilibrium of a structure or parts of it as a rigid body (e.g. overturning), attainment of the maximum resistance capacity, transformation of the structure or part of it into a mechanism or instability of the structure of part of it. The serviceability limit states concern the cases where the following are considered: the functioning of the infrastructure or infrastructural element under normal use, the comfort of passengers and the appearance. Often fatigue limit states are part of either the serviceability or the ultimate limit states. This is because, although fatigue may lead to the collapse of the structure and should therefore be considered as an ultimate limit state, the normal service loads are used in checking the limit state. Therefore, it is recommended in this Guideline to handle fatigue separately. Assessment of service life belongs to the class of durability limit state.

It should be noted that, in comparison to road bridges, railway bridge assessments require special attention to the fatigue limit state and serviceability limit states taking into account ballast instability and comfort requirements. In fact, when assessing bridges for higher speeds, the ballast instability requirement often results in a need for strengthening even though the ultimate limit state satisfies the requirements.

2.4. Classification of assessment

The core objectives of an assessment are to analyse the current load carrying capacity and predict the future performance with maximum accuracy and minimum effort. In most cases it is wise to start

with simple conservative methods and advance to more sophisticated assessment methods only when the evaluated load carrying capacity is insufficient.

In general, assessment procedures can be classified into three groups (SAMCO, 2006): non-formal assessment, measurement based assessment and model based assessment, Table 2.1.

Non-formal assessment

Non formal assessment methods include those which are based on the experience and judgement of the assessing engineer. Most non-formal assessments take place within an infrastructure management system, where the structural condition is evaluated on the basis of visual inspections.

Results of a visual inspection can be considered to be conservative. Nevertheless, they allow:

1. A rapid evaluation of the overall condition of a large number of structures
2. Prediction of future trends based on past observations and experience
3. Easy collection of data for defining maintenance and repair strategies and their associated costs

The results from a visual inspection, the visual observations (extent and severity of damage), are used to assess the conditions of infrastructure based on an arbitrary scale, generally ranging from “good” condition to “very poor” condition. The main advantages of a visual inspection are their simplicity, low cost and easy link with maintenance strategies, as maintenance options may be directly associated with condition ratings and classes of visual deterioration. Their main disadvantages are their subjectivity, they cannot detect latent defects or defects at early stages of deterioration (e.g. initiation of corrosion) and no direct information may be derived on the structural deterioration (SAMARIS D30, 2006).

Measurement based assessment

In this category are assessments where the load effects are not determined by structural analysis but directly by measurement (e.g. performance of structural health monitoring, proof load tests, Weigh in Motion (WIM) systems). The method is only able to verify structural sufficiency within the Serviceability Limit State since only serviceability measures can be determined directly. It is a two-component procedure involving:

- measurement of load effects
- serviceability verification

In general, measurement based assessments are not complex. An example application is the evaluation of serviceability limit states like displacement or dynamic behaviour after installing instrumentation on a structure. The assessment of monitored structures and those which are deemed to be almost structurally insufficient may also be based on this method. Measurement based assessment will therefore not be described in detail within this document.

Model based assessment

This category includes all assessments where the load effects are determined by model based structural analysis. This document will focus primarily on these assessment procedures where assessments are ranked from level 1 to level 5, with the level of complexity and detail increasing with increasing levels, as discussed in Section 2.5.

Using this method, Ultimate Limit States and Serviceability Limit States can be modelled and therefore assessed. Each assessment level consists of 3 components (SAMCO, 2006):

- acquisition of data of loading and resistance (condition assessment)
- calculation of load effects using structural models (structural analysis)
- safety and serviceability verification

The condition assessment consists of examining existing documents and visiting the infrastructural element being assessed for an inspection. The aim of the inspection is to identify areas of deterioration (e.g. delamination, material losses, cracking, etc.) that need to be investigated in more detail (e.g. by more detailed inspections or employing instrumentation/structural health monitoring) in order to determine the cause and extent of damage and its effect on the behaviour and load carrying capacity. For most railway infrastructure, simple checks based on information from existing documentation and visual inspections may be enough to prove safety. However, in some cases, for example ’substandard bridges’ or 'critical bridges', more detailed investigation and sophisticated analysis (e.g. non-linear structural analysis, probabilistic safety analysis, etc.) may be necessary. In this step, structural analysis is performed to determine the load effects in the structure due to the actual applied loading.

Finally, safety and serviceability verification can be carried out with different levels of sophistication. Generally, deterministic, semi-probabilistic and probabilistic formats can be used. In general, safety and serviceability verifications should be carried out using limit state principles with characteristic values and partial safety factors. If more refined methods are necessary, probabilistic approaches may be applied, as appropriate (O’Connor, 2009).

2.5. Assessment levels (for model based assessment)

Safety assessments are performed to check the capacity to safely carry or resist a specific loading level and to identify those elements of the infrastructure which are inadequate to carry or resist a required loading, e.g. structures which have an unacceptable probability of failure. The consequences of finding a structure to be inadequate can be costly to both owners and users. The main options available after deeming inadequacy are replacement or strengthening to ensure safety with respect to the required loading, or, to restrict the loading to facilitate temporary operation. It is therefore critical to perform assessments of doubtful elements as accurately as possible. However, theoretically complex and rigorous assessment can be costly and time consuming. Therefore, it is advisable that when an element of railway infrastructural fails an initial assessment, that the cost and time implications should be considered when advancing to more rigorous levels. The likelihood of changing the result should also be carefully considered. In some cases, the end result becomes self-evident at an early stage and then the decision to terminate or continue the assessment can be taken at that stage.

Generally, when carrying out a particular assessment, each of the steps within the assessment (i.e. condition assessment, structural analysis and safety verification) should be of the same level of sophistication. For example, it is not advisable to obtain resistance and load parameters using simple but imprecise methods and then using full probability based methods for the safety verification.

There are, however, some exceptional cases where the combination of methods with low and high complexity is advisable (SAMCO, 2006). For example, if a structure fails the first low level assessment and the structure specific resistance and load parameters are then obtained for the next step assessment using more refined investigation methods like non-destructive testing (NDT), the structural analysis and the verification can be carried out with the same simple methods as in the first step.

The five levels of assessment recommended, in this document, vary in complexity from simple but conservative to complex but more accurate. These levels of assessment, numbered 1 to 5 with Level 1 being the simplest and Level 5 the most sophisticated, are well explained in the literature, including the COST 345 report (2004). Details from the COST 345 report are also given below and in Table 2.1 (from SAMCO, 2006).

An assessment at level 1 is carried out with *traditional methods* of analysis (simple, convenient and 'often' conservative) while assessment at higher levels will involve more refined methods of analysis. The number of parameters required increases with the level of assessment. Therefore, parameters

for lower levels of assessment can be based on visual observations, but parameters for higher levels of assessment should be estimated from testing. Hence, full partial factors from assessment standards (which are typically less conservative than those employed at the design stage) can be used for level 1. However, characteristic strengths of materials must be based on existing data for level 2 (from the same or similar infrastructure) and on tests on the infrastructural element being assessed for level 3 or higher. Level 4 uses modified partial safety factors to account for any additional safety characteristics specific to the infrastructure being assessed and level 5 uses structural reliability analysis instead of partial safety factors. Analysis methods which are recommended for different assessment levels are presented in Table 2.2 (from Cost 345, 2004).

Level 1 assessment

In a level 1 assessment, only simple analysis methods are necessary and deterministic safety verifications (calculated based on permissible stresses) are used to give a conservative estimate of load carrying capacity.

Level 2 assessment

Level 2 assessment involves the use of more refined analysis and better structural idealisation. The more refined analysis may include, e.g. grillage analysis or possibly finite element analysis when it is considered that these may improve the result. Non-linear and plastic methods of analysis (e.g. yield line or orthotropic grillages) may also be used (COST 345, 2004).

This level also includes the determination of characteristic strengths for materials based on existing available data. This may be in the form of existing mill test certificates or recent tests on similar railway infrastructure. No new tests would be carried out for a Level 2 assessment. If any new tests are to be carried out on the structure being assessed then this should be considered as a Level 3 assessment. Safety and serviceability verification is based on partial factors.

Level 3 assessment

Level 1 and Level 2 assessments make use of Assessment Live loadings given in the standards or estimated as generally applicable to the network. In a Level 3 assessment, the assessor has the option of determining and using structure specific loading. For many elements of railway infrastructure, the use of specific live loading can be quite beneficial. Level 3 assessments may also make use of material testing results to determine the characteristic strength or yield stress. Furthermore, in Level 3, consideration may be given to the use of load testing in the form of

diagnostic load tests. Where deemed necessary, proof load testing should be performed with the greatest possible care in order to avoid damage.

In a level 3 assessment, analysis is carried out using refined methods and detailed models. Safety and serviceability verification is based on partial factors.

Level 4 assessment

Levels 1 to 3 assessments are based on code implicit levels of safety, incorporated in the nominal values of loads and resistance parameters and the corresponding partial safety factors. The corresponding safety is related by implication to past satisfactory performance of the infrastructure stock or through calibrations where these have been carried out.

Any calibration involves an element of averaging which makes the results acceptable for the bulk of infrastructures of the type concerned. Nevertheless, the resulting rules may be overly conservative for a particular case which may be significantly different in some way from the norm used in the calibration. Level 4 assessments can take account of any additional safety characteristics of that specific case and amend the assessment criteria accordingly. Any changes to the criteria used in this level may be determined through rigorous reliability analysis, or by judgemental changes to the partial safety factors. The Level 4 method allows modifications to partial factors based on information available and safety characteristics specific to the railway infrastructure in terms of dimensional surveys, material testing, age, consequences of failure, reserve strength and redundancy, etc. For the analysis of railway infrastructure at assessment Level 4, care should be taken not to double count infrastructure-specific benefits. For instance, if system analysis based methods such as the yield line method have been used in Levels 2 or 3, system effects should not be utilised in Level 4 to further optimise the structural model.

Level 4 assessment may be particularly beneficial in the following circumstances:

1. The bridge assessment criteria have been primarily devised for longitudinal effects on main deck members. All other elements such as cantilever slabs, cross beams, pier heads etc. may be examined in Level 4 for determining element specific target reliability.
2. The failure of a retaining wall adjacent to a minor road will obviously have much lesser consequences than the failure of a major bridge. Such considerations may be used in a Level 4 assessment.

Level 5 assessment

Level 5 assessment involves reliability analysis of particular railway infrastructures or types of railway infrastructures. Structural reliability analysis is used directly instead of partial factors. Uncertainties are modelled probabilistically. Such analyses require statistical data for all the variables defined in the loading and resistance equations. The techniques for determining the probability of failure from such data are now readily available and can be undertaken in modest time frames. Care should be taken to ensure this form of sophisticated analysis is performed by professionals with adequate and relevant experience. Level 5 assessments provide greater flexibility but it should be noted that the results can be sensitive to the statistical parameters and the methods of analysis used. The Level 5 methodology may also be employed to assess/optimise the maintenance management strategies for railway infrastructure for their remaining/required service life (O'Connor 2009).

Table 2.1 Classes and levels of assessment (SAMCO, 2006)

Classes of Assessment	**Level**	**Methodology**		
Non-formal assessment	-	Visual Inspections Based on the experience of the assessing engineer		
Measurement based assessment	-	Determination of Load Effects		Verification
		Load effects determined directly by measurement for Serviceability Limit States		Compare with threshold values
Model based assessment		Determination of Load Effects		Verification
		Condition Assessment	Structural Analysis	
	1	Document review Inspections	Basic structural models	Deterministic (Permissible stress) Semi-probabilistic (partial safety factors)
	2	Monitoring of static load effects and deterioration (deformation, stresses, cracks, corrosion etc.)	Refined models (FEM, Non-linear analysis)	
	3	Monitoring of live load and environmental influences		
	4	Testing and measurement of material properties and dimensions	Adaptive FE models	Probabilistic approximation methods (First Order Reliability Method (FORM), Second Order Reliability Method (SORM))
	5	Monitoring of dynamic load effects (eigenfrequencies, mode shapes)	Stochastic FE Models	Probabilistic simulation methods (MCS, LHC)

Table 2.2 Analysis methods recommended for each level of assessment (COST 345, 2004)

Structure Type		Level of Assessment				
		1	2	3	4	5
Bridges	Not skew beam	1-D linear elastic (beam theory or plane frame analysis)	1-,2- or 3-D linear or non-linear; elastic or plastic; allowing for cracking	2- or 3-D; linear or non-linear; elastic or plastic; grillage or FEM (upstand model if necessary); allowing for soil-structure interaction, cracking, surface irregularities and 'specific' live loading & material properties	FEM analysis of specific details of the structure being assessed not considered in previous levels	Reliability analysis based on probabilistic models
	Not skew slab		2- or 3-D linear or non-linear; elastic or plastic; allowing for cracking; grillage or FEM (upstand model if necessary)			
	Not skew beam & slab					
	Not skew cellular					
	Skew, tapered and curved	Frame linear elastic allowing torsion				
	Arch	Empirical or 1-D linear elastic arch frame	1-, 2- or 3-D linear or non-linear; elastic or plastic; allowing for cracking			
	Cable Stayed	1-D linear elastic with modified modulus of elasticity for the cables	1-, 2- or 3-D linear or non-linear; elastic or plastic; allowing for cracking and modelling cable sag more accurately			
Culverts	Rigid	Frame linear elastic	2- or 3-D FEM linear or non-linear; elastic or plastic; allowing for soil-structure interaction, cracking	2- or 3-D FEM, linear or non-linear; elastic or plastic; allowing for soil-structure interaction, cracking, surface irregularities and 'specific' live loading & material properties		
	Flexible	Frame linear elastic allowing for soil-structure interaction (beam & spring)				
Earth-retaining walls		Simple method of analysis	Beam, 2- or 3-D non-linear FEM on elastic foundation or elasto-plastic continuum	3-D non-linear FEM, allowing for soil constitutive models and 'specific' live loading & material properties		
Reinforced soil		Empirical models or 1-D linear elastic	2- or 3-D FEM of soil	2- or 3-D FEM of soil in combination with existing structure and 'specific' live loading and material properties		
Tunnels		Empirical models or beam-and-spring models (non-cohesive soil)	2- or 3-D FEM; linear or non-linear; elasto-plastic	3-D non-linear FEM with bedding, fracture planes, ... and 'specific' live loading & material properties		

2.6. Possible refinement of assessment

2.6.1. General overview

As already discussed in previous sections, the assessment of existing railway infrastructure may be improved (or refined) by carrying out more detailed analysis and/or by collecting additional data. The improvement of analysis methods may be achieved by using more accurate structural analysis methods (e.g. linear elastic analysis but with more accurate idealization, plastic analysis, non-linear analysis, etc.) and/or by using more appropriate safety verification methods (e.g. semi-probabilistic, simplified probabilistic, fully probabilistic, etc.). Additional data can be collected to improve load models as well as resistance models (including material resistance properties) used in the assessment. All of these areas of possible refinement are discussed in SB-LRA (2007), SAMCO (2006) and in the following sections.

2.6.2. Data acquisition

To determine load effects, in most cases of assessment it is necessary to gather information on material and structural properties and dimensions as well as previous, current and/or future loading. In addition, environmental conditions of physical, chemical or biological nature can have an effect on material properties.

The main difference between design and assessment is that in the latter, uncertainties can be reduced significantly by site specific data. There are a wide range of methods which may be employed in this regard with varying expense and accuracy. The choice of the data acquisition method highly depends on the assessment objective and the assessment procedure. Usually simple methods, like the study of documents, are applied in the beginning. To reduce uncertainty at higher assessment levels, more sophisticated test methods need to be applied. Non-destructive test (NDT) methods are preferred to destructive methods whenever possible.

Besides the provision of data which describes the current state of the structure, information relating to time dependant processes, like deterioration, should also be acquired. This can take place with periodic or permanent measurement (i.e. structural health monitoring).

Load models

One of the first tasks in the assessment of existing railway infrastructure is the definition of the live load. In most European countries assessment codes or guidelines do not exist. Therefore, assessment of the load carrying capacity is often performed on the basis of design codes which are usually very conservative due to the fact that they have to cover a wide range of bridges and loading

conditions. It is obvious that it can be very advantageous to perform assessments of existing bridges using specific load models designed for assessment purposes. An overview of the train assessment loads specified in selected European countries is presented in SB4.3.1 (2005). Special assessment train loads may be connected directly to the classification of heavy goods wagons (UIC, 2004). In this way it is possible to classify the line or bridge capacity according to railway traffic that the railway line, and/or bridge, is actually experiencing.

Detailed information regarding this subject, including guidance on methods to determine the assessment of train loads and railway infrastructure specific dynamic amplification factors, is presented in Chapter 5. Traffic load models used in assessment can also be based on measurements of the actual loads on bridges, performed using, for example, Weigh in Motion (WIM) or similar technologies. Furthermore, the load can be modelled as a random variable with an associated probability distribution and extreme value(s), meaning the complete information in the whole load range can be used. In some situations the model(s) can also contain information regarding all the loading history (e.g. for fatigue analysis).

The choice of the most appropriate load models (i.e. railway traffic loads but also permanent loads) for the assessment of the railway infrastructure under consideration will depend on the specific type of infrastructure, the level of assessment and the analysed effects (local or global effects, ultimate strength or fatigue, etc.). Generally, for a level 1 assessment, load models from design or assessment codes will be sufficient. For level 2 or level 3 assessments, loads which are especially calibrated for the assessment of existing railway infrastructure should be applied or some simple probabilistic models may be used. However, for level 4 or level 5 assessments, the semi-probabilistic or fully probabilistic load models based on real traffic records (e.g. obtained by WIM) should be used.

Resistance models

As with load models, the resistance models used for assessment may be refined during the assessment process. Generally this can be done by collecting additional data (e.g. performing some non-destructive, minor destructive or destructive test, monitoring the behaviour, etc.).

The choice of the most appropriate resistance model for each assessment would be made based on information such as the railway infrastructure type, the construction material, the level of assessment, the analysed effects (local or global effects, ultimate analysis, fatigue, etc.) and the condition. Generally, level 1 assessments can be performed using resistance models based on available data (design drawings and calculations, records from the construction phase, results of previously performed tests, etc.) and the available design or assessment codes. The design codes

from the time when the railway infrastructure was constructed can provide background information for the assessment. However, the assessment should be performed using modern codes. Level 2 or level 3 assessments can be performed using resistance models calibrated using information from simple tests performed on the analysed structure (usually non-destructive or minor destructive tests). Sometimes, probabilistic models can also be used. Level 4 or level 5 assessment should generally be performed using fully probabilistic models calibrated against reliable test results (usually minor destructive or destructive). Semi-probabilistic models derived from the fully probabilistic models can also be used (e.g. for the assessment of masonry arch bridges or when the use of a probabilistic format for assessment is not necessary).

2.6.3. Structural analysis methods

The purpose of structural analysis is to determine internal forces, or stresses, strains and deformations. Cross-sectional forces and moments are used for capacity checks in the analysis of cross-sections or local parts of a bridge. Stresses and strains are used to determine the capacity directly using the material resistance.

Structural analysis involves an idealisation of the bridge geometry, the material behaviour and the structural behaviour. A structural analysis can be made on different levels with respect to the idealisations made on the material and structural behaviour. Generally four different methods of structural analysis may be distinguished:

- Linear elastic analysis
- Linear elastic analysis with limited redistribution
- Plastic analysis
- Non-linear analysis

Linear elastic analysis can be used for the verification of SLS as well as ULS. It can be effectively used to get a first estimate of deflections for SLS or to calculate cross sectional forces for cross-section verification using standard design formulas or more advanced methods, such as, probabilistic approaches.

Linear elastic analysis with limited redistribution can be used for the verification of ULS. It provides a more realistic distribution of internal forces than the linear elastic analysis where the concentration of sectional moments and forces may appear (e.g. where there are concentrated supports or loads, in corners of slab frame bridges etc.). It can be used for cross-sectional checks using standard design formulas or probabilistic approaches.

Plastic analysis can be based on lower or upper bound theory (static or kinematic), e.g. frame analysis with plastic hinges, yield line theory and strip method for slabs, strut and tie models. It is an efficient method for verification for all bridge types in ULS. In this method it is necessary to verify the capacity for plastic deformation. Plastic analysis can help to verify additional load carrying capacity of structures due to the redistribution of internal forces. It provides a more realistic distribution of internal forces that can be used for cross-sectional checks using standard design formulas or probabilistic approaches.

Non-linear analysis is the most appropriate method that can be used to describe the behaviour of the structure in the most abnormal situations (excessive loading, cracking, buckling, etc.). It can be used when the non-linear response of the materials and/or non-linear geometrical effects should be taken into account directly in the structural analysis. The method can be used for all bridge types at SLS as well as ULS. It may be used for the determination of sectional forces and moments, but also for direct study of the stress-strain response and the analysis of failure or load carrying capacity.

The choice of the appropriate analysis method for each particular assessment depends on the type of railway infrastructure, the level of assessment and the analysed effects (local or global effects). Refer to Table 2.2 for more information on recommended structural analysis methods for different levels of assessment.

For lower assessment levels it is often effective to calculate load effects with basic conservative methods with simple structural models. Typical simple analysis methods are, among others, space frame and grillage analysis combined with a simple load distribution and linear elastic material behaviour, which results in a lower bound equilibrium solution.

In cases where low level assessments fail, refined load effect calculation methods may be performed to gain a more accurate indication of load capacity. Refined methods include mainly finite element analysis and non-linear methods such as yield line analysis. Detailed modelling of material behaviour to include time-variant behaviour (e.g. shrinkage and creep in RC structures) and the interaction between material components (e.g. bond, tension stiffening in RC) may uncover hidden capacity reserves and reduce conservatism. For higher levels of assessment a stochastic finite element model can be used to analyse the structure. The difference between conventional finite element models and stochastic finite element models is that the stochastic elements take the spatial correlation of the random variables into account.

2.6.4. Safety formats

While data acquisition (condition assessment) and structural analysis are procedures to obtain information about the structural state, the third component of the model based assessment process considers the actual evaluation of the safety and serviceability margin. This can be described as the distance between the actual real state of the railway infrastructure and the limit state, and can be carried out using different methods of varying sophistication, Figure 2.2. The verification should normally be carried out to ensure a target reliability level, that represents the required level of performance, is achieved.

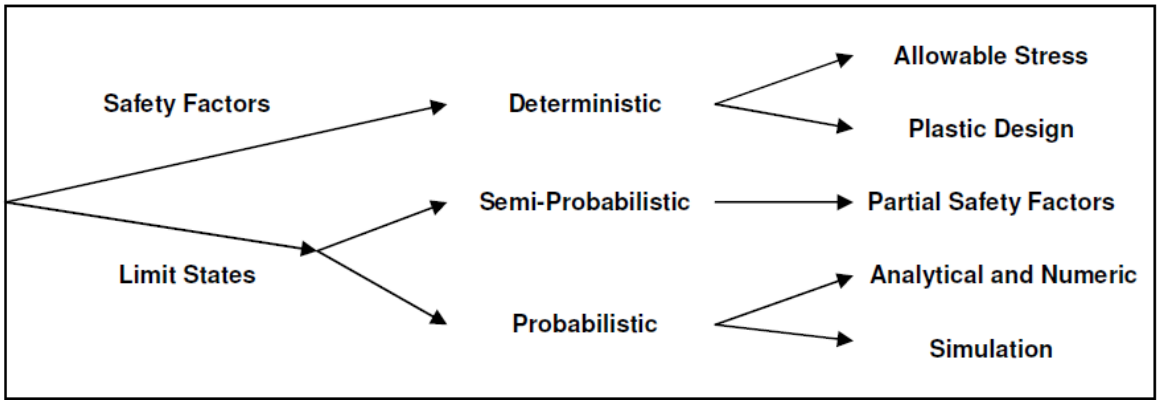

Figure 2.2 Reliability verification approaches (from SAMCO, 2006)

Deterministic verification with global safety factors

The deterministic approach is the traditional means of defining safety. It is fully based on experience and the safety measures are of an empirical nature. Deterministic verification is characterised by simplifications and associated conservative safety measures. The most common deterministic safety measure is the global 'factor of safety'. It is the ratio of the resistance to the load effect and is applied mostly on the resistance side.

The concept of the permissible stresses is a typical deterministic verification method, where failure is assumed to occur when any stressed part reaches the permissible stress. The accuracy depends on how well the value of permissible stress represents the failure stress of the real material and how well the calculated stress represents the actual stress in the real structure. Another concept is the load factor method, where the safety measure is represented by the 'load factor', which is the ratio of the ultimate strength of a member to its working loads.

Partial safety factors

This semi-probabilistic approach is based on the limit state principle. The primary concern is to ensure that failure does not occur in a component or the structure itself, which is defined as the *Ultimate Limit State* (ULS). For structural assessment it may also be important to analyse the serviceability performance where the structural effects of loading may lead to a serviceability failure, defined by the *Serviceability Limit State* (SLS).

As a safety measure, *partial safety factors* are well established. They have been developed/calibrated with reliability analysis for specific target reliability and are applied to design parameters. Partial safety factors guard against the extreme variations of the design parameters, which could possibly occur during their use, and are applied on both the resistance and the load side.

The semi-probabilistic verification method can much better reflect reality because uncertainties can be taken into account on the design parameters where they occur. Since partial factor based verification methods have been developed for design reasons, most design codes use them. Also, in design, a safe criterion is more important than a realistic one and an economic design can mean ease of construction instead of efficiency. For those reasons semi-probabilistic methods tend to be conservative for the majority of railway infrastructure. The level of conservatism varies at a network and local scale (i.e. from structure to structure and from load effect to load effect).

Probabilistic verification

Probabilistic verification procedures are also based on the principle of limit states as described above. Within assessment it will be intended to identify the real values of the design parameters by inspection, testing, monitoring or other methods and to minimise uncertainties. In the safety verification the uncertainties of these design parameters are taken into account to calculate the probability of failure of the railway infrastructure or railway infrastructural element. The measures of whether the railway infrastructure is adequately safe or not, are the *probability of failure,* p_f, and the associated *reliability index,* β.

Probabilistic verification methods are by now well developed and are being used more and more in design and assessment of buildings, bridges and industrial structures (O'Connor 2008, 2009). The procedure is sensitive to the chosen probability distributions which represent the basic random variables and also to the analysis methods and models for calculating the load effects (e.g. grillage

analysis, FE analysis). Therefore while this is an extremely effective tool for assessments, it is necessary to have an adequate knowledge to perform this type of analysis.

3. Probability Based Assessment

3.1. Introduction

The objective of the assessment of railway infrastructure, and assessments in general, are to determine whether the requirements to functionality, service life and safety, are fulfilled or not. In the context of this guideline, the general requirements for a Probability Based Assessment or Reliability-Based Classification of railway infrastructure (DRD, 2004) is that there is:

1. Sufficient safety against failure during the design lifetime
2. Satisfactory function with normal use
3. Adequate durability and robustness

The criteria that indicate whether a railway infrastructure functions satisfactorily are prescribed by limit states (section 3.2). In a probability-based analysis one or more critical limit state(s) are generally defined on the basis of a deterministic analysis (i.e. lower level assessment). The critical limit state found in the deterministic analysis is given by a function that depends on the modelled resistance and load parameters. The chosen reliability-based analysis method will then depend on the limit state function's complexity and the safety requirement. Detailed descriptions and reviews of reliability-based analysis methods can be found in Melchers (1999).

The reliability requirements described in this chapter correspond to verification at component level. The railway infrastructure or a part of it is assumed to have failed when one of the limit states has been violated. The safety requirements depend on which limit state is under consideration, the consequences of failure and the type of possible failure.

The following sections describe some possible limit states to be considered, the consequences of failure (also referred to as reliability class) and the types of failure. Target reliability levels, prescribed by various codes of practice and guidelines, are presented in advance of brief discussions on the reliability of systems, time variant reliability assessment and sensitivity analysis in a reliability assessment.

3.2. Limit states

As the current practice in the Eurocodes is to design new structures based on the limit states philosophy, it is proposed that the same philosophy be adopted in the case of assessing existing infrastructure. In the following section, the limit states to be considered for railway infrastructure assessment are presented as they are in the Guideline for Load and Resistance Assessment of

Existing European Railway Bridges (SB-LRA) published by the Sustainable Bridges project (SB-LRA, 2007).

The limit states relevant to railway infrastructure were introduced in Chapter 2. In general, they are divided into the following:

- ultimate limit states
- serviceability limit states
- fatigue limit states
- durability limit states

As mentioned in Section 2.3, fatigue limit states are often included in either the serviceability or the ultimate limit states. This is because, although fatigue may lead to the collapse of the structure and could therefore be considered as an ultimate limit state, the normal service loads are used in checking the fatigue limit state. Therefore, corresponding to the recommendation of SB-LRA (2007), it is recommended in this guideline to handle fatigue separately.

Masonry arch bridges can also be a source of ambiguity, with respect to limit states. While it may be easy to differentiate between the serviceability, fatigue and durability limit states for metal and concrete bridges, it is not so easy for masonry arch bridges. Therefore, in the case of masonry arch bridges these three limit states can be put together to check the residual life of the bridge. The Permissible Limit State (PLS), defined as the limit at which there is a loss of structural integrity which will measurably affect the ability of the bridge to carry its working loads for the expected life of the bridge, is often mentioned when discussing the assessment of masonry arch bridges SB-LRA (2007).

When performing a safety assessment, it may not always be necessary to check all limit states. For example, the verification of a limit state may be omitted if sufficient information is available to prove that the requirements of this limit state are met by one of the other limit states.

3.2.1. Ultimate limit states

The ultimate limit state includes collapse and structural failure. The ultimate limit state concerns safety of the railway infrastructure and its contents as well as the safety of its users. Ultimate limit states which may require consideration include, e.g. (SB-LRA, 2007):

- loss of equilibrium of the structure or any part of it, considered as a rigid body
- failure by excessive deformation
- transformation of the structure or any part of it into a mechanism

- rupture
- loss of stability of the structure or any part of it, including supports and foundations
- slope failure

3.2.2. Serviceability limit states

Serviceability limit states relate to conditions beyond which the specified service requirements are no longer met. The serviceability requirements concern the functioning of the railway infrastructure or parts of it, comfort to the user and appearance.

If relevant, a distinction should be made between reversible and irreversible serviceability limit states. The reliability requirements for an irreversible limit state will generally depend on the relation between the cost of preventing the state in question from arising and the cost of repair after the state has arisen (DRD, 2004).

Serviceability limit states which may require considerations include (SB-LRA, 2007):

- deformations and displacements which affect appearance or effective use or cause damage to non-structural elements
- vibrations which cause discomfort to people, induce damage or which limit functional effectiveness
- damage, including cracking, which is likely to affect appearance, durability or function adversely

For railway infrastructures attention should especially be made to (SB-LRA, 2007):

- performance criteria (to avoid passenger discomfort)
- deformation
- vibrations
- traffic safety
- vertical acceleration of the deck
- deck twist
- rotations at the end of the deck (ballasted tracks)
- horizontal deflection of the deck

3.2.3. Fatigue limit states

The fatigue limit state includes:

- failure caused by fatigue or other time-dependant effects
- observable damage caused by fatigue and other time-dependent effects

Fatigue is a local material deterioration caused by repeated variations of stresses or strains. A distinction is made between low cycle fatigue (few load cycles) and high cycle fatigue (numerous load cycles). Low cycle fatigue is associated with non-linear material and geometric behaviour, e.g. alternating plastic strains in plastic zones. High cycle fatigue is mainly governed by elastic behaviour and as a consequence elastic models should be used.

Whether fatigue assessment is needed or not has to be evaluated in each case.

3.2.4. Durability limit states

The durability limit state refers to:

- Requirements to attain a specified design service life
- Assessment of remaining service life

and is concerned with the degradation mechanisms induced by the environment that may affect the service life. Also related to remaining service life issues, fatigue can be considered as a degradation process. However the degradation in the case of fatigue is due to mechanical effects in the material due to the stress level induced by external actions and, therefore, is considered apart from the durability limit state. In this sense, durability and fatigue limit states could be grouped into a more global “permissible” limit state. The term permissible refers to the condition at which, although not viewing extremely high load levels (ULS), the stresses incurred at normal operation levels (service loads) can lead to the failure. This situation is of special relevance in the strength assessment of existing masonry arch bridges.

In the case of corrosion of concrete structures, the durability limit state includes the corrosion *initiation* and *propagation* periods. The initiation period may refer to the following limit states (among others):

- depassivation of the reinforcement by carbonation
- depassivation of the reinforcement by chlorides
- frost damage causing cracking and scaling

and the propagation period to:

- corrosion-induced cracking
- corrosion-induced spalling and collapse
- frost-induced cracking/deflection
- sulphate attack cracking

3.3. Reliability class

For the purpose of reliability differentiation, consequences classes (CC) have been established by considering the consequences of failure or malfunction of the railway infrastructure. These CC are presented in EN 1990 (2002) and given here in Table 3.1.

Table 3.1 Definition of consequence classes (from EN 1990)

Consequence Class	Description	Examples of buildings and civil engineering works
CC3	**High** consequence for loss of human life, or economic, social *or* environmental consequences **very great**	Grandstands, public buildings where consequences of failure are high (e.g. a concert hall)
CC2	**Medium** consequence for loss of human life, economic, social or environmental consequences **considerable**	Residential and office buildings, public buildings where consequences of failure are medium (e.g. an office building)
CC1	**Low** consequences for loss of human life, and economic, social or environmental consequences **small or negligible**	Agricultural buildings where people do not normally enter (e.g. storage buildings, greenhouses)

The three consequence classes can be associated with reliability classes (RC). The reliability classes are defined by the reliability index, β. β is calculated using the equation, $\beta = -\Phi(P_f)$, where Φ is the distribution function of the standardised normal distribution and P_f is the probability of the limit state under consideration being exceeded. The relationship if further outlined in Section 3.5.

Three reliability classes RC1, RC2 and RC3 exist to correspond with the three consequences classes CC1, CC2 and CC3. Table 3.2 gives the recommended minimum values for the reliability index associated with the three reliability classes.

Table 3.2 Recommended minimum values for reliability index β (ultimate limit states)

Reliability Class	Minimum values for β	
	1 year reference period	50 years reference period
RC3	5.2	4.3
RC2	4.7	3.8
RC1	4.2	3.3

3.4. Types of failure

In a load-bearing capacity evaluation, the safety requirement for the ultimate limit state depends on the type of failure anticipated (NKB 1978). The type of failure is assessed on the basis of the characteristics for the given material, component or structure.

The following are the types of failure that may be investigated (DRD, 2004):

- Type I - *Failure with warning and with load-bearing capacity reserve*, which includes ductile failure
- Type 2 - *Failure with warning but without load-bearing capacity reserve,* which includes ductile failure without extra load-bearing capacity
- Type 3 - *Failure without warning*, which includes brittle failure and stability failure

3.5. Target reliability levels

The target reliability level is the level of reliability prescribed by the railway infrastructure owner/manager to ensure acceptable safety and serviceability of the infrastructural element/network analysed. The choice of the target level of reliability should take into account the possible consequences of failure in terms of risk to life or injury, potential economic losses and the degree of societal inconvenience. The choice of the target level of reliability should also take into account the amount of expense and effort required to reduce the risk of failure.

Although the requirements for safety and serviceability in the assessment of existing railway infrastructure are in principle the same as for the design of new infrastructure, there are large differences in the outcome of the necessary considerations. As such, due attention should be given to differentiating the reliability level of infrastructure to be designed and that of existing infrastructure. The main differences in the considerations are (COST345):

- *economic considerations:* the incremental cost between acceptance and upgrading can be very large whereas the cost increment of increasing the safety of a new build is generally very small (relative to the overall project cost); consequently conservative criteria are used in the design standards
- *social considerations:* these include disruption (or displacement) of occupants and activities as well as heritage values, considerations that do not affect the design of new infrastructure
- *sustainability considerations:* considerations relating to reduction of waste and recycling, are more prevalent in the rehabilitation of existing infrastructure

In order to make the right choice for the target β values, the reference period, the consequences of failure and the cost of safety measures shall be analysed for the specific case considered. The maximum acceptable failure probability depends on the type of the limit state and considered consequences of failure for the relevant construction work.

Reliability requirements correspond to a formal annual probability of failure. This means that the formal probability of failure in the course of one year must not exceed a specified value. The reliability requirement is given in the form of the safety index, β, which is defined as:

$$\beta = -\Phi(P_f) \qquad 3.1$$

where Φ is the distribution function of the standardised normal distribution and P_f is the probability of the limit state under consideration being exceeded. The relationship between the reliability index β and the probability of failure P_f is given in Table 3.3.

Table 3.3 Relationship between β *and* P_f (from SAMCO, 2006)

P_f	10^{-1}	10^{-2}	10^{-3}	10^{-4}	10^{-5}	10^{-6}	10^{-7}
β	1.3	2.3	3.1	3.7	4.2	4.7	5.2

Note that the reliability requirement is related to the defined limit state, and that exceeding the limit does not necessarily imply collapse of the railway infrastructure. It is important not to confuse limit state violation with collapse.

The COST 345 report (2004) compared the target reliability indices of various codes and standards. Those comparisons are presented in the following subsections along with other relevant codes and standards. The distribution types which were used for the derivation of the reliability levels are included where available. When comparing the values in the tables presented and deciding on a reliability level, one must always consider the different reference periods used in the various documents (e.g. one year, life-time of the structure, etc.).

3.5.1. ISO/CD 13822:1999

In the ISO/CD 13822:1999 "Bases for Design of Structures - Assessment of Existing Structures" code, the target reliability mainly depends on the type of limit state examined as well as on the consequences of failure. As Table 3.4 shows, for ultimate limit states the target reliability index ranges from 2.3 for very low consequences of a structural failure to 4.3 for structures whose failure would have very high consequences.

Table 3.4 ISO/CD 13822:1999 – Target reliabilities

Limit States	Target reliability index β	Reference period
Serviceability		
Reversible	0.0	Intended remaining working life
Irreversible	1.5	Intended remaining working life
Fatigue		
Inspectable	2.3	Intended remaining working life
Not inspectable	3.1	Intended remaining working life
Ultimate		
Very low consequences of failure	2.3	L_s years *
Low consequences of failure	3.1	L_s years *
Medium consequences of failure	3.8	L_s years *
High consequences of failure	4.3	L_s years *

* L_s is a minimum standard period of safety (e.g. 50 years)

3.5.2. ISO 2394:1998

In ISO 2394:1998 “General Principles on Reliability for Structures” the target reliability index to be chosen for assessment of existing structures depends on the consequences of a structural failure as well as the costs of a safety measure (Table 3.5). The following distribution types were used for the derivation of the reliability level:

- Resistance: Lognormal or Weibull distributions
- Permanent loads: Gaussian distributions
- Time-varying loads: Gumbel Extreme Value distributions

Table 3.5 ISO/CD 2394:1998 Target reliabilities

Relative costs of safety measures	**Consequences of failure** small	some	moderate	great
High	0	1.5*	2.3	3.1[†]
Moderate	1.3	2.3	3.1	3.8[‡]
Low	2.3	3.1	3.8	4.3

* for SLS, use β = 0 for reversible and β = 1.5 for irreversible limit states
[†] for Fatigue Limit State, use β = 2.3 to β = 3.1 depending on the possibility of inspection
[‡] for ULS, use β = 3.1, 3.8 and 4.3

3.5.3. NKB Report No. 36:1978

The NKB Report No. 36 "Guidelines for Loading and Safety regulations for Structural Design" gives reliability indices depending on the failure type and consequence. The values recommended for the ultimate limit state for a reference period of one year are given in Table 3.6. For the serviceability limit state NKB recommends values of β = 1 to 2. The values presented in Table 3.6 are also the basis of the PIARC report "Reliability Based Assessment of Highway Bridges" (PIARC, 2000).

Table 3.6 NKB Report No. 36:1978 – Target reliabilities, ultimate limit state

Failure consequences	**Failure Type** Failure Type I, ductile failure with remaining capacity	Failure Type II, ductile failure without remaining capacity	Failure Type III, brittle failure
Less serious	3.1	3.7	4.2
Serious	3.7	4.2	4.7
Very serious	4.2	4.7	5.2

3.5.4. JCSS 2000

The publication of the Joint Committee of Structural Safety "Probabilistic Evaluation of Existing Structures" (JCSS, 2000) is devoted directly to existing structures and probabilistic evaluation. The target reliability indices, Table 3.7, given for the ultimate limit state and a reference period of one year depend on the failure consequence and the costs of safety measures similar to ISO 2394:1998. For the serviceability limit state, values of β = 1 to 2 are recommended. From this target reliability indices the standard code calibration process can be applied to obtain modified partial safety factors.

Table 3.7 JCSS Model Code I:2000 - Tentative target reliability indices β related to one year reference period and ultimate limit state

Relative cost of safety measure	**Consequences of failure** Minor	Moderate	Large
Large	3.1	3.3	3.7
Normal	3.7	4.2	4.4
Small	4.2	4.4	4.7

According to JCSS 2000, the value of 4.2 in Table 3.7 (corresponding to 'moderate' consequence of failure and 'normal' relative cost of safety measure) should be considered as the most common design situation. As previously mentioned, the costs of achieving a higher reliability level for existing structures are usually high compared to structures under design. For this reason the target level for existing structures usually should be lower.

For irreversible serviceability limit states tentative target values are given in Table 3.8. A variation from the target serviceability indexes of the order of 0.3 can be considered. For reversible serviceability limit states no general values are given.

Table 3.8 JCSS Model Code I:2000 - Tentative target reliability indices β related to one year reference period and serviceability limit state

Relative cost of safety measure	**Target index (irreversible SLS)**
High	1.3
Normal	1.7
Low	2.3

3.5.5. EN 1990:2002

Recommended values from EN 1990 (2002) for the reliability index β for various design situations (for reference periods of 1 year and 50 years) are indicated in Table 3.9. The values of β in Table 3.9 correspond to levels of safety for reliability class RC2 structural members.

Table 3.9 EN 1990:2002 – Target reliability index for Class RC2 structural members

Limit state	**Target reliability index**	
	1 year	50 years
Ultimate	4.7	3.8
Fatigue		1.5 to 3.8*
Serviceability (irreversible)	2.9	1.5

* Depends on degree of inspectability, reparability and damage tolerance

The following distribution types were used for the derivation of these evaluations of β:

- Lognormal or Weibull distributions have usually been used for material and structural resistance parameters and model uncertainties;
- Normal distributions have usually been used for self-weight;
- For simplicity, when considering non-fatigue verifications, Normal distributions have been used for variable actions. Extreme value distributions would be used where appropriate.

3.5.6. fib Bulletin 65

The fib Bulletin 65 (Model Code 2010) provides the following recommendations for target reliabilities for the design of structures:

Table 3.10 *fib* Bulletin 65:2012 – Recommended target reliability indices for structures to be designed, related to specific reference periods

Limit states	Target reliability index β	Reference period
Serviceability		
Reversible	0.0	Service Life
Irreversible	1.5	50 years
Irreversible	3.0	1 year
Ultimate		
Low consequence of failure	3.1	50 years
	4.1	1 year
Medium consequence of failure	3.8	50 years
	4.7	1 year
High consequence of failure	4.3	50 years
	5.1	1 year

The fib Bulletin 65 suggests that the β values given in Table 3.10 may also be used for the assessment of existing structures, but also suggests that a differentiation of the target reliability level for the new structures and for the existing structures may need to be considered. However, it warns that the decision to choose a different target reliability level for existing structures may be taken only on the basis of well-founded analysis of consequences of failure and the cost of safety measures for any specific case may need to be considered. The suggestions for the reliability indices for existing structures are given in Table 3.11 for the specified reference periods.

Table 3.11 *fib* Bulletin 65:2012 – Suggested range of target reliability indices for existing structures, related to specific reference periods

Limit states	Target reliability index β	Reference period
Serviceability	1.5	Residual service life
Ultimate	In the range of 3.1-3.8*	50 years
	In the range of 3.4-4.1*	15 years
	In the range of 4.1-4.7*	1 year

* depending on costs of safety measures for upgrading the existing structure

The requirements for the reliability of the components of the system shall depend on the system characteristics. The target reliability indices given Table 3.10 and Table 3.11 relate to the system or in approximation to the dominant failure mode or component dominating system failure. Therefore, railway infrastructures with multiple, equally important failure modes should be designed for a higher level of reliability per component than recommended in this Model Code. It should be noted that the recommendations in the other codes and standards presented above relate to component reliability rather than system reliability (Section 3.6).

The target reliability indices given in Table 3.10 and Table 3.11 are valid for ductile railway infrastructural components or redundant systems for which a collapse is preceded by some kind of warning, which allows measures to be taken to avoid severe consequences. Therefore by explicit requirements or by appropriate detailing it shall be assured that brittle failure does not occur. A component or system which would be likely to collapse suddenly without warning should be designed for a higher level of reliability than is recommended in this Model Code for ductile components.

3.5.7. Target reliability levels

When a reliability assessment of existing railway infrastructure is performed, it has to be decided if the probability of failure is acceptable. As can be seen in this chapter, there is no easy answer to that question. The Engineer carrying out the assessment has to decide which of the values are most suited and best applied to the problem at hand as the estimated probability of failure associated with a project is very much a function of the understanding of the issues, the modelling of the data, etc. Furthermore, it depends on costs as well as consequences of failure. Still, the target reliability indices presented in the subsections above can be helpful when a decision on the acceptable probability of failure has to be made (COST 345, 2004).

3.6. Reliability of structural systems

The reliability of railway infrastructure can be determined at two levels:

1. Safety at the component level, in which the safety of a component (or when a mechanism is considered, several components) with respect to a single form of failure is taken into account.
2. System safety, in which all components of the system and all forms of failure are taken into account.

The following types of systems can be classified:

- *redundant systems* where the components are “fail safe”, i.e. local behaviour of one component does not directly result in overall failure;
- *non-redundant* systems where local failure of one component leads rapidly to overall failure

The likelihood of system failure following an initial component failure should be assessed. In particular, it is necessary to determine the system characteristics in relation to damage tolerance or robustness with respect to accidental events (JCSS, 2000).

3.7. Time variant reliability assessment

Live load and resistance change with time, particularly where a structure is subjected to deterioration processes like environmental or chemical attack, or fluctuating stresses. Climate change is also an important consideration in this regard. A reliability analysis should therefore consider time-variance in the basic variables that describe loads and/or resistances.

Even in considering a relatively simple safety margin for component reliability analysis such as $M = R - S$, where *R* is the resistance at a critical section and *S* is the corresponding load effect, it is generally the case that both *S* and resistance *R* are functions of time, *R(t)* or *S(t).* Changes in both mean values and standard deviations could occur for either *R(t)* or *S(t).*

For example, the mean value of *R(t)* may change as a result of deterioration (e.g. corrosion of reinforcement in an RC bridge results in a loss of area, hence a reduction in the mean resistance) and its standard deviation may also change (e.g. uncertainty in predicting the effect of corrosion on loss of area may increase as the periods considered become longer). On the other hand, the mean value of *S(t)* may increase over time (e.g. due to higher train flow and/or higher vehicle weights) and, equally, the estimate of its standard deviation may increase due to lower confidence in predicting the correct mix of live load for longer periods. Figure 3.1 illustrates this process by undertaking a number of reliability analyses at specified time intervals. This type of time-integrated analysis is of particular use in cases where future crossing of an unacceptable threshold (e.g. a minimum acceptable target level) is part of the decision making progress. Clearly, inspection and maintenance planning as well as prioritisation of alternatives in railway infrastructure management may depend on such considerations.

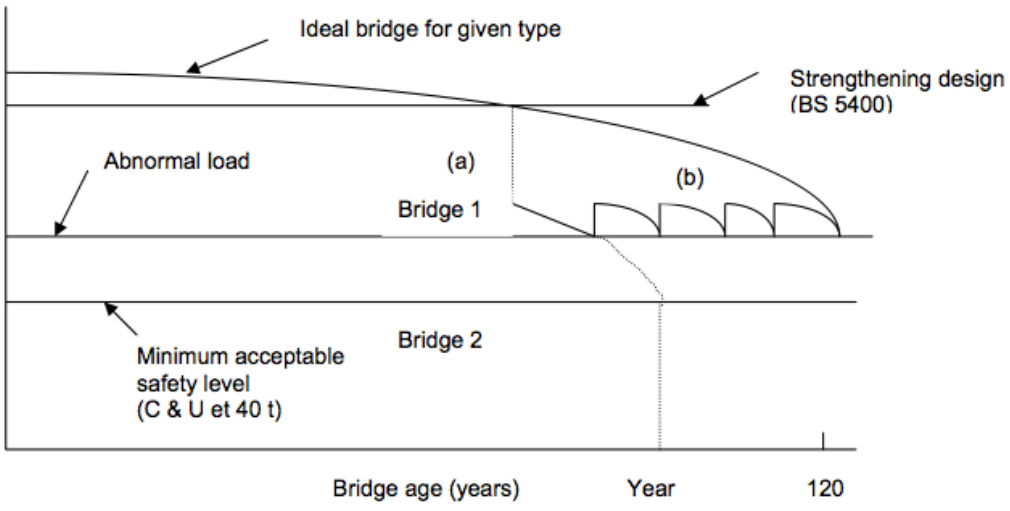

Figure 3.1: Whole life reliability profile (PIRAC 2000)

3.8. Sensitivity analysis

A reliability-based classification should always include a sensitivity analysis (DRD, 2004). The sensitivity analysis should be performed to ensure confidence in the result of the reliability analysis and to verify that the result is sufficiently robust. The models used should be checked to determine whether they give rise to unusually high sensitivity.

The sensitivity of the variables and parameters used should also be checked and it should be decided whether the sensitivities are acceptable. In practice, the implication is that when the sensitivity to a random variable $\left(\partial_{\beta}/\partial_{RV}\right)$ is small the variable could be treated as a deterministic quantity, with only a minor error being introduced. Furthermore, the values at the β point (the realisation of the stochastic variables at the most probable failure point) should also be verified by comparing the results with a deterministic assessment.

Finally, performing a sensitivity analysis can also identify the parameters that can, with advantage, be supplemented by additional information as discussed in Chapter 7.

4. Modelling Uncertainty

4.1. Introduction

For defined limit states the probability of failure, or the associated reliability index, is calculated for components or the overall structure. The design parameters that are involved in the definition of a limit state, i.e. loading, strength or geometry, have uncertainties associated with them and are thus described through the introduction of random variables. These uncertainties are therefore modelled using appropriate probability distribution functions for each basic variable.

The main sources of uncertainty that are relevant for reliability evaluation can be classified according to the nature of the uncertainty (PIRAC, 2000):

- Physical uncertainty
- Statistical uncertainty
- Model uncertainty

The sources of physical uncertainty can be considered as a result of inherent variation in the parameter (i.e. material strength, load intensity). The physical uncertainty in a basic random variable is represented by adopting a suitable probability distribution, described in terms of its type and relevant distribution parameters. The choice of distribution type is very important as the results of the analysis can be sensitive to the tail of the probability distribution, which depends primarily on the type of distribution adopted. Section 4.3 provides recommendations on suitable distributions for different properties.

Statistical uncertainty represents uncertainty resulting from the lack of sufficiently large samples of data to obtain a stable, even though empirical, probability distribution function for the data. For existing railway infrastructure, supplemental information (if obtainable) on material parameters or dimensions or loads can improve probability distributions through updating. 'A priori' values for probability distribution functions for various random variables can be used together with any site specific data in order to provide 'posterior' distribution functions. Material properties, including damage and deterioration, as well as loads could be subjected to updating. The process of Updating is discussed in more detail in Chapter 7.

The third source of uncertainty, model uncertainty, is caused by simplifications introduced in describing model behaviour. This can be as result of either the modelling used in global analysis or the modelling employed in describing the local capacity. It is possible to determine the errors

introduced through the simplifications of the models through comparison with a more sophisticated representation. Section 4.4 deals with model uncertainty in more detail.

In addition to discussing model uncertainty, this chapter will also briefly discuss the methods of analysis available when including uncertainties as well as the properties of probabilistic distributions.

4.2. Methods of Analysis

In a deterministic analysis the critical limit state is given by a function that depends on the resistance and load parameters. When performing a reliability-based analysis, the function will also depend on the model uncertainty parameters.

There are many reliability-based analysis methods and the selection for a particular situation is dependent on the limit state function's complexity and safety requirement. Details of the different reliability-based analysis methods are widely available in the literature, including Melchers (1999) who gives a detailed review of each. A very brief summary is given here.

FORM (First Order Reliability Method) is usually used as a starting point for ultimate limit states (DRD, 2004). This is considered the simplest method but its accuracy depends on the linearity of the limit state function. Depending on the limit state function's linearity it may be necessary to check that the use of the analysis method SORM (Second Order Reliability Method) does not give significantly different values of the safety index β.

For serviceability limit states, where the requirement for β is lower than for ultimate limit states, the difference between FORM and SORM can be significant (depending on the linearity of the limit state function). In such cases SORM, or possibly simulation (e.g. the Monte Carlo Simulation method), could be used to provide a more accurate estimation of the safety index.

There can be limit states of such complexity that both FORM and SORM are inappropriate. In such cases simulation methods should be considered (Ditlevsen & Madsen 1989, Melchers 1999).

4.3. Probability Distributions

Similar to the methods of reliability-based analysis, information on probability distributions is also widely available in the literature (e.g. Melchers, 1999). The following points are provided in JCSS (2000) and may also be helpful in providing information and in selecting suitable probabilistic models for various parameters.

Material properties

- the frequency of negative values is normally zero, therefore, a log-normal distribution can often be used
- distribution type and parameters should, in general, be derived from large homogeneous samples taking account of established distributions for similar variables (e.g. for a new high strength steel grade, the information on properties of existing grades should be consulted); tests should be planned so that they are, as far as possible, a realistic description of the potential use of the material in real applications.

Geometric parameters

- the variability in railway infrastructure dimensions and overall geometry tends to be small
- dimensional variables can be adequately modelled by the normal or log-normal distribution
- if the variable is physically bounded, a truncated distribution may be appropriate (e.g. location of reinforcement); such bounds should always be carefully considered to avoid entering into a physically inadmissible range
- variables linked to manufacturing can have large coefficients of variation (e.g. due to imperfections, misalignments, residual stresses, weld defects etc.)

Load variables

- loads should be divided according to their time variation (e.g. permanent, variable, accidental)
- in certain cases, permanent loads consist of the sum of many individual elements; in such cases they may be represented by a normal distribution
- for single variable loads, the form of the point-in-time distribution is seldom of immediate relevance; often the important random variable is the magnitude of the largest extreme load that occurs during a specified reference period for which the probability of failure is calculated (e.g. annual, lifetime)
- the probability distribution of the largest extreme could be approximated by one of the asymptotic extreme-value distributions (i.e. Gumbel, Frechet, Weibull)
- when more than one variable loads act in combination, load modelling is often undertaken using simplified rules suitable for FORM/SORM analysis.

In selecting a distribution type to account for physical uncertainty of a basic random variable, JCSS (2000) suggests the following procedure:

- based on experience from similar types of variables and physical knowledge, choose a set of possible distributions
- obtain a reasonable sample of observations ensuring that, as far as possible, the sample points are from a homogeneous group (i.e. avoid systematic variations within the sample) and that the sampling reflects potential uses and applications
- evaluate by an appropriate method the parameters of the random variable distributions using the sample data; the method of maximum likelihood is recommended but evaluation by alternative methods (e.g. moment estimates, least-square fit, graphical methods) may also be carried out for comparison
- compare the sample data with the resulting distributions; this can be done graphically (i.e. histogram vs. pdf, probability paper plots) or through the use of goodness-of-fit tests (i.e. Chi-square, Kolmogorov-Smirnov tests)

If more than one distribution gives equally good results (or if the goodness-of-fit tests are acceptable to the same significance level), it is recommended to choose the distribution that will result in the smaller reliability. This implies choosing distributions with heavy left tails for resistance variables (i.e. material properties, geometry excluding tolerances) and heavy right tails for loading variables (i.e. manufacturing tolerances, defects and loads).

The other two types of uncertainty mentioned above (statistical and model) also play an important role in the evaluation of reliability. These uncertainties are also modelled as random variables. Physical uncertainty is discussed further in Chapters 5 (Loading) and 6 (Materials) while statistical uncertainty is covered in Chapter 7. The remainder of this chapter focuses on categorising/evaluating model uncertainty.

4.4. Model uncertainty

Model uncertainty is concerned with the differences between results predicted by mathematical models and the actual condition. It has both a systematic component (bias) and a random component. The systematic component (e.g. a constant underestimation of material strength) is often built into design equations to ensure that engineers are conservative. The random component is due to the inability to define the actual condition exactly.

Model uncertainties, denoted θ, are often modelled as normal or lognormal distributed variables. If the model uncertainty is normally distributed, it has a mean value about zero and is commonly introduced into the calculation model as follows:

$$Y = \theta + f(X_1 \dots \dots X_n) \quad 4.1$$

Or if the variable is lognormal distributed, it has a mean value about 1.0 and is introduced into the calculation models as follows:

$$Y = \theta \text{ x } f(X_1 \dots \dots X_n) \quad 4.2$$

where *Y* is the response of the structure and $f(X_1 \dots X_n)$ is the model with the inherent basic variables that describes the capacity or load effect.

It should be kept in mind that in this way the statistical properties of the model uncertainties depend on the exact definition of the model output. JCSS (2000) provides an elegant theoretically way to avoid these definition dependencies by linking the model uncertainties directly to the basic variables, that is to introduce $X_i' = \theta X_i$.

4.4.1. Model uncertainty for capacity

In the Danish Road Directorate Report (DRD, 2004), which borrows heavily from earlier NKB reports (NKB, 1978 & 1987), the model uncertainty is taken into account by introducing the stochastic variable I_m for material capacities. The variable I_m is introduced into the model by multiplying the relevant basic strength parameters (e.g. concrete strength, steel strength, strength of reinforcement bars etc.) by I_m. This model uncertainty parameter, I_m, incorporates:

1. The accuracy of the computation model, I_1. The computation model specifies the role of the materials in the mathematical model in converting loads to load effects and the mathematical model for determining capacity.

2. Possible deviations from the strength of material properties in the railway infrastructure considered as compared with that derived from control specimens, I_2

3. The uncertainty in the identification of materials in existing railway infrastructures, I_3

The variable I_m is logarithmic-normally distributed with mean value of 1.0 and a coefficient of variation, V_{I_m}. The variation of I_m may be incorporated into the analysis by increasing the coefficient of variation of the basic material variable V_m (i.e. the physical uncertainty) as per the NKB recommendation (1978):

$$V^2 = V_m^2 + V_{I_m}^2 \quad 4.3$$

where V_{I_m}, is calculated as:

$$V_{I_m}=\sqrt{V_{I_1}^2+V_{I_2}^2+V_{I_3}^2+2\left(\rho_1 V_{I_1}+\rho_2 V_{I_2}+\rho_3 V_{I_3}\right)V_m} \quad 4.4$$

where V_m is the variation coefficient for the material parameter and the variation and correlation coefficients, V_{I_i} and ρ_i respectively, are as specified in Table 4.1.

Table 4.1. Model Uncertainty Factors (NKB, 1978)

Accuracy of the calculation model			
	Good	**Normal**	**Poor**
V_{I_1}	0.04	0.06	0.09
ρ_1	-0.3	0.0	0.3
Material property deviations			
	Small	**Medium**	**Large**
V_{I_2}	0.04	0.06	0.09
ρ_2	-0.3	0.0	0.3
Material identity			
	Good	**Normal**	**Poor**
V_{I_3}	0.04	0.06	0.09
ρ_3	-0.3	0.0	0.3

In considering Table 4.1, for uncertainty factors associated with the accuracy of the calculation model it should be noted that: (a) Good computation models can for example be used (i) where the model is so simple (corresponding to a simple structure) that only small variations can arise, (ii) where attention has been paid to eccentricities, secondary moments, etc., (iii) where the model has been verified for the railway infrastructure in question, or (iv) where an improved model has resulted in a reduction of the uncertainty of an important stochastic variable; (b) Normal calculation accuracy is used in situations where computation models are used that are generally accepted as being in conformity with normal practice and (c) a Poor computation model is one that has been excessively simplified and does not meet the requirements for a model of normal accuracy. The uncertainty associated with determining material parameters is dependent upon the amount of information available and on the availability of test results etc. For uncertainty factors associated with material identity it should be noted that: (a) Good material identity can be assumed if the identity of the materials has been verified e or if the identity of materials used subsequently can be documented, (e.g. "as built" drawings); (b) Normally material identity is assumed when the materials are assigned on the basis of the project material and there is no reason to doubt that the railway

infrastructure in question was not built in accordance with the project material and (c) Poor material identity arises when estimated values are used or where the project material is dubious or incomplete (O'Connor and Enevoldsen 2008).

In the absence of structure specific data the JCSS Model Code III (2000) provides the following recommendations for model uncertainties:

Table 4.2 Recommended model uncertainties for material capacities (JCSS Model Code III, 2000)

Model type	Distribution	Mean	CoV
Resistance models steel (static)			
Bending moment capacity *	LN	1.0	0.05
Shear capacity	LN	1.0	0.05
Welded connection capacity	LN	1.15	0.15
Bolted connection capacity	LN	1.25	0.15
Resistance models concrete (static)			
Bending moment capacity *	LN	1.2	0.15
Shear capacity	LN	1.4	0.25
Connection capacity	LN	1.0	0.10

* including the effects of normal and shear forces

4.4.2. Model uncertainty for loading

In terms of the load side of the failure equation, the model uncertainties take care of uncertainties such as:

- uncertainties in the load calculation model
- uncertainties in the load effect calculation model

In the Danish Road Directorate Report (DRD, 2004) uncertainties in the load calculation models are taken into account by introducing the stochastic variable I_f. From NKB-rapport nr. 35 (1978), if the material properties are assumed to be normally distributed, the variation of I_f may be incorporated into the analysis by increasing the coefficient of variation of the action, V_f, as:

$$V^2 = V_f^2 + V_{I_f}^2 \qquad 4.5$$

If the action is non-normal, the variable I_f should be considered as a basic variable, which is stochastically independent of other variables in the limit state function.

Permanent loads

The variable I_f is modelled for each permanent load by an independent normally distributed stochastic variable with mean value 0.0 and a standard deviation of 5% of the mean value of the

permanent load. I_f is introduced into the computation model by the addition of I_f to the relevant basic variables (NKB, 1978).

Variable loads

The model uncertainty for variable loads is introduced into the computation model by multiplying the basic parameters by I_f, where the variable I_f is normally distributed with mean value 1.0 and variation coefficient V_{If} as given in Table 4.3 (DRD, 2004).

Table 4.3 Variation coefficient for uncertainties in the load calculation model for variable loads (from DRD Report 291, 2004)

	Uncertainty in load calculation model		
	Low	Medium	High
V_{If}	0.10	0.15	0.20

The uncertainty of the loading model can generally be evaluated on the basis of the confidence in the modelling. For a 90% confidence level, *Low uncertainty* corresponds to a variation coefficient of 0.10 and an accuracy of approx. 15%, *Medium uncertainty* to a variation coefficient of 0.15 and an accuracy of approx. 25% and *High uncertainty* to a variation coefficient of 0.20 and an accuracy of approx. 35%. Note: these values of uncertainties were calibrated for road bridges. The level of uncertainty associated with railway structures is lower; therefore, the uncertainty associated with railway load models could be reasonably taken as low, i.e. variation coefficient of 0.10 (O'Connor et al. 2009).

The load effect calculation models facilitate linear or nonlinear calculation of stresses, axial forces, shear forces and bending and torsional moments etc. In this regard, model uncertainties can arise as a result of failure to consider for example 3D effects, inhomogeneities, interactions, boundary effects, simplification of connection behaviour, imperfections and so on. The scatter of the model uncertainty will also depend on the type of infrastructure considered (e.g. frame, plates, shell, solids, etc.). The JCSS Model Code III (2000) provides recommendations for model uncertainties associated with load effect calculations as outlined in Table 4.4.

Table 4.4 Recommended probabilistic models for uncertainties in load effect calculation models (JCSS Model Code III, 2000)

Model type	Distribution	Mean	CoV
Load effect calculation			
Moments in frames	LN	1.0	0.10
Axial forces in frames	LN	1.0	0.05
Shear forces in frames	LN	1.0	0.10
Moments in plates	LN	1.0	0.20
Forces in plates	LN	1.0	0.10
Stresses in 2D solids	N	0.0	0.05
Stresses in 3D solids	N	0.0	0.05

Model uncertainties for capacity and loading in geotechnical engineering depend largely on the type of analysis being carried out. There is limited information available on appropriate values to use for model uncertainty when carrying out probabilistic assessments in geotechnical engineering.

The following references provide some guidance.

- Al-Homoud and Tanash (2004) – This research considers modelling uncertainty in stability analysis for design of embankment dams on difficult foundations. As part of the analysis the sensitivity of results to the model uncertainty parameters are examined. In this case the model uncertainty bias varies between 1.0 and 1.3 and the CoV varies between 0.11 and 0.25.
- Yucemen and Al.Homoud (1990) – As part of this study the authors carried out a three-dimensional probabilistic analysis of slope stability. In this case a bias and CoV of 1.16 and 0.11, respectively, were assumed as input parameters for model uncertainty.
- Phoon (2005) – This paper examines model uncertainty parameters for laterally loaded rigid drilled shafts and provides results from laboratory controlled tests and full-scale field tests. Log-normally distributed model uncertainty parameters are provided for the lateral (or moment) limit and the hyperbolic capacity where the bias varies between 0.85 and 2.26 and the CoV varies between 0.27 and 0.4.
- Forrest and Orr (2011) – This paper investigates the effect of model uncertainty on the reliability of spread foundations. The authors concluded that the CoV for the model uncertainty parameter needs to be greater than 0.15 to have a significant effect on the calculation of β. The CoV is generally much less than 0.15 when using the bearing resistance equation for spread foundation. The results tend to be more sensitive to physical uncertainties associated with the soil strength parameters. The effect of model uncertainty

is more significant for drained conditions than undrained conditions since the physical uncertainty associated with soil parameters is lower for drained conditions.

5. Load Modelling

5.1. Introduction

When assessing existing infrastructure it is possible to have a more accurate assessment of the loading than in design. The consequence of a more accurate load assessment is that it is justifiable to reduce the associated load partial safety factors at the ultimate and serviceability limit states and in the load combinations, to reflect the increased knowledge of the loads (COST 345, 2004). Using knowledge of the actual loads also results in a more accurate evaluation of the reliability index in a probabilistic assessment.

When determining load models for the assessment of railway infrastructure, special attention must be given to the modelling of the railway load and dynamic effects. The following chapter gives details of the loads to be considered with particular emphasis on train loads and associated dynamic effects.

In performing an assessment, the assessor should take account of all likely loading scenarios. Where relevant, the scenarios should include environmental effects such as those due to wind, air pollution, moisture, chlorides etc. Environmental effects, including those due to Climate Change, are not covered by this chapter but it should be noted that some of these are important inputs for the degradation analysis. This chapter instead details permanent loads (such as gravity, rails, sleepers, ballast) and variable loads (such as traffic and other variable loads). Load distribution by the rails, sleepers and ballast is also discussed (Section 5.3).

The final section of this chapter discusses load combinations. In the reliability analysis it will often be necessary to combine several load processes, e.g. load on two or more tracks. With variable loads and combinations of variable loads a distinction is made between the distribution of immediate values and extreme values, where the distribution of extreme values is adjusted to the reference period of the safety assessment.

5.2. Permanent gravity loads

The permanent loads generally include the weight of the structure and earth pressures.

In a probabilistic safety assessment, permanent loads are generally modelled by normally distributed variables (NKB, 1978). A distinction is generally made between the dead load of the structure itself, G, and the superimposed dead load, G_W.

In line with DRD (2004), the following can be used as a starting point:

- G is assumed to be normally distributed with a variation coefficient of 5%
- GW is assumed to be normally distributed with a variation coefficient of 10%

Note that permanent loads from different sources are assumed to be stochastically independent and it is possible to reduce uncertainties by measurement. Note also that in addition to the given variations, the uncertainty of the model should also be taken into account (as discussed in Section 4.4).

5.2.1. Self-weight

Self-weight includes the weight of the structure and the weight resulting from service cables, ducting and other miscellaneous items such as walkways (any assumptions made regarding such equipment should be clearly stated in the assessment calculations.) When calculating the self-weight for assessment, the dimensions should, where possible, be based on dimensions verified during the inspection. For the most conservative assessment level analysis, the recommended values of unit weight given in JCSS (2000) and SB-LRA (2007) or from drawings should be used. However, if the initial assessment shows inadequacies, or there is doubt about the nature of particular material, tests should be carried out to determine actual densities (SB-LRA, 2007).

5.2.2. Ballast

The ballast depth can either be determined from the drawings or from direct site measurements. It is recommended to measure ballast depth (SB-LRA, 2007). When performing more advanced assessments (such as Assessment level 3, see Chapter 2) measurements of actual ballast depth and weight are essential.

When the ballast depth is measured, the weight should be based on the measured depth with unit weight varying between 1600-2100 kg/m³ (SB-LRA, 2007). The density of the ballast is dependent on its condition (e.g. older crushed ballast absorbs more water). Therefore the type and condition (clean/dry or wet/contaminated etc.) should always be noted when estimating the density. Where required by the railway administration, any future requirements for increase in ballast depth should also be taken into account.

UIC 776-1 (2006) recommends an additional factor of either 1.33 (ballast load effect unfavourable) or 0.75 (ballast load effect favourable) should be applied to the nominal depth of ballast beneath the underside of the sleeper to take account of the variability of the ballast depth. The minimum and maximum nominal depths of ballast beneath the sleeper to be taken into account should be

specified by the commissioning body. Any additional ballast provided below the nominal depth of ballast may be considered as an imposed moveable load. Additionally, the ballast density (or range of ballast densities) to be taken into account may also be specified by the commissioning party.

5.2.3. Track

A large range of sleepers, rails, ballast profiles and other track equipment exist. For enhanced assessment, these loads have to be checked by the track maintenance office (SB-LRA, 2007).

SB-LRA (2007) provides the various loads due to track components. Where a different configuration of sleepers and rails has been identified during the inspection, the self-weight to be used should be determined by measurement of dimensions of the configuration and by reference to data on weights of components produced by the manufacturer. In a probabilistic assessment, a coefficient of variation of 3% for steel elements, 8% for pre-cast concrete sleepers and 15% for timber sleepers can be assumed (JCSS, 2000).

5.2.4. Other permanent loads

Other permanent loads that should be considered are:

- Soil pressure
- Water pressure
- Differential settlement
- Concrete creep and shrinkage
- Prestress
- Movable loads (self-weight of non-structural elements, loading from overhead line equipment, loading from other railway infrastructure equipment).

Further information can be found in EN 1991-2:2003 section 6.7.3.

5.3. Load distribution by the rails, sleepers and ballast

When assessing existing infrastructure, more sophisticated load distribution models than those used for design should be used. Design codes (for examples EN 1991-2:2003) often contain simplified models for the load distribution. Though such models are acceptable for new structures and usually give safe values, for existing structures considering a more sophisticated load distribution taking into account the contribution of the track can increase the assessed load capacity, decrease the vertical bridge acceleration and decrease the deflections. For Level 1 assessment (see Chapter 2) it is adequate to directly apply the axle loads to the bridge deck as concentrated point forces. However,

in intermediate and enhanced assessment (i.e. assessment level 2 and 3), the beneficial effect of the track (i.e. the rails, sleepers and ballast) should be considered. This requires often complex models and commercial Finite Element (FE) packages in order to include a length of the track on the approaches to the structure, across the structure and on the departure from the structure (SB-LRA, 2007).

5.4. Vertical Train loads

5.4.1. WIM data available

When performing a probability based assessment, the inherent variables in the limit state function should be described by statistical distributions (as discussed in Chapter 4). In this subsection focus is on the statistical distributions suitable for modelling train loads. These statistical distributions are generated using measurements of real train loads. Such measurements can be carried out by using WIM techniques. WIM is well documented in the literature and has been the focus of, and used in, many European projects (e.g. COST 323 (1999), WAVE (2001) and SAMARIS (2006)).

Individual train load models

The load and location of each axle of passing trains can be obtained from WIM measurements and the corresponding load effects in different locations of the railway infrastructure and in different types of railway infrastructure elements can be calculated very accurately using the measurement information. If the measurements of the train loads are made during a sufficiently long time period and it can be assumed that the train loads are time invariant, i.e. there are not systematic changes in e.g. traffic type and train intensities, then it is possible to fit the measured data to a common statistical distribution with a cumulative distribution function, F_x (SB-LRA, 2007). F_x describes the natural variation of the load on the specific line where the measurements were performed and is also valid for other similar lines (O'Connor et al. 2009).

For variable loads, such as traffic loads which fluctuate in time, the interesting statistical distributions, at least in the ultimate limit state, are the maximum distributions. The maximum distributions describe the variation of the maximum loads during a reference period, *T*. Where it is time consuming and due to economical reasons, not possible to collect data to determine such distributions, other techniques such as simulation and extrapolation are used to determine these distributions. Such techniques are described in the report SB4.3.2 (2006). A simple approach to determine the maximum distribution F_Y is given by:

$$F_Y(y) = [F_X(x)]^n \qquad 5.1$$

where $F_X(x)$ is the parent distribution and $F_Y(y)$ is the maximum distribution of *n* samples of *X* all of which are independently identically distributed (e.g. $F_X(x)$ is the distribution of 3000 trains passing over the bridge in one day and $F_Y(y)$ is the distribution of max per day where n=3000 OR $F_X(x)$ is the distribution of 3000 trains passing over the bridge in one day and $F_Y(Y)$ is the distribution of max per year where n=3000*250 OR take $F_X(x)$ as max per day and $F_Y(Y)$ is the max per year where n= 250, assuming 250 working days per year). In this situation *n* is the number of trains that passes the bridge during the reference period. The reference period for variable loads are generally set to one year. The choice of reference period is directly linked to the safety index, β in design.

As an illustration, Figure 5.1 taken from SB-LRA (2007) shows the maximum distributions for different *n* if $F_X(x)$ is assumed standard normal distributed. As can be seen, the mean value increases and the standard deviation decreases when n increases.

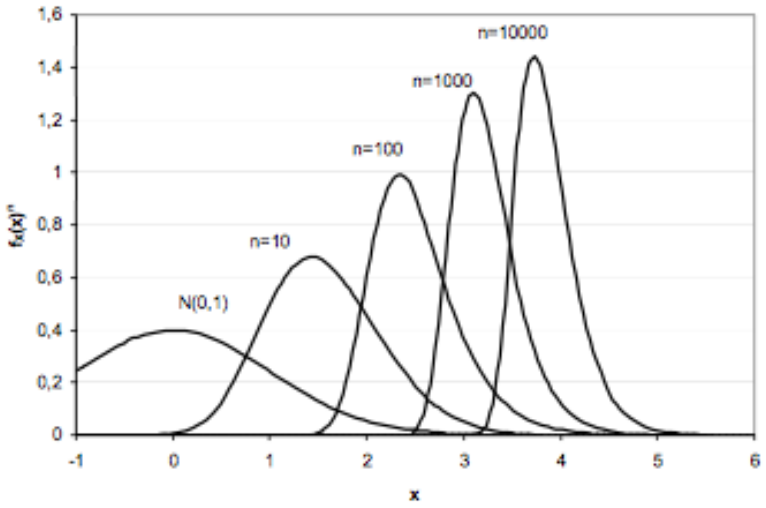

Figure 5.1 Maximum of standard normal distributed independent random variables

From SB-D4.3.2 (2007), Equation 5.1 is the exact probability function for maxima, but it is not always useful in practice because it doesn't follow any standard distribution and it is often very difficult to use analytically. Two exceptions are the cases when F_X is exponential or normally distributed. In both cases $F_{max}(X)$ (where $F_{max}(X) = F_Y(y) = [F_X(x)]^n$) becomes Gumbel distributed with cumulative distribution function given as:

$$F_{MAX}(X) = e^{-e^{-\left(\frac{x-b}{a}\right)}} \qquad 5.2$$

where *a* and *b* are parameters of the Gumbel distribution. For the case that F_X is exponential distributed with cumulative distribution function

$$F_{MAX}(X) = 1 - e^{-\frac{x}{m}} \qquad 5.3$$

where m is the parameter in the exponential distribution. The Maximum of n independent identically exponential distributed random variables is Gumbel distributed with parameters according to:

$$\begin{aligned} a &= m \\ b &= m \cdot \ln(n) \end{aligned} \qquad 5.4$$

For the other case when F_X is normal distributed, the parameters of the Gumbel distribution become

$$\begin{aligned} a &= \frac{1}{f_X(b) \cdot n} \\ b &= F_X{}^{-1}\left(1 - \left(\frac{1}{n}\right)\right) \end{aligned} \qquad 5.5$$

Where f_X is the probability density function for the normal distributed random variable *X*. Finally, the parent distribution influences both the convergence and the variation of the extreme value distribution, e.g. an exponential distributed variable converges faster than a normal distributed variable, $n \approx 5$ and $n \approx 20$ respectively (SB-D4.3.2, 2007).

It has been found that equation 5.1 converges towards an asymptotic distribution when $n \to \infty$ (SB-D4.3.2, 2007). There is a family of three types of such maximum distribution types I, II and III also called the Gumbel, Fréchet and Weibull distribution respectively. The cumulative distribution functions for maximum Type I, II and III are given in SB-D4.3.2 (2007), and below:

The cumulative distribution function of a Gumbel distribution, Type I is given by

$$G_X(x) = \exp\left(-\exp\left(-\left(\frac{x-b}{a}\right)\right)\right) \qquad 5.6$$

The cumulative distribution function of a Fréchet distribution, Type II is given by

$$\begin{aligned} G_X(x) &= 0 && x \le b \\ G_X(x) &= \exp\left(-\left(\frac{x-b}{a}\right)^{-k}\right) && x > b \end{aligned} \qquad 5.7$$

The cumulative distribution function of a Weibull distribution, Type III is given by

$$G_X(x) = \exp\left(-\left(-\frac{x-b}{a}\right)^{-k}\right) \qquad x > b$$
$$G_X(x) = 0 \qquad x \le b \qquad 5.8$$

where *a*, *b* and *k* are the scale, location and shape parameter respectively. It is postulated in equations 5.6-5.8 that the parameters *a* and *b* are > 0 and that parameter *k* in equations 5.5 and 5.6 is ≠ 0.

The three extreme value distributions, type I, II and III described above can be compounded into one distribution called the General Extreme Value distribution (GEV), see WAFO (2000) and Coles (2001), with cumulative distribution function given by:

$$F_X(x) = \exp\left(-\left(1-k\frac{x-b}{a}\right)^{\frac{1}{k}}\right) \qquad \text{if } k \neq 0 \qquad 5.9$$

$$F_X(x) = \exp\left(-\exp\left(-\frac{x-b}{a}\right)\right) \qquad \text{if } k = 0$$

where *a* , *b* and *k* are the scale, location and shape parameter respectively. Equation 5.9 is valid for $k(x-b) < a$, $a > 0$ and *k*, *b* arbitrary. The shape parameter *k* is often called the Extreme Value Index (EVI), because, if $k > 0$ the GEV is a Weibull distribution, if $k = 0$ the GEV is Gumbel distributed and finally if $k < 0$ the GEV is Fréchet distributed. Figure 5.2 from SB-D4.3.2 (2007) shows three GEV distributions with different shape parameter.

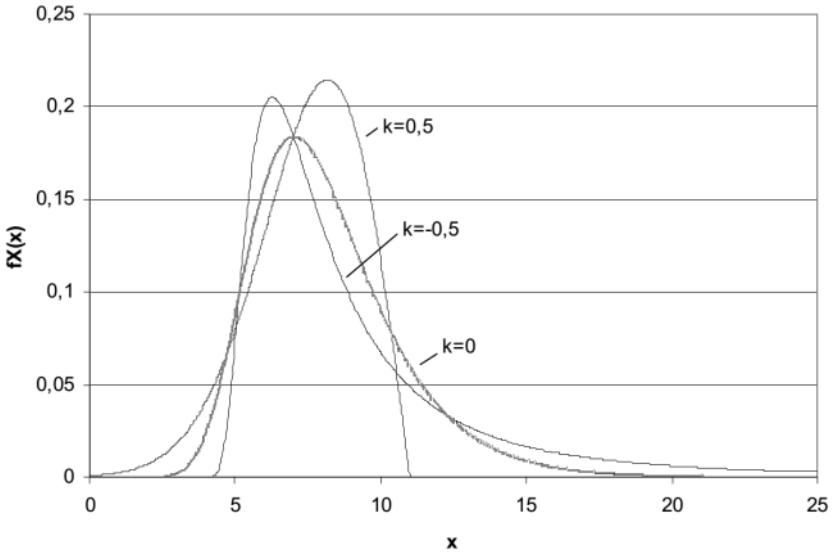

Figure 5.2 Probability distribution functions for GEV distributions with different shape parameters, with equal scale and location parameters, a=2 and b=7 respectively (SB-D4.3.2, 2007)

The above method, of determining the statistical distribution from measurements is known as the Extreme Value Theory (EVT). The Peaks Over Threshold (POT) method is used to estimate quantities outside the range of observed data. The objective with the method is to only use the extreme tails of the distribution of the observed data. A distribution which fits the tail data well is chosen. This is done by choosing a suitable, relatively high threshold, *u* and only uses the events, *x* that exceed *u* in the future analysis. The differences between *x* and *u* are fitted to a standard distribution and from that distribution the extreme quantities are estimated (SB-D4.3.2, 2007).

5.4.2. No WIM data available

Where WIM data is not available, alternative load models must be used in the probabilistic assessment. This is not ideal and is rather a quasi-probabilistic rather than a probabilistic analysis. In such cases, deterministic load model parameters may be taken from EN 1991-2:2003, for example, and assigned appropriate coefficients of variation. Examples of some of these load models are given here.

Note that the load models defined in EN 1991-2:2003 do not describe actual loads. They have been designed so that their effects, with dynamic enhancements taken into account separately, represent the characteristic effects of service traffic.

The following load models are provided in EN 1991-2:2003:

- Load Model 71 to represent normal rail traffic on mainline railways
- Load Model SW/0 for continuous bridges to represent normal rail traffic
- Load Model SW/2 to represent heavy loads
- Load Model “unloaded train”

5.5. Other variable loads

5.5.1. Thermal actions

Thermal effects may often have to be included in the assessment of capacity and performance. They are particularly important for interaction between bridge and track and have to be taken into account when assessing piers or abutments receiving fixed bearings. Some information can be found in EN 1991-2:2003 Section 6.5.4. Principles and rules for calculating thermal actions can be found in EN 1991-1-5 (2003).

Thermal action can be divided into:

1. change over time of the average temperature
2. maximum and minimum temperature gradients
3. differential temperatures between different sub elements

Thermal actions for a specific railway infrastructure at a specific site depend on the climate conditions at the site (i.e. air temperature, solar radiation and wind), geometry and the thermal properties of the material. Thermal actions associated with changes in average temperature of the cross section are normally handled by appropriate boundary conditions allowing more or less free movements so that stresses are not induced in the structure except, e.g. frame bridges and bridges with seized bearings.

For thermal actions giving rise to gradients and differential temperatures the associated movements are often restrained so that stresses are induced, especially for statically indeterminate structures. Such imposed stresses may contribute to cracking. Thermal actions have the most significant effect for serviceability limit states, but also for ultimate limit states associated with brittle type failure modes and fatigue.

A correct estimation of the temperature loads is essential when the serviceability or fatigue limit states are of concern. In the case of the assessment in the ultimate limit state, the temperature load may be neglected for verification of failure modes where sufficient ductility to allow for redistribution of the internal forces can be expected before the ultimate state is reached. In such cases thermal actions will have no influence on the capacity (SB-LRA, 2007).

5.5.2. Equivalent vertical loading for earthworks and earth pressure effects

According to UIC 776-1 (2006), for global effects the equivalent characteristic vertical loading due to rail traffic actions for earthworks under or adjacent to the track may be taken as the appropriate load model (LM71, or classified vertical load where required, and SW/2 where required). The load model should be uniformly distributed over a width of 3.00 m at a level 0.70 m below the running surface of the track. No dynamic factor or enhancement needs to be applied to the uniformly distributed load.

5.5.3. Centrifugal forces

The centrifugal force on the track should be taken into account when the track on a bridge is curved over the whole or part of the length of the bridge. According to EN 1991-2:2003 and UIC 776-1 (2006), the centrifugal forces should be taken to act outwards in the horizontal direction at a height

of 1.80 m above the running surface. The centrifugal force should always be combined with the vertical traffic load and the centrifugal force should not be multiplied by the dynamic factor.

The characteristic value of the centrifugal force (deterministic) shall be determined according to the following equations provided in UIC 776-1 (2006):

$$Q_{tk} = \frac{v^2}{g \times r}\left(f \times Q_{vk}\right) = \frac{V^2}{127r}\left(f \times Q_{vk}\right) \qquad 5.10$$

$$q_{tk} = \frac{v^2}{g \times r}\left(f \times q_{vk}\right) = \frac{V^2}{127r}\left(f \times q_{vk}\right) \qquad 5.11$$

where:

Q_{tk}, q_{tk}	are characteristic values of the centrifugal forces [kN, kN/m],
Q_{vk}, q_{vk}	are characteristic values of the vertical loads for Load Models 71, SW/0, SW/2 and "unloaded train"
f	reduction factor [f =1 for V ≤ 120 km/h, see EN 1991-2:2003 for more details]
v	maximum speed [m/s]
V	maximum speed [km/h]
g	acceleration due to gravity [9.81 m/s^2]
r	radius of curvature [m]

5.5.4. Nosing force

EN 1991-2:2003 recommends that the nosing force should be taken as a concentrated force acting horizontally, at the top of the rails, perpendicular to the centre-line of the track. It should be applied on both straight track and curved track. The characteristic value of the nosing force should be taken as $Q_{sk} = 100kN$. The nosing force should always be combined with a vertical traffic load. The nosing force should not be multiplied by the dynamic factor.

The characteristic value of the nosing force should be multiplied by the factor α for values of α ≥ 1. Further details can be obtained in EN 1991-2:2003, Section 6.5.2.

5.5.5. Actions due to traction and braking

Recommendations for traction and braking forces are given in EN 1991-2:2003 Section 6.5.3. These forces act at the top of the rails in the longitudinal direction of the track. They should be considered as uniformly distributed over the corresponding influence length $L_{a,b}$ for traction and braking effects

for the structural element considered. The direction of the traction and braking forces should take account of the permitted direction(s) of travel on each track.

The characteristic values of traction and braking forces recommended in the Eurocode are as follows:

Traction force: $Q_{l_{ak}} = 33[kN/m]\ L_{a,b}$ [m] ≤ 1000 [kN] for Load Models 71, SW/0 and SW/2

Braking force: $Q_{l_{bk}} = 20[kN/m]\ L_{a,b}$ [m] ≤ 6000 [kN] for Load Models 71 and SW/0

$Q_{l_{bk}} = 35[kN/m]\ L_{a,b}$ [m] for Load Model SW/2

Notes on traction and braking forces:

- Traction and braking may be neglected for the load model “unloaded train”
- The characteristic values of traction and braking forces shall not be multiplied by the dynamic factor
- Traction and braking forces should be combined with the corresponding vertical loads
- In the case of a bridge carrying two or more tracks, the braking forces on one track should be considered with the traction forces on one other track
- The characteristic values given above for Load Models SW/0 and SW/2 should be multiplied by the factor α

When the track is continuous at one or both ends of the bridge, only a proportion of the traction or braking force is transferred through the deck to the bearings, the remainder of the force being transmitted through the track where it is resisted behind the abutments. The proportion of the force transferred through the deck to the bearings should be determined by taking into account the combined response of the structure and track in accordance with UIC Leaflet 774-3.

5.5.6. Track bridge interaction

Relative displacements of the track and of the bridge, caused by a possible combination of effects such as thermal variations, train braking or deflection of the deck under vertical traffic loads lead to the track-bridge phenomenon that can result in additional stresses to the bridge and the track Calgaro et al (2010). Where the rails are continuous over discontinuities in the support to the track (e.g. between a bridge structure and an embankment), longitudinal actions are transmitted partly by the rails to the embankment behind the abutment and partly by the bridge bearings and the substructure to the foundations. It is important to underline that the limit states for the track depend on its design and state of maintenance.

It is also important to minimise the forces lifting the rail fastening systems (vertical displacement at deck ends), as well as horizontal displacements (under braking/starting) which could weaken the ballast and destabilise the track. It is also essential to limit angular discontinuity at expansion joints and switches near abutments in order to reduce any risk of derailment Calgaro et al (2010).

Note: In principal, interaction should be taken into account as a serviceability limit state (SLS) as regards the bridge, as well as being an ultimate limit state (railway traffic safety) as regards the rail.

5.5.7. Other variable loads

Other variable loads that need to be considered for the assessment of existing bridges include (EN 1991-2, 2003):

- horizontal mass action
- snow load
- wind load (characteristic values are given in EN 1991-1-4 (2003))
- pressure from ice and currents
- actions from waves and flowing water
- water pressure (ground water, free water, uplift)
- actions from soil
- frictional forces from bearings
- loads on footpaths (5kN/m^2 for non-public footpaths, for use by authorised persons)
- longitudinal forces (from designer's guide, interaction between track and structure)
- live load surcharge horizontal earth pressure
- the effects of scour
- water borne debris
- avalanche (where required by relevant authority)
- mud slides (where required by relevant authority)
- aerodynamic actions from passing trains (EN 1991-2:2003 Section 6.6 – to be taken into account when designing structures adjacent to railway tracks, noise barriers etc.)

5.6. Accidental Loads

Accidental loads include:

- Derailment of rail traffic on the bridge (EN1991-2:2003, Section 6.7.1)
- Derailment of rail traffic beneath or adjacent to the bridge (EN 1991-1-7)
- Accidental loading from errant road vehicles beneath the bridge
- Accidental loading from over height road vehicles beneath the bridge

- Ship impact
- Actions due to rupture of catenaries
- Actions due to accidental breakage of rails
- Fire (where required by relevant authority)

Other actions for Accidental Design Situations are given in EN 1991-1-7 and should be taken into account if necessary.

5.7. Dynamic effects

The load effect generated by trains consists of two parts; one static and one dynamic. The static part is due to the gravity effect of the train at rest and the dynamic effect occurs when the train moves. The dynamic effect comes in the form of vertical vibration. In this section the magnitude of the dynamic effect is described. SB- D4.3.2 (2007) explores and presents a recommendation for the statistical description of the dynamic effect.

The principal factors which influence dynamic behaviour are:

1. the speed of traffic
2. the span *L* of the element and the influence line length for deflection of the element being considered
3. the mass of the railway infrastructure
4. the natural frequencies of the whole structure and relevant elements of the structure and the associated mode shapes (eigenforms) along the line of the track
5. the number of axles, axle loads and the spacing of axles
6. the degree of damping
7. vertical irregularities in the track
8. the unsprung/sprung mass and suspension characteristics of the vehicle
9. the presence of regularly spaced supports of the deck slab and/or track (cross girders, sleepers etc.)
10. vehicle imperfections (wheel flats, out of round wheels, suspension defects etc.)
11. the dynamic characteristics of the track (ballast, sleepers, track components etc.)

The criteria for determining whether a dynamic analysis is required are given in UIC leaflet 776-2. It is important that the natural frequency of all structures subject to dynamic loading should be checked.

5.8. Fatigue loads

According to EN1991-2:2003, a fatigue damage assessment should be carried out for all structural elements, which are subjected to fluctuations of stress. For normal traffic based on characteristic values of Load Model 71, including the dynamic factor ϕ, the fatigue assessment should be carried out on the basis of the traffic mixes, "standard traffic", "traffic with 250 kN-axles" or ”light traffic mix“ depending on whether the structure carries mixed traffic, predominantly heavy freight traffic or lightweight passenger traffic in accordance with the requirements specified. Details of the service trains and traffic mixes considered and the dynamic enhancement to be applied are given in Annex D of EN 1991-2:2003. Each of the mixes is based on an annual traffic tonnage of 25×10^6 tonnes passing over the bridge on each track. Note that a special traffic mix may be specified in the National Annex or for the individual project.

For structures carrying multiple tracks, the fatigue loading should be applied to a maximum of two tracks in the most unfavourable positions. Alternatively, the fatigue assessment may be carried out on the basis of a special traffic mix.

Vertical rail traffic actions including dynamic effects and centrifugal forces should be taken into account in the fatigue assessment. Generally nosing and longitudinal traffic actions may be neglected in the fatigue assessment.

SB-LRA (2007) recommends that probabilistic train load models for the fatigue analysis may be deduced from reliable traffic data (from WIM or other measurements) using the same approach outlined in Section 5.4.1. The likelihood that a concrete section will crack under the proposed future loading can be determined using the POT approach. The rain-flow analysis from measured data and the use of the cumulative damage hypothesis (Miner´s rule) can be used for the fatigue analysis. A method for the probabilistic fatigue assessment including the uncertainty and variability of both the fatigue loads and resistance is explained in Crespo and Casas (1998) and Casas and Crespo (1997). The uncertainty of the variables can be included in the cumulative damage hypothesis so long as the probabilistic S-N curve is defined for the material or detail under consideration.

5.9. Application of traffic loads on railway bridges

EN1991-2:2003 recommends that a structure should be designed for the required number and position(s) of the tracks in accordance with the track positions and tolerances specified. However, each structure should also be designed for the greatest number of tracks geometrically and structurally possible in the least favourable position, irrespective of the position of the intended

tracks taking into account the minimum spacing of tracks and structural gauge clearance requirements specified. In an assessment the most adverse effects should also be checked.

5.10. Groups of loads – characteristic values of the multicomponent action

The simultaneous action of the vertical, horizontal and derailment loading may be taken into account by considering the groups of loads defined in Table 6.11 in EN 1991-2:2003. Each of these groups of loads, which are mutually exclusive, should be considered as defining a single variable characteristic action for combination with non-traffic loads. Each group of loads should be applied as a single variable action.

6. Modelling of Resistance Variables

6.1. Introduction

When performing a safety assessment it is important to accurately model resistance. The resistance models require information of the material properties (such as strength and stiffness) as well as the dimensions. Consideration of the temporal nature of resistance is also important. This chapter considers different material properties and pays particular attention to the associated probabilistic distributions. The chapter firstly looks at reinforced concrete and this is followed by prestressed concrete, steel, masonry and finally soil.

6.2. Reinforced concrete

6.2.1. Concrete

Material models for concrete must include the compressive strength, f_c', the modulus of elasticity, E_c, the compressive strain and information on shrinkage and creep. COST345 (2004) identifies that the main sources of uncertainty in these concrete properties are due to variations in the properties of the concrete and proportion of concrete mix, variations in mixing, transporting, placing and curing methods, variations in testing procedures, and variations due to concrete being in a structure rather than in test specimens (Mirza, 1979).

Concrete compressive strength is a very important parameter as it is generally included in models defining the load carrying capacity of a concrete structure and is also often used as the basis variable for determining a number of other parameters (DRD, 2004). Normal and lognormal distributions have both been used in the literature to represent the probability density function of this parameter, although lognormal is generally preferred (COST 345, 2004; PIARC, 2000).

When defining the mean value of the compressive strength for an existing structure, it is vital that original documentation, including design codes at the time of the original design, is consulted. It is very important to know the relationship between the characteristic and mean strengths and this relationship can be code dependent (O'Connor & Enevoldsen, 2008). The COV is generally higher for lower strength concrete. In DRD (2004) the values range from 0.12 for the higher strength concretes, i.e. 40MPa to 50MPa to 0.22 for 5MPa. PIARC (2000) suggests a COV of 0.2 to reflect the uncertainties associated with the material properties and the condition at the time of assessment.

The other material properties of concrete (i.e. tensile strength, modulus of elasticity and ultimate strain) can be determined from the compressive strength.

The shrinkage and creep of the concrete can be determined by considering the available information on the age and geometry of the structure, the w/c ratio of the concrete and the surrounding site climate. When assessing an existing structure, the age will usually be such that shrinkage and creep can be considered as having terminated. If they are to be included, the mean values of both shrinkage and creep can be determined using the approach in Section 2.1.6.4 in the CEB-FIP Model Code (1991). Adopting that approach, the shrinkage strain can be taken as normally distributed with a COV of 0.35 and creep strain can also be taken as normally distributed with a COV of 0.2 (DRD, 2004).

Model uncertainty, discussed in Section 4.4.1, should be included in analyses. Note that the model uncertainty can be reduced if the structure has been tested to an extent sufficient to document variations.

6.2.2. Reinforcing steel

The uncertainties in the estimation of the strength of steel reinforcement are due to the variation in the strength of material, variation in the cross-section, effect of rate of loading, effect of bar diameter on properties of the bar and effect of strain at which yield is defined (Mirza, 1979). Also, different tests can sometimes be performed to measure the same property. For example, yield strength recorded by the manufacturer in mill tests is approximately 8% greater than the actual static yield strength so there are often two quoted steel strengths, the mill strength and the static strength. The mill strength tests are performed at a rapid rate of loading and use actual areas while the static strengths are determined based on nominal area and use a strain of rate that is similar to that expected in a structure.

DRD (2004) suggests that the tensile yield stress, f_y, can be assumed to be lognormally distributed with a constant standard deviation of 25 MPa independent of the grade. A table (Table 6.4) is presented with the recommended mean for smooth round bars, ribbed bars and cold-formed bars with characteristic strengths ranging from 235 MPa to 550 MPa. The PIARC (1999) report also suggests a lognormal distribution for the yield strength of steel. The lognormal distribution follows the positive skewness of obtained data and also precludes non-negative values of strength. For high strength steel the suggested standard deviation is 30-35 MPa which corresponds with JCSS III (2000) which suggests 30 MPa.

In terms of the cross-section, the actual areas of the reinforcing bars can differ from the nominal areas due to the rolling process. COST 345 (2004) suggests a normal distribution to represent the uncertainty. For groups of bars, PIARC (1999) suggests a lognormal random variable and presents an

approach for calculating the resistance provided by a group of bars as a sum of the resistances of individual bars. In this case, the mean value and standard deviation (of the group of bars) can be obtained as a function of individual bar characteristics and, possibly, different models for the correlation between areas and between strengths of bars.

PIRAC (1999) also suggests that the effective depth (distance from the compressive face of the section to the centre of reinforcement) of the reinforcement is modelled as a random variable. This parameter can be affected by inaccuracies in slab thickness, height and spacing of supporting formwork or the diameters of the bars. While the mean values for the probabilistic distribution for this random variable can be taken as equal to the nominal value, the COV will vary depending on the placement (i.e. top or bottom) and for possible deterioration. It can be in the range of 5%to 20%.

The depth of cover to reinforcement is also suggested to be taken as a random variable with a lognormal distribution (PIARC, 1999). The modulus of elasticity and the ultimate strain of the reinforcement can however, often be modelled deterministically. Such an assumption will not significantly affect the safety calculation (DRD, 2004). The compressive stress can be determined from the tensile yield stress if no other information is available. If the reinforcement is not cold-formed then they can be assumed to be equal, and, in the case of cold-formed reinforcement the compressive yield stress is reasonably taken as 0.8 times the tensile yield stress (DRD, 2004).

Model uncertainty should be included in analyses to account for the uncertainty in the determination of the parameters. Where tests have been carried out on the structure, the model uncertainty can be reduced.

6.3. Prestressed concrete

In general, concrete standards do not give characteristic values for relevant material parameters for prestressed reinforcement. These values must therefore be based on documentation from the design or the manufacturer's documentation (DRD, 2004).

In a probabilistic safety assessment involving a prestressed concrete bridge, the strength of the prestressing steel can modelled as a lognormally distributed variable (O'Connor & Enevoldsen, 2008). A low COV, circa 0.04 is generally sufficient for prestress steel. The ultimate strain and the modulus of elasticity for the prestressing steel can be modelled deterministically without affecting the safety calculations. The prestressing force at any given time should be determined by taking the relevant losses into account.

Model uncertainty should also be included with calculations involving prestressed concrete.

6.4. Structural Steel

For the probabilistic model for the yield stress, f_y, of structural steel, a lognormal distribution is recommended (JCSS III 2000; DRD 2004). The mean value is dependent on the steel grade and the thickness, t, and is greater than the characteristic value. JCSS III (2000) proposes a probabilistic model and DRD (2004) presents a table with recommended mean values for various grades of steel.

Studies differ on whether the standard deviation or the COV of the yield stress should remain constant. DRD (2004) suggests 25 MPa for all grades of steel whereas JCSS III (2000) suggests a COV of 0.07.

A lognormal distribution is also recommended for the ultimate tensile stress of structural steel. Again, DRD (2004) recommends a constant standard deviation of 25 MPa for all steel grades while JCSS III (2000) recommends a constant COV of 0.04.

The modulus of elasticity, shear modulus and Possion's ratio can either be taken as deterministic or a lognormal distribution with small COV of 0.03 suggested.

6.5. Masonry

The main materials used in masonry construction include a variety of bricks and stone typically separated by bed and vertical joints consisting of some type of mortar. The quantity of mortar depends on the construction type (e.g. the percentage of mortar per unit volume in multi-ring brickwork arches is 20% but is only 2% in the case of dressed stone voussoir arches).

Most methods of assessment for masonry arch bridges require the assessing engineer to make some assumptions regarding the properties of the constituent materials. The assumptions are dependent on the method of analysis and range from simplifying assumptions like infinite stiffness and strength in compression and no tensile strength to very sophisticated mathematical models which consider interface bond and non-linear behaviour of heterogeneous assemblies. Determining the material properties of masonry bridges is a difficult task and methods for determining the properties and the assessment of masonry bridges was a significant aspect of the Sustainable Bridges project. Chapter 8 in the final report (SB-LRA, 2007) is dedicated to Masonry Bridge Structures as well as the background document SB4.7.

The basic properties of masonry structures that should be included in an assessment are: elastic modulus, compressive and tensile strengths, bond strengths and shear strengths. Other properties include thermal coefficient, viscous deformation and fatigue properties. A good deal of experience is needed to determine realistic values for these properties.

6.6. Soil

There is great uncertainty associated with soil parameters and the geology of different sites can vary greatly even within short distances. It is therefore generally necessary to base an evaluation of the relevant strength parameters for soil on geotechnical investigations and tests in the specific locality of the bridge. The uncertainty in the parameters can be determined on the basis of the guidelines in NKB-rapport nr. 35 (1978) and/or JCSS (2006) (Phoon 2005).

7. Updating of Variables and Distributions

7.1. Introduction

Uncertainty due to inherent variability is unavoidable. In some cases it cannot be reduced. For example, the wind loads on a structure cannot be modified by human intervention in a reasonable way (COST 345, 2004). At the design stage uncertainty due to inherent variability may be reduced by ensuring quality control measures (e.g. of concrete strength). This is not helpful however for assessing existing railway infrastructures. When performing a safety evaluation of an existing railway infrastructure there is uncertainty associated with determining material parameters and resistance models as well as loading models. The magnitude of the uncertainty is dependent on the amount of information available on the materials and on the availability of test results, for both resistance and loading. There are methods to reduce the uncertainties associated with the assessment and this chapter discusses these methods.

In Chapter 4 uncertainties were discussed in detail. Statistical uncertainty represents uncertainty resulting from the lack of sufficiently large samples of data to obtain a stable probability distribution function for the data whereas modelling uncertainty is associated with the accuracy of the models employed. These uncertainties can be reduced by adopting more accurate models and updating existing models. In updating an existing model, 'a priori' values for probability distribution function for various random variables can be used together with any site specific data in order to provide 'posterior' distribution functions. Material properties, including damage and deterioration, as well as loads can benefit from updating.

This chapter discusses updating and presents information on how testing and inspection results can be incorporated to update initial estimations or distributions. The chapter looks at updating and presenting methodologies for incorporating the results of testing or monitoring.

7.2. Testing and inspection results

When deriving theoretical models of resistance and loading, the assessor must make assumptions based on the literature and his/her knowledge and experience. Testing and monitoring can be used to validate and, if necessary, update the assumptions. Testing is generally in reference to the behaviour of the railway infrastructure at a particular point in time whereas monitoring refers to continuous observation by means of sensors.

Testing and monitoring are only employed in advanced levels of assessment (see Chapter 2) and the cost associated with them is really only justifiable if a critical element of railway infrastructure fails

at the first levels of assessment. When employed however, they can greatly improve the knowledge of the condition of the railway infrastructures and its evolution over time. They can also provide greatly improved information on the actual loads.

Testing is an expensive process and as such, it must be carefully planned prior to commencement. It is important to remember that the aim of testing is to gather information about the parameters that are relevant for the assessment calculations. It is recommended that the following should be considered in the planning stage (SB-LRA, 2007):

- Type of tests to be carried out
- The number of measurements necessary to obtain reliable results
- The limitations of the testing procedures
- The location for which representative values can be found
- The need of complementary devices to carry out the tests.

Testing can be used to obtain details of the structural geometry and integrity, material properties (mechanical and durability), performance of structural components and the structure itself and the condition of the railway infrastructure (i.e. presence and intensity of defects and deterioration). Testing can also provide information on permanent and variable loads.

The railway infrastructure geometry and integrity can be obtained in the first instance from visual inspection and some simple superficial measurements. This may not always provide sufficient or accurate information and in such cases measurements and other tests, preferably non-destructive, must be performed. There are many guidelines and reports available on Non Destructive Testing (NDT), Minor Destructive Testing (MDT) and Destructive Testing (DT) (SB-ICA, 2007; IAEA, 2002; OFM, 2005; NI, 2003; Scott et al. 2001).

Mechanical material properties can be determined by tests performed on the structure or on specimens taken from the structure. The most reliable way is by performing destructive tests on samples taken from the structure (SB-ICA, 2007). Durability properties can also be determined using both destructive and NDT. Further information can be obtained from SB-ICA (2007) and SB-LRA (2007).

Theoretical models can be used to determine the structural behaviour of structural components or the structure as a whole. If necessary however, they should be calibrated using the laboratory tests. Such tests can be performed on specimens taken from the structure (or similar structure) or specially constructed samples can be used. In a deterministic analysis the theoretical models can be

calibrated or upgraded using 'Annex D – Design assisted by testing' of EN 1990 (2002) and in a probabilistic analysis the methods described in Sections 7.4 and 7.5 can be used.

Load tests can also be performed. The objective of these tests is to apply a controlled load to the structure and monitor the response. There are two types: diagnostic tests and proof tests. Within diagnostic there are static and dynamic tests. Further information can be found in SB-LRA (2007).

In a safety assessment, an accurate knowledge of real loads acting on the railway infrastructure can have a significant influence on the results. Therefore, when necessary, there are many tests available to obtain more loading information. For example, the permanent load can be obtained using the results of the geometrical survey and the expected or measured material densities. Or, the permanent load can be directly obtained by e.g. weighing the bridge deck using hydraulic jacks. The variable loads, such as traffic loading, can be determined using WIM (as mentioned in Section 5.4).

It can be seen that testing is useful for providing information on the actual state of the railway infrastructure. Monitoring, on the other hand, can provide information on how the infrastructure and the loads acting on it are changing. Monitoring not only provides information on time dependent parameters, but it also provides more data and therefore the quantification of the parameters for the models is more reliable (SB-LRA, 2007).

The information that can be collected by monitoring includes:

- Deck deflection and rotation
- Stress levels and changes
- Change of water level
- Vibration characteristics
- Temperature variations
- Wind speed and direction
- Corrosion rates and crack widths
- Water speed and rise of rivers
- Scour at abutments and piers
- Rise and fall of tides
- Bridge traffic loads

Obtaining this information can greatly increase the understanding of condition, performance, evolution of degradation processes and loads acting on the railway infrastructure.

7.3. Updating individual structural properties or whole structure properties

After obtaining supplemental information from tests or monitoring, the results can be used in two ways:

- Update the distribution parameters of a particular variable using observations obtained on that variable (e.g. concrete compressive strength)
- Directly update the structural failure probability of the structure (e.g. test loading).

7.3.1. Individual parameters

For a particular variable (material or load), the distribution parameters such as mean and standard deviation can be estimated and updated. When doing so, the uncertainty in the measurement should be stated and taken into account in the estimation of the distribution parameters. Therefore the estimation of the distribution parameters should be carried out using a method which determines the statistical uncertainty of the parameters (DRD, 2004). This means that the distribution parameters can be estimated on the basis of, e.g. Maximum likelihood or Bayesian statistics. The statistical uncertainty of the distribution should then be taken into account in the subsequent reliability analysis.

Maximum likelihood and Bayesian statistics are well documented in the literature (Raiffa & Schkaifer, 1961; Box & Tiao, 1972; Lindley, 1976). The maximum likelihood method allows the quantification of the uncertainty of the estimated distribution parameters, but the database must be sufficiently large to determine the statistical uncertainty. Bayesian statistics can be used, however, even if the database is small, to determine both the uncertainty of the estimated distribution parameters and the statistical uncertainty.

Bayesian statistics assume '*a priori*' knowledge of the distribution parameters. The distribution parameters can be the mean or the standard deviation or both (or any other parameters that describe the distribution). The distribution descriptors or parameters can come from subjective knowledge based on expert opinion but it is important that all information on the '*a priori*' data must be well documented and care must be taken to avoid inappropriate assumptions or conclusions (i.e. the *a priori* knowledge must be as accurate as is reasonably possible). The Bayesian statistics method is based on the updating of distribution parameters for a particular variable, so therefore the *a priori* knowledge consists of a distribution function for the mean and/or standard deviation of the variable under consideration.

The *a priori* distribution function can then be updated to *a posteriori* distribution function using measurement or evidence data or any supplemental data available. The measurement data is used to create a likelihood function, and, using Bayes Theorem the likelihood function is combined with the *a prior* information to create the *a posteriori* distribution. The expressions are well documented in the literature (e.g. Raiffa and Schlaifer, 1961; JCSS, 2001) and SB-LRA (2007) also gives detailed description of the method. A summary of the method is given here.

The updating of the individual or multivariate probability distribution is achieved using the following equations:

$$P(X|E) = P(X)P(E|X)/P(E) \qquad 7.1$$

Where

P = probability mass (or density)

X = random variable in question

E = the evidence or information available (may also be denoted as *I*)

P(X) = prior probability mass or density function of *x*

P(E|X) = the conditional likelihood function (likelihood of finding information *E* for given value *x* of *X*) – it can also be written as *L(x|E)*

P(E) = normalising factor

Once the updated distribution for the basic variable, *P(X|E),* is obtained, it can be directly included in the reliability analysis to determine the updated safety estimation for the railway infrastructure. Any number of variables can be updated depending on the information available.

7.3.2. Direct updating of the probability of failure

Bayesian statistics can also be used to directly update the reliability of a structure based on a given event or considering a measured property. The event could be a test loading or the observation of a crack in a structure or a geometrical measurement. The deflection of a bridge at midspan, for example, can be determined with certain accuracy. The probability of failure can then be directly updated taking the measurement or event into account:

$$P_f = P(F|I) = \frac{P(F \cap I)}{P(I)} \qquad 7.2$$

Where:

F = local or global structural failure

I = information obtained from investigation or measurements

∩ = intersection of two events

| = conditional upon

This method can also be used to update reliability with indirect information, i.e. information from similar structures. In such situations the updating must be carried out using correlations between the stochastic variables, so that the uncertainties in the information are taken into account (DRD, 2004). More information can be found in JCSS (2001) and in Madsen et al (1986).

8. Consideration of Climate Change

8.1. Introduction

Climate change can impact on the safety of railway infrastructures during the course of their design lives through influencing rates of deterioration and environmental load frequency and intensity. Deterioration significantly alters the long term performance of railway infrastructures. When considering deterioration in an assessment, it should be remembered that the deterioration rate not only depends on material compositions and construction processes, but also relies on the on-going climatic environment during the service life. Climate change may alter this environment. Increases in atmospheric CO_2 concentrations and changes in temperature and humidity, as a result of climate change, can cause acceleration of the deterioration process and in rates of e.g. corrosion-induced cracking and spalling. In addition to increasing rates of deterioration, climate change can impact railway infrastructures through the impacts of extreme weather events and rising sea levels, e.g. increased intensity of precipitation can have a significant effect on slope stability.

8.2. Impacts of climate change

Climate change can be defined as a change in the state of the climate that continues for an extended period, typically decades or centuries (Wang *et al.*, 2010). It is generally considered that climate change is taking place today as a result of anthropogenic (human) activity such as burning fossil fuels and clearing forests and this is resulting in significant increases in greenhouse gases, atmospheric CO_2 in particular. The increase is quantified in the fourth assessment report of the Intergovernmental Panel on Climate Change (IPCC, 2007), which indicates an increase in the concentration of CO_2 in the atmosphere, from 280 parts per million (ppm) in 1750 to 380 ppm in 2005, with an accelerating trend. Comparing with pre-industrial temperatures, the best estimate of the increase in temperature caused by elevated concentrations of greenhouse gases in the atmosphere is 2.1°C for 550 ppm CO_2, 3.0°C for 700 ppm, and 4.4°C for 1000 ppm CO_2 by 2100 (IPCC, 2007).

8.3. Probabilisitic modelling of reinforced concrete corrosion considering climate change

Corrosion induced reinforced concrete deterioration is characterised by three stages: corrosion initiation, corrosion progress, and cracking and spalling Stewart et al. (2011).

8.3.1. Carbonation-induced corrosion

Time to Corrosion Initiation,T_i

Concrete quality, concrete cover, relative humidity, ambient carbon dioxide concentration and others all determine the time to corrosion initiation, T_i, from the perspective of carbonation induced corrosion. The impact of carbonation has been studied by many researchers and various mathematical models have been developed with the purpose of predicting carbonation depths (e.g. Duracrete 1998, Stewart et al 2002). It is observed that corrosion may occur when the distance between the carbonation front and the reinforcement bar surface is less than 1-5 mm (e.g. Yoon et al 2007). However, probabilistic analyses for assessing durability design specifications tend to ignore this effect (Duracrete 2000, fib 2006). Hence, the time to corrosion initiation (T_i) is taken as the time for the carbonation front to equal the concrete cover depth (Stewart et al. 2011):

$$x_c(t) = \sqrt{\frac{2D_{CO_2}(t)}{a} k_{urban} C_{CO_2}(t-1999)} \left(\frac{t_0}{t-1999}\right)^{n_m} \qquad t \geq 2000 \qquad 8.1$$

$$D_{CO_2} = D_1 (t-1999)^{-n_d} \text{ and } a = 0.75 C_e C_a O \alpha_H \frac{M_{CO_2}}{M_{C_aO}} \qquad 8.2$$

where $C_{CO_2}(t)$ is the time-dependent mass concentration of ambient CO_2 (10^{-3}kg/m^3) with $\mu_{CO_2}(t)$ and COV equal to $\sigma_{CO_2}(t)/\mu_{CO_2}(t)$ obtained from projection of CO_2 concentrations from 1990 based on the Model for Assessment of Greenhouse-gas Induced Climate Change, known as MAGICC (Wigley et al. 1996), (using the conversion factor 1 ppm = 0.0019×10^{-3} kg/m^3). k_{urban} is a factor to account for increased CO_2 levels in urban environments; D_{CO_2} is the CO_2 diffusion coefficient in concrete; D_1 is the CO_2 diffusion coefficient after one year; n_d is the age factor for the CO_2 diffusion coefficient; t_0 is one year; C_e is cement content (kg/m^3); C_aO is the C_aO content in cement (0.65); α_H is the degree of hydration; M_{C_aO} is molar mass of C_aO and equal to 56 g/mol and M_{CO_2} is molar mass of CO_2 equal to 44 g/mol. The age factor for microclimatic conditions (n_m) associated with the frequency of wetting and drying cycles is n_m=0 for sheltered outdoor and n_m=0.12 for unsheltered outdoor.

The mean values for D_1 and n_d are presented in Table 8.1. The standard deviation for D_1 is approximately 0.15, and COV for n_d is approximately 0.12 for all w/c ratios. These statistics represent model error. The diffusion coefficient D_1 is less than 5×10^{-4} cm^2s^{-1} which is appropriate for good quality concrete (Sanjuan & del Olmo, 2001). These parameters are based on T=20°C and relative humidity, RH, =65%. The degree of hydration after more than 400 days is estimated as (de Larrard, 1999):

$$\alpha_H \approx 1 - e^{-3.38w/c} \qquad 8.3$$

Table 8.1 Mean Parameter Values (Stewart, 2011)

w/c	$D_1\times10^{-4}cm^2s^{-1}$	n_d
0.45	0.65	0.218
0.50	1.24	0.235
0.55	2.22	0.240

A higher temperature will cause an increase in diffusion coefficient leading to increased carbonation depths (e.g. Baccay et al., 2006). The effect of temperature on diffusion coefficient is modelled using the Arrhenius Law (e.g. Yoon et al 2007), where the time-dependent change in diffusion coefficient when compared to a temperature of 20°C is:

$$f_T(t) \approx e^{\frac{E}{R}\left(\frac{1}{293}-\frac{1}{273+T_{av}(t)}\right)} \quad T_{av} = \frac{\sum_{i=2000}^{t} T(t)}{t-1999} \qquad 8.4$$

where *T(t)* is the temperature (°C) at time *t*, *E* is the activation energy of the diffusion process (40 kJ/mol (Kada-Benameur et al. 2000)) and *R* is the gas constant ($8.314\text{x}10^{-3}$ kJ/mol·K). As temperature increases over time then $D_{CO2}(t)$ is averaged over time and so *T(t)* is also averaged over time. A 2°C temperature increase will therefore increase the diffusion coefficient by 12% (Stewart et al., 2011).

Equation 8.1 was used by Yoon et al (2007) to predict carbonation depths for increases in CO_2 concentrations. However, as this assumes that $CO_2(t)$ is constant for all times up to time *t*, it could lead to an overestimation of the carbonation depth as CO_2 concentration will be gradually increasing with time up to the peak value $CO_2(t)$. Stewart et al (2002) considered this phenomenon and calculated carbonation depths due to enhanced greenhouse CO_2 conditions using the average CO_2 concentration over the time period, and not the peak value at time *t*. As such, Equation 8.1 can be rewritten as (Stewart et al., 2011):

$$x_c(t) = \sqrt{\frac{2 f_T(t) D_{CO_2}(t)}{a} k_{urban} \int_{2000} C_{CO_2}(t) dt \left(\frac{1}{t - 1999} \right)^{n_m}} \qquad t \geq 2000 \qquad 8.5$$

Stewart et al. (2011) stress that equation 8.5 is an approximation and there is a need for an improved carbonation model that considers the time-dependent effect of CO_2 concentration and other parameters such as temperature or humidity.

As mentioned, the parameters given above assume temperature, *T*, is 20°C and relative humidity, *RH(t),* is 65%. It is recognised that carbonation tends to be highest for relative humidities *RH(t)* of 50% to 70% (Russell et al., 2001). Additionally, Al-Khaiat and Fattuhi (2002) report that little or no carbonation occurs below a relative humidity of 30%, whereas Russell et al. (2001) state that below 50% relative humidity there is insufficient moisture for carbonation reactions to take place. Most carbonation models assume relative humidity of greater than 50%. To be conservative, analyses can assume that if *RH(t)* is less than 40% then the carbonation front ceases to advance (i.e. carbonation depth does not increase with time) (Stewart et al., 2011).

Corrosion Propagation

Corrosion rates and models can be reviewed in Raupach (2006) and Peng & Stewart (2008). It should be noted that the carbonation-induced corrosion rate is variable and highly dependent on exposure conditions and atmospheric situations. The corrosion rate for carbonation or chlorides becomes negligible when relative humidity *RH(t)* is less than 50% (e.g. Enevoldsen et al 1994, Neville 1995), and in the probabilistic approach developed by Stewart et al (2011) a negligible corrosion rate is defined as a corrosion current density (i_{corr}) of 0.1 µA/cm^2 where a corrosion rate (i_{corr}) of 1 µA/cm^2 = 0.0116 mm/year. Stewart et al (2011) suggest the corrosion rate can be assumed lognormally distributed with statistical parameters for a temperature of 20°C given by Duracrete (1998). These values take into account the concrete grades suggested for the corresponding exposure classes. An increase in temperature will increase corrosion rate, and the model described by Duracrete (2000) is used:

$$i_{corr}(t) = i_{corr-20}\left[1 + K\left(T(t) - 20\right)\right] \qquad 8.6$$

where $i_{corr-20}$ is the corrosion rate at 20°C (given in Stewart et al., 2011), and K=0.025 if T(t)<20°C and K=0.073 if T(t)>20°C. Duracrete (2000) notes that Equation 8.6 is a close correlation to Arrhenius equation, at least for temperature below 20°C, but may be conservative for T(t)>20°C. A 2°C temperature increase will increase the corrosion rate by 15%.

As there is little data on time-dependent effects on corrosion rate for carbonated RC structures a time-invariant corrosion rate for carbonation can be assumed. This is likely to be a conservative assumption as corrosion rate will generally decrease with time due to the build-up of rust products thus impeding the corrosion process (see for example Vu and Stewart, 2000).

8.3.2. Chloride-induced corrosion

Time to Corrosion Initiation, T_i

The penetration of chlorides is given empirically by Fick's second law of diffusion. However, chloride penetration processes and field conditions differ from that assumed with Fick's law (Val and Stewart, 2009). However, Fick's law is often used to describe chloride penetration into concrete due to its computational convenience; namely, surface chloride concentration (C_o) and diffusion coefficients (D_c) are easily calculated by fitting Fick's law to measured chloride profiles. An improved model utilising a time-dependent chloride diffusion coefficient proposed by Duracrete (2000b) is used to calculate chloride concentration. The time to corrosion initiation (T_i) is assumed to occur when chloride concentration at the level of reinforcement exceeds the critical chloride concentration (C_{cr}). The chloride concentration at depth x (mm) at time t is:

$$C(x,t) = C_0\left[1 - erf\left(\frac{x}{2\sqrt{k_e \cdot k_t \cdot k_c \cdot f_T(t) \cdot D_c\left(\frac{t_0}{t-1999}\right)^n \cdot (t-1999)}}\right)\right] \quad t \geq 2000 \qquad 8.7$$

where D_c is the chloride diffusion coefficient, n is the ageing factor, k_e is the environment factor, k_t is the test method factor (1.0), k_c is the curing factor (1.0), t_o is the reference time in years (28 days or 0.0767 years), and $f_T(t)$ is the temperature effect on diffusion coefficient given by Equation 8.4.

The surface chloride concentration (C_o) is generally assumed as a time-invariant variable as exposure to chlorides for a specific member would not change from year to year. However, climate change may cause changes in wetting/drying cycles, rainfall and wind patterns could vary, etc. but there is no data to support how this might affect C_o. The surface chloride concentration can be categorised into specific exposure categories: submerged zone, splash and tidal zones, and atmospheric zone. The critical chloride concentration is normally distributed with mean and COV of 3.35 kg/m3 and 0.375, respectively, truncated at 0.35 kg/m^3 (Val and Stewart 2003). The critical chloride concentration is not affected by concrete quality (Duracrete, 2000b).

Corrosion Propagation

Corrosion rates are highly variable and dependent on concrete grade, cover and environment. For example, the British Standard BS 6349-1 (2000) suggests that mean corrosion rate for the atmospheric zone is 0.04 mm/yr (3.45 µA/cm2), 0.08 mm/yr (6.9 µA/cm2) for the splash zone, and 0.04 mm/yr (3.45 µA/cm2) for the tidal zone. The corrosion rates recommended by Duracrete (1998) shown are not dissimilar from those reported in BS 6349-1 (2000). These values take into account the concrete grades suggested for the corresponding exposure classes. Since corrosion rate data assumes time-invariant corrosion rate so this guideline will also assume a time-invariant corrosion rate. This is a conservative assumption. The effect of temperature on corrosion rate is modelled using Equation 8.6.

8.4. Probabilisitic modelling of structural steel deterioration considering climate change

The effect of climate change on structural steel deterioration was modelled by Minh N. Nguyena et. al (2013). The calculation was done for the two Australian cities of Melbourne and Brisbane. The effects of pollution and changing CO_2 concentration on deterioration were stated to be secondary and thus, were excluded from the analysis. The projected relative corrosion rate of steel due to temperature change (C_{temp}) was calculated as:

$$C_{temp} = \frac{C_{0,Tprojected}}{C_{0,Tref}} = \exp\left[260 \times \left(\frac{1}{T_{ref}} - \frac{1}{T_{projected}}\right)\right] \qquad 8.8$$

Where T_{ref} is the absolute yearly average temperature at a reference year, $T_{projected}$ is the projected absolute yearly average temperature due to climate change in the future; $C_{0,T\ projected}$ and $C_{0,T\ ref}$ are corrosion rate parameters at T_{ref} and $T_{projected}$, respectively.

Variations in temperature for the period from 2000-2100 may be taken from the Intergovernmental Panel on Climate Change (IPCC) Fourth assessment report: Climate Change 2007 (Figure 9.1). The temperature variations may be considered as normally distributed. Mean values may be taken as the multimodal average for a given SRES scenario. The standard deviation may be taken from the assessed ranges as shown for each SRES scenario in Figure 8.1. Alternatively, a more broad distribution may be modelled using a standard deviation which accounts for a number of SRES scenarios. A steel corrosion model, such as the model used by Komp (1987) can then be modified by the projected relative corrosion rates of steel (Ctemp) due to temperature change. It should be noted that the effects of period of surface wetness and airborne salinity are not considered herein. These effects are not crucial in rural inland areas.

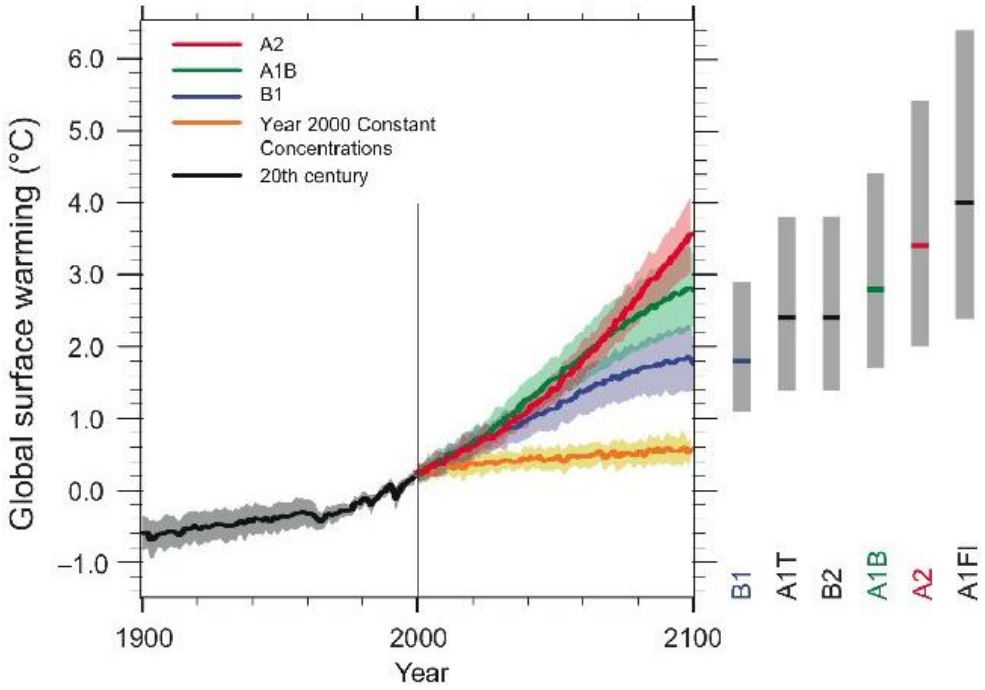

Figure 8.1: Multimodal averages and assessed ranges for surface warming (IPCC, 2007)

8.5. Probabilisitic modelling of embankment stability considering climate change

Introduction

Climate change effects are resulting in rainfall with increased intensity and duration in many regions of the world. These events can lead to shallow translational landslides on natural and man-made slopes, which although often small in volume can have devastating effects on down slope habitats and infrastructure. The effect of climate change can be severe on ageing transport networks, in particular railways, many of which were built in the mid 1800's. On the 12th of April 2010 a landslide initiated by heavy rainfall, caused the derailment of a train at Merano, Italy in which 9 people died and 28 were injured. Similar recent incidents occurred in Guilin, China, on the 23rd of May 2010 where a landslide on the track caused a crash which resulted in 19 fatalities and near Wellington, New Zealand, on 30th September 2010, a landslide caused a passenger train to derail and hit an oncoming service.

During the first decade of the 21st century, the ECTP Implementation Action Plan (ECTP, 2007) estimated the cost of natural and man-made hazards at €7.35 billion/year (excluding the cost of fatalities). The effect of increased rainfall due to climate change, increased populations, Eastward expansion of the EU and ageing infrastructure will result in an increase in natural hazards over the next 50 years in the European Economic Area (EEA 2013). In many countries the transport infrastructure was built before the introduction of modern design standards. Owners and managers

of soil structures such as embankments, cuttings and dams need to be able to quantify the safety of these structures and assess their resilience to climate change.

Stability analysis of unsaturated soil slopes

In embankments and cuttings formed along transport networks the water table is usually at some depth. As a result the soil between ground level and the water table (below which the soil is saturated) exists in a partially saturated state with the voids being filled by air and water. The presence of air and water allows suctions to develop which increase the soil strength and provide stability, allowing slopes to stand at angles much higher than their natural friction angle. During rainfall, infiltrating water reduces suction and can trigger failure over some critical depth in the slope, known as the wetting front.

Soil must be described as a three phase material due to the effect of partial saturation. Fredlund et al. (1978) expanded the Mohr-Coulomb soil model to incorporate negative porewater pressure (matric suction) effects:

$$\tau = c' + (\sigma_n - u_a)\tan\phi' + (u_a - u_w)\tan\phi^b \qquad 8.9$$

where τ=shear strength of unsaturated soils, c' is the effective cohesion', σ_n is the total normal strength on the failure plane, u_a is the pore-air pressure on the failure plane, ϕ' is the angle of internal friction associated with the net normal stress state variable σ_n-u_a, u_w is the pore-water pressure on the failure plane, u_a-u_w is the matric suction on the failure plane, and ϕ^b is the angle indicating the rate of increase in shear strength relative to the matric suction.

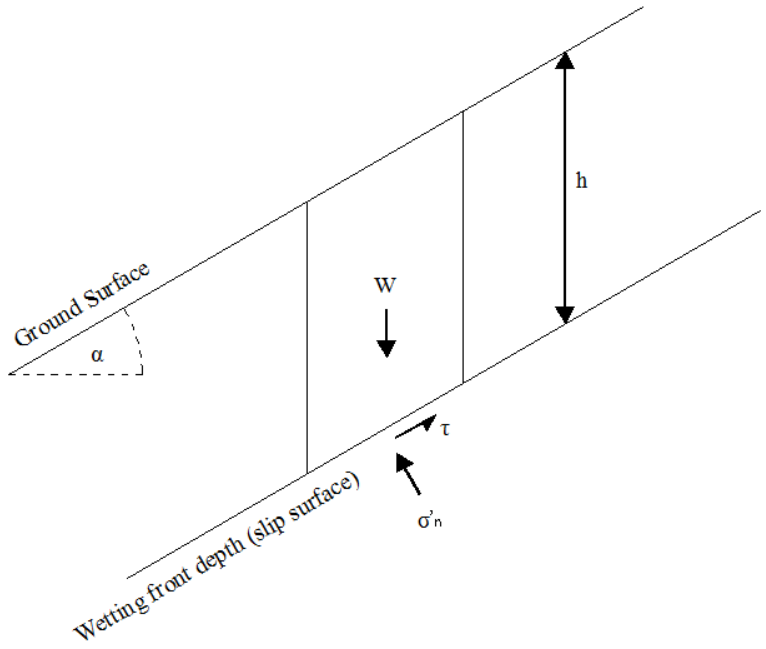

Figure 8.2: Infinite slip surface model.

Fourie et al. (1999) and Cho and Lee (2002) note that in most slope failures caused by infiltration, the failure plane forms parallel to the existing slope surface, see Figure 8.2. The authors suggest using an infinite slope model in which the soil strength is described by an expression of the form given in Equation (8.9). The Factor of Safety (F) is given in Equation (8.10).

$$F = \frac{c' + (u_a - u_w)\tan\phi^b + \gamma h \cos^2\alpha \tan\phi}{\gamma h \cos\alpha \sin\alpha} \qquad 8.10$$

where α is the slope angle, γ is the unit weight of soil and h is the wetting front depth.

By combining the effects of c' and the contribution of matric suction $(u_a\text{-}u_w)\tan\phi^b$ into a single parameter, apparent cohesion (C), Equation (8.9), takes the form of the conventional Mohr-Coulomb model, and can be implemented into slope stability software developed to analyse saturated soil slopes, see Equation (8.11):

$$F = \frac{C + \gamma h \cos^2\alpha \tan\phi}{\gamma h \cos\alpha \sin\alpha} \qquad 8.11$$

The value of C can be obtained from laboratory testing or by direct in-situ tests (Springman et al., 2003). At the point of failure, F = 1, and therefore the critical wetting front depth (h_c) is given by Equation (8.12)

$$h_c = \frac{C}{\gamma \cos\alpha (\sin\alpha - \cos\alpha \tan\phi)} \qquad 8.12$$

Understanding the critical wetting front depth is crucial in determining whether a particular rainfall event provides sufficient rainfall to initiate failure and is therefore fundamental in determining the safety of a slope.

The variables in Equation 8.12 include C, h, ϕ' and γ. The total cohesion (C) depends on the matric suction and ϕ^b, the wetting front depth increases throughout the infiltration event, the friction angle of the soil varies because of natural variability in soil properties, and the unit weight of the soil increases as the water content increases during the rainfall event.

Although as noted by Hassan and Wolff (1999) these parameters are most likely, log normally distributed, Whitman (1984) notes that the reliability index is not very sensitive to the distribution of the parameters provided that β<2.5 and the standard deviation of the parameters is not very large.

Reliability Model for Unsaturated Soil Slopes

At the limit state (FOS=1), the limit state function Equation 8.11, can be written as:

$$g(X) = C + \gamma h \cos^2\alpha \tan\varphi - \gamma h \cos\alpha \sin\alpha \qquad 8.13$$

and the probability of failure (P_f) is given as:

$$P_f = P(g(X) \le 0) = \int_{C+\gamma h \cos^2\alpha \tan\varphi - \gamma h \cos\alpha \sin\alpha \le 0} f(X)dX \qquad 8.14$$

in which *f(X)* is the probability density function (range of likely values) of the random variables, (*C, φ, γ, h)*. P_f can be obtained by integrating Equation 8.14. However, this is rarely practicable, partly due to the highly nonlinear form of the limit state function and to difficulties accessing the probability density distribution functions of the random variables. The reliability index, which allows comparative reliability to be assessed for a system, where the probability distributions are unknown, is often employed to solve these problems.

Hasofer and Lind (1974), propose an invariant approach to calculate the reliability index in which the random variables are transformed into non-dimensional form:

$$\overline{X_i} = \frac{X_i - E[X_i]}{\sigma[X_i]} \qquad (i=1,2,.....,n) \qquad 8.15$$

where $E[X_i]$ and $\sigma[X_i]$ are the mean value and standard deviation of the variable X_i. The limit state function can be written in terms of the reduced variables:

$$g(\overline{X}) = g(\overline{x}_1, \overline{x}_2, \overline{x}_3, \cdots, \overline{x}_n) \qquad 8.16$$

The reliability index (β_{HL}) is the minimum distance from the origin of the reduced variable space ($\overline{X}$) to the limit state surface (g($\overline{X}$) = 0), see Figure 8.3. The determination of this *minimum* distance (distance from the origin to the design point) is normally carried out by performing a cosine directional search along the limit state surface (Hassan and Wolff 1999, Bhattacharya et al. 2003). Val et al. (1996) note a tendency for the identification local minima when using the cosine directional search method on highly non-linear functions, and state that the method is unlikely to find the true minimum reliability index. They suggest transforming the rectangular co-ordinates to polar co-ordinates to avoid this problem. Although the minimisation problem could be solved equally well using a full population technique (such as the Monte-Carlo method), the polar coordinate conversion was adopted by Xue and Gavin (2007), and offers the critical advantage of simplifying the formulation of the objective function in the minimisation problem which must be solved to find the true reliability index of a slope.

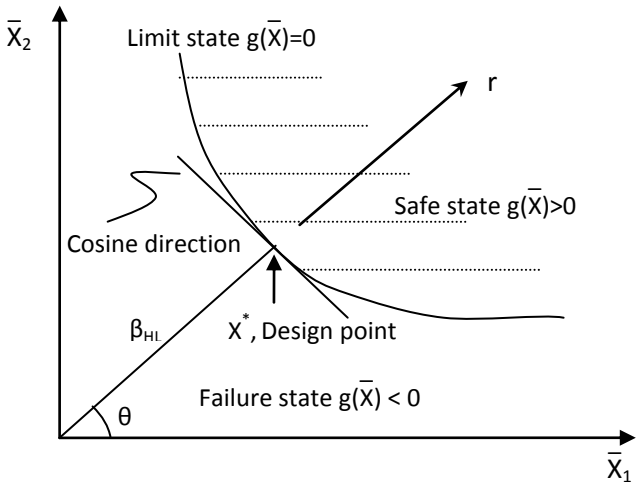

Figure 8.3: Definition of reliability Index in Polar Coordinates

Xue and Gavin (2007) and Gavin and Xue (2009) solved this constrained nonlinear programming problem using the Genetic Algorithm (GA) method, in a reliability based slope stability model known as GASSA. The model considers only variables which affect the slope resistance. In the SMARTRAIL project the model is being developed to include correlated variables (Reale et al 2014) which will be particularly important if the model is to consider both the load and resistance components, as variables such as the precipitation rate will affect both the load and resistance (i.e. the wetting front depth). For a simplified approach a range of wetting front depths will be calculated using simple empirical models (Gavin and Xue 2008) or finite element analyses (Ng and Shi 1998), and the likely values of wetting front depth and the uncertainty associated with the assessment of these can be included in the reliability analysis. An application of the model to analyse the effect of wetting front development to the stability of a 150 year old railway slope is described in Appendix B. The slope was used to monitor the in-situ suction over a 5 month period of normal rainfall and the effect of extreme rainfall on slope stability in the SMARTRAIL project.

9. Simplified Approach

9.1. Introduction

A comprehensive reliability framework is suitable for sophisticated users and for the management of network infrastructure at a regional or national level. Engineers at a local level may prefer a simpler approach for everyday use such as a Load and Resistance Factor Design (LRFD). LRFD is used for design by structural engineers – whereby the factored effect of load is compared to the factored resistance to determine if the structure is safe. This chapter shows the development of simpler approaches to infrastructure assessment which are benchmarked against the comprehensive safety framework described in the preceding chapters.

9.2. Motivation for optimisation of partial safety factors

Partial safety factors, subsequently referred to as γ-factors, within modern codes are derived to ensure that the desired reliability is achieved for a lot of different types of structures and load situations. An example of this approach for Danish codes is described in Sørensen et al (2001). For a limited set of structures with similar characteristics (e.g. a set of single span steel bridges) it can be reasonable to optimise the γ-factors through recalibration, for example for some of the following reasons:

- For a specific set of structures the γ-factors can be calibrated more accurately than for a large set of different structures.
- It can be justified to use a lower target reliability β_T for aged structures due to economic, social and sustainability considerations.
- Load- and resistance can have changed since the design phase of the structures. For example, the loads on a railway line can be higher than during the design phase, or the whole set of structures show comparable degeneration due to corrosion in a maritime environment.

The outcome of the calibration should usually be a simplified tool, e.g. a diagram, where the practical engineer can select the proper γ-factors for the given optimisation objective and conduct an assessment based on the principles of LRFD without the need for full probabilistic calculations of the individual structures. To achieve this, the calibration procedure has to be carried out a number of times for different optimisation objectives. The objective of the optimisation can be chosen as a function of different factors, depending on the individual set of structures. For example, some

reasonable optimisation objectives for a set of comparable steel bridges can be the recalibration of the γ-factors as a function of:

- the target reliability level β_T
- the rate of corrosion
- dimensions of the bridge

The optimisation objective has to be chosen carefully by experienced engineers. Also an estimation of the possible advantage of the recalibration over full probabilistic assessment of single bridges has to be considered.

9.3. Calibration procedure

The calibration procedure (see Madsen et al. (1986), Gayton et al. (2004), Moser et al. (2011) or the proceedings of the JCSS Workshop (2002)) for a given optimisation objective generally contains the following steps:

1. Scope of calibration
2. Target reliability level β_T
3. Design situations and input parameters
4. Optimisation of γ-factors
5. Verification of γ-factors

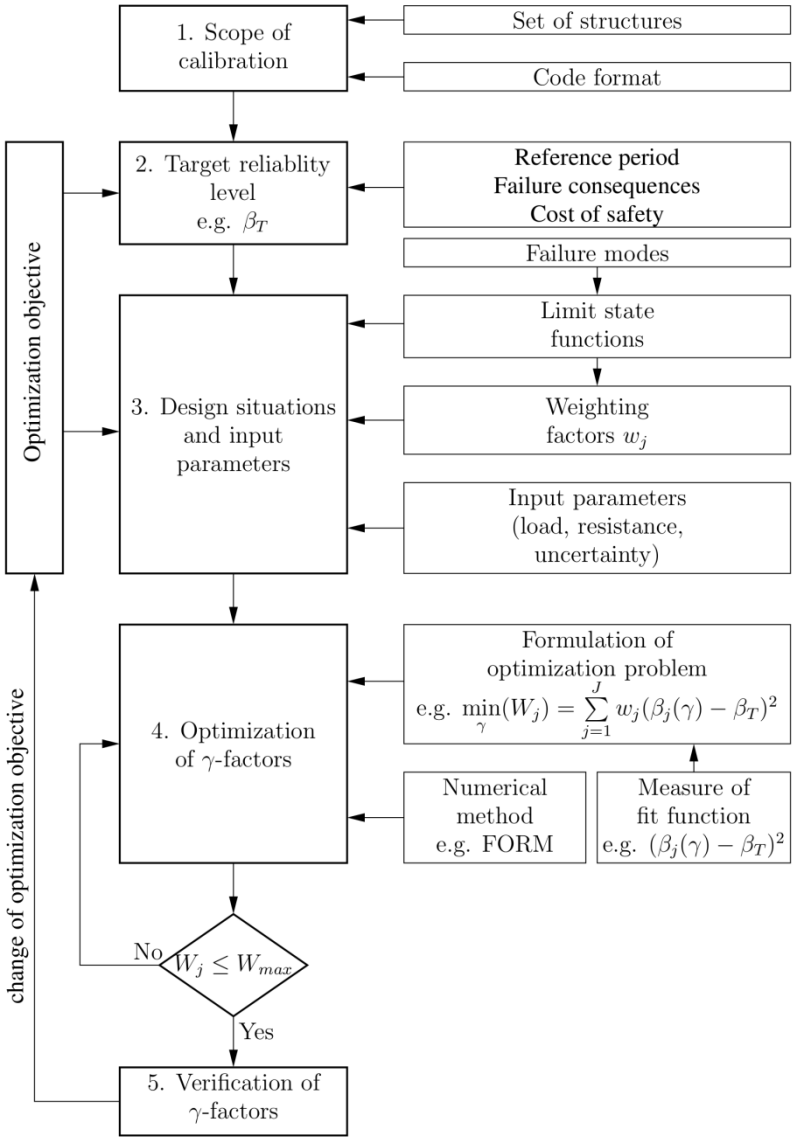

Figure 9.1 Flow-chart for the calibration procedure

After each calibration the optimisation objective is changed for the next calibration process as described before. The main parts of the calibration procedure are shown in Figure 9.1 and are subsequently described below.

9.3.1. Scope of calibration

In this step the specific domain of structures for which the γ-factors will be calibrated is specified. For example, a set of same-age bridges of similar construction type on a railway line that show comparable grades of deterioration.

Also the code format and the limit state that will be used for the design situations have to be specified. This will set the γ-factors as well as the load combination factors (ψ-factors). It is

recommended to use the current building code valid at the time of the optimisation process. Limits for the γ factors can be set when assumed necessary (e.g. γ≥1).

It is important to remember that the outcome of the optimisation process is only valid for structures specified in this step.

9.3.2. Target reliability level

This step defines the target reliability level of the calibration procedure. Usually the target reliability factor β_T or the target failure probability $p_{f,T}=\phi(-\beta_T)$ (valid for normally distributed limit state functions) is specified. This is a difficult task which requires an experienced engineer. The target reliability for an aged structure can be set at a different value to that of the design process depending on failure consequences, cost of safety measures and reference period. For more information, see chapter 3.5 of this report.

9.3.3. Design situations and input parameters

In this step the J design situations (main failure modes) for the given set of structures and limit states are identified. Formulation of the corresponding J limit state functions g_j and design equations G_j, see Eq. 9.1 and 9.2, are carried out within this step.

$$g_j(X, p_j, z)=0,\ j=1,\ldots,J \qquad 9.1$$

$$G_j(x_c, p_j, z, \gamma)=0,\ j=1,\ldots,J \qquad 9.2$$

With **X** presenting the stochastic variables, $\mathbf{p}_j$ the vector of deterministic parameters, **z** the design variables and $\mathbf{x}_c$ the characteristic values.

The design variables **z** in Eq. 9.1 can be expressed dependent on the γ-factors with the use of the deterministic design equations G_j according to the code format.

Each of the design situations can be weighted with a weighting factor w_j according to their relative frequency and importance.

$$\sum_{j=1}^{J} w_j = 1;\ w_j > 0 \qquad 9.3$$

When using the finite element method (FEM) for the calibration procedure there are no analytical or empirical limit state functions and design equations available. This problem can be treated for example, by approximation of the failure surface with the response surface method (RSM), as

introduced by Box & Wilson (1954) or described in Khuri & Cornell (1987). First order RSM requires an iterative linesearch procedure to find the most probable point of failure, while second order RSM gives a better estimation of the failure surface. But finding the most probable point of failure can still require an iterative process, especially for highly nonlinear limit state functions and to reach an adequate accuracy for small failure probabilities.

The distributions of the uncertain input parameters **X** for load and resistance variables and model uncertainties are determined in this step. For the determination of the uncertain parameters, refer to chapters 4, 5 and 6 of this report.

9.3.4. Optimisation of γ-factors

The γ-factors are calibrated to get as close as possible to the calibration objective (e.g. β_T) for each of the J design situations. Therefore a measure of fit to the calibration objective is needed. A very simple measure of fit function is to use the least square function of the calculation results to the calibration objective during the iterative optimisation process (e.g. $(\beta_j(\gamma) - \beta_T)^2$).

With this simple approach and taking the weighting factor w_j into account, the optimisation problem can be formulated (for calibration on β_T) as shown in Eq. 9.4:

$$\min_{\gamma}(W_j) = \sum_{j=1}^{J} w_j(\beta_j(\gamma) - \beta_T)^2 \qquad 9.4$$

In a similar way this problem can be formulated for other calibration objectives (e.g. $p_{f,T}$) and measure of fit functions. The formulation of the optimisation problem with the square deviation as a measure of fit is easy to implement and gives good results. On the downside it is weighted symmetrically around the given calibration objective and needs numerous calculations to obtain satisfying results. Different approaches for the measure of fit function are discussed and compared in literature, for example in Gayton et al. (2004).

The iterative optimisation process will be stopped when the weighted measure of fit W_j is smaller than a given threshold value W_{max}.

The numerical method used during the calibration process has to be carefully chosen with respect to the chosen design situations, aspired precision of the results and calculation time. Crude Monte Carlo simulation should be avoided as it needs a high number of calculations to achieve the desired precision. Advanced methods like Latin Hypercube Sampling, first and second order reliability method (FORM & SORM) or RSM should be used to obtain reasonable calculation times.

The outcomes of this step are the calibrated γ-factors for the given set of structures, design situations and optimisation objective. It has to be noted that in most cases, there will be interdependencies between the resulting γ-factors.

9.3.5. Verification of γ-factors

It is highly recommended to check the design equations with the calibrated γ-factors with reasonable values for the input parameters to verify that the results of the calibration process are reasonable.

10. Conclusions

This document provides a framework for the safety assessment of rail transport infrastructure. The safety and serviceability of railway infrastructure may need to be evaluated for a variety of reasons, which may include:

- changes of use or increase of loads,
- effects of deterioration (e.g. corrosion, fatigue, climate change),
- an extension of the service life,
- damage as a result of extreme loading events or accidental actions,
- concern about design/construction errors or the quality of building materials/workmanship.

The level of detail associated with an assessment can range from whole-line assessment, to bridge assessment, to individual element assessment, depending on the reasons for performing the assessment. In general, assessments start with a simple non-formal approach which is typically conservative. If the evaluated load carrying capacity is not sufficient, the assessment will then progress to more complex measurement based and model based assessments.

Probability based assessment guidelines have been discussed in this framework. Approaches for assessing the ultimate, serviceability, durability and fatigue limit states have been detailed and the required levels of reliability discussed. Physical uncertainty, statistical uncertainty and model uncertainty are considered. The modelling of uncertainty can have a significant impact on the results of reliability analysis. Appropriate statistical distributions and coefficients of variation for each type of uncertainty were discussed.

Load modelling, which is another crucial aspect of probability based assessment, has also been discussed. Guidelines are provided for the modelling of permanent gravity loads (e.g. self-weight of structures, tracks and ballast), vertical train loads and various other types of live loading (nosing, braking & traction etc.). The modelling of resistance variables, which are equally as important as load variables, was investigated. A detailed summary is provided for probabilistic modelling of the strength parameters of reinforced/prestressed concrete, structural steel, masonry and soil.

The effect of climate change on the safety of railway infrastructure has also been addressed. Methods are given for calculating the effect of climate change on carbonation and chloride induced corrosion in reinforced concrete as well as well as corrosion rates in structural steel. The effect of increased intensity and duration of rainfall events on the stability on soil embankment is also investigated and probabilistic methods for analysing the stability of soil slopes are given.

In addition, a simplified approach to reliability based assessment has been described. This is applicable to engineers at a local level who may prefer to avoid the more sophisticated analysis techniques. The approach involves the optimisation of partial safety factors based on different factors depending on the individual set of structures. The approach also allows each failure mode to be weighted according to its relative frequency and importance.

References

Al-Homoud, A. S. and Tanash, N. (2004), Modelling uncertainty in stability analysis for design of embankment dams on difficult foundations, Engineering Geology, 71 (3-4), pp. 323-342.

Al-Khaiat, H. & Fattuhi, N. (2002), Carbonation of Concrete Exposed to Hot and Arid Climate, Journal of Materials in Civil Engineering, 14(2): 97-107.

Babu, G.L, Murthy D.S (2005), Reliability Analysis of Unsaturated Soil Slopes, Journal of Geotechnical and Geoenvironmental Engineering, 131(11).

Baccay, M.A., Otsuki, N., Nishida, T. and Maruyama, S. (2006), Influence of Cement Type and Temperature on the Rate of Corrosion of Steel in Concrete Exposed to Carbonation, Corrosion, 62(9): 811-821.

Balaguru, P., (1995). Comparison of Normal and Lognormal Frequency Distributions for Representing Variations of Concrete Compressive Strength, ACI Material Journal, Vol. 92, No. 5, March-April

Baecher, G.B., Christian J.T. (2003). Reliability and Statistics in Geotechnical Engineering, Wiley, Chichester, England.

Bhattacharya, G., D. Jana, et al. (2003). Direct search for minimum reliability index of earth slopes. Computers and Geotechnics 30: 445-462.

Box, G.E.P. & Tiao, G.C., (1972), Bayesian Inference in Statistical Analysis, Assison-Wesley, Reading, MA, USA.

Box, G.E.P., Wilson, K.B., (1954), The exploitation of response surfaces: some general considerations and examples. Biometrics 1954, pp 10:16-60

BRIME, (2001), Bridge management in Europe. Final Report D14, 4th Framework Programme, Brussels. Available from: http://www.trl.co.uk/brime

Calgaro, J.A., Tschumi, M. and Gulvanessian, H. (2010), Designer's guide to Eurocode 1: Actions on bridges. Thomas Telford Limited.

CEB-FIP, (1990), Model Code, Bulletin d'information No. 203, Final draft, Lausanne.

CHLORtest (2003-2005), EU Funded Research Project under 5FP GROWTH Programme, Resistance of concrete to chloride ingress – From laboratory tests to in-field performance. Available from:

http://www20.vv.se/fud-esultat/Publikationer_000201_000300/Publikation_000256/ChlorTest%20-%20Slutrapport.pdf [Accessed 23 May 2013].

Choi, S-K., Grandhi, V., Canfield, R.A. (2007), Reliability-Based Structural Design. London: Springer.

Cho, S.E., (2007), Effects of spatial variability of soil properties on slope stability, Engineering Geology 92 (2007) 97–109

Coles, S., (2001). An introduction to statistical modelling of extreme values. Springer-Verlag, ISBN 1-85233-459-2.

COST 323, (1999), European Specification on Weigh-in-Motion of Road Vehicles, EUCO-COST/323/8/99, LCPC, Paris, August, 66pp, 1999

COST345, (2004), Procedures required for the assessment of highway structures, Numerical techniques for safety and serviceability assessment, Report of the Working Groups 4 and 6. Cooperation in the Field of Scientific and Technical Research, Brussels. Available from: http://cost345.zag.si

Crespo-Minguillón, C. and Casas, J.R. (1998). Fatigue Reliabilty Analysis of Prestressed Concrete Bridges, Journal of Structural Engineering, 124(12): 1458-1466.

Casas, J.R. and Crespo-Minguillón, C. (1998). A Comprehensive Traffic Load Model for Bridge Safety Checking, Structural Safety, 19(4): 339-359.

Cho, S. E. and S. R. Lee (2002). Evaluation of surficial stability for homogeneous slopes considering rainfall characteristics. Journal of Geotechnical and Geoenvironmental Engineering. ASCE 128(9): 756-763

de Larrard, F. (1999), Concrete Mixtures Proportioning: a Scientific Approach, E&FN Spon, London.

Ditlevsen, O. & Madsen, H.O. (1989), Proposal for a code for the direct use of reliability in structural design, Joint Committee on Structural Safety. IABSE-AIPC-IUBH, ETH-Honggerberg, Zurich.

DRD, (2004), Report 291, Reliability-Based Classification of the Load Carrying Capacity of Existing Bridges, Road Directorate, Ministry of Transport, Denmark, 2004.

DURATINET (2009-2011), INTERREG Project, Development of a Network of Durable Transport Infrastructure in the Atlantic Area, http://www.duratinet.org/

DuraCrete, (1998), Modelling of Degradation, DuraCrete - Probabilistic Performance based Durability Design of Concrete Structures, EU - Brite EuRam III, Contract BRPR-CT95-0132, Project BE95-1347/R4-5, December 1998, 174 p.

DuraCrete, (2000), Probabilistic Calculations, DuraCrete - Probabilistic Performance based Durability Design of Concrete Structures, EU - Brite EuRam III, Contract BRPR-CT95-0132, Project BE95-1347/R12-13, May 2000, 41 p.

DuraCrete, (2000b), Statistical Quantification of the Variables in the Limit State Functions, DuraCrete - Probabilistic Performance based Durability Design of Concrete Structures, EU - Brite EuRam III, Contract BRPR-CT95-0132, Project BE95-1347/R9, January 2000, 130 p.

EEA. (2013). Annual report 2012 and Environmental statement 2013.

ECTP. (2007). Strategic Research Agenda for the European Construction Sector Implementation Action Plan.

Embrechts, P., Kluppelberg, C., Mikosch, T., (1999). Modelling extremal events for insurance and influence. Springer-Verlag, ISBN 3-40-60931-8.

EN 1990,(2002), Eurocode – Basis of Structural Design. European Standard, CEN, Brussels, 2002.

EN 1991-2, (2003), Eurocode 1: Actions on structures – Part 2: Traffic loads on bridges, European Standard, CEN, Brussels, 2003.

EN 1991-1-4, (2005), Eurocode 1: Actions on structures – Part 1-4: General actions – wind actions, European Standard, CEN, Brussels, 2005.

EN 1991-1-5 (2003), Eurocode 1; Actions on Structures – Part 1-5: General actions – Thermal actions, CEN, Brussels

EN 1993-2 (2010), Eurocode 3; Design of steel structures – Part 2: Steel Bridges, European Standard, CEN, Brussels

EN 1993-9 (2005) Eurocode 3; Design of steel structures – Part 1-9: Fatigue, European Standard, CEN, Brussels

Enevoldsen, J.N., Hansson, C.M. and Hope, B.B. (1994), The Influence of Internal Relative Humidity on the Rate of Corrosion of Steel Embedded in Concrete and Mortar, Cement and Concrete Research, 24(7): 1372-1382.

Fib, (2006), Model Code for Service Life Design, fib, Bulletin 34, February 2006, Lausanne

Fib, (2010), Bulletin 65: Model Code, Final draft – Volume 1, 2012

Forrest, W. S. and Orr, T. L. L. (2011), The effect of model uncertainty on the reliability of spread foundations, Third International Symposium on Geotechnical Safety and Risk (ISGSR2011), Munich, Germany, June.

Fourie, A. B., Rowe, D., Blight, G. E. (1999),The effect of infiltration on the stability of the slopes of a dry ash dump, Geotechnique, 49(1):1-13

Fredlund, D.G., Morgenstern, N. R., Widger, R. A. (1978),The shear strength of unsaturated soils, Canadian Geotechnical Journal, 15(3): 313-321

Fredlund, D.G., Rahardjo, H, (1993), Soil Mechanics for Unsaturated Soils, Wiley, USA.

Gan J. K. M., Fredlund, D.G. and Rahardjo, H. (1988), Determination of the shear strength parameters of an unsaturated soil using the direct shear test, Can. Geotech. J. 25, 500-510

Gavin, K.G. and Xue, J.F. (2008) A simple method to analyse infiltration into unsaturated slopes, Computers and Geotechnics, Volume 35, Issue 2, March, pp 223-230.

Gavin, K.G. and Xue, J.F. (2009) Use of a genetic algorithm to perform reliability analysis of unsaturated soil slopes, Vol. 59, No. 6, pp 545-549. DOI 10.1680/geot.8.T.004

Gayton N., Mohamed A., Sorensen J.D., Pendola M., Lemaire M., (2004), Calibration methods for reliability-based design codes. Structural Safety 26, 2004, pp 91-121

Hassan, A. M., and Wolff, T. F. (1999). Search algorithm for minimum reliability index of earth slopes. Journal of Geotechnical and Geoenvironmental Engineering. ASCE, 125(4), 301-308.

Hasofer, A. M. and Lind, N. C. (1974). Exact and invariant Second-Moment code format. Journal of the Engineering Mechanics Division, ASCE, 100, 111-121.

IPCC, (2007), Climate Change 2007 – the Fourth Assessment Report. Intergovernmental Panel on Climate Change. Cambridge University Press, United Kingdom.

ISO/CD 13822, (1999), Basis for Design of Structures - Assessment of Existing Structures.

ISO 2394, (1998), General Principles on Reliability for Structures.

JCSS, (2000), Joint Committee of Structural Safety, Probabilistic Model Code I – Basis of Design.

JCSS (2000), Joint Committee of Structural Safety, Probabilistic Model Code III – Resistance Models.

JCSS, (2006), Probabilisitic Model Code, Section 3.7: Soil Properties, Updated version.

Jennings, P and Muldoon, P. (2003), "Assessment of Stability of Man-made Slopes in Glacial Till: Case Study of Railway Slopes, Southwest Ireland", Proceeding of the 13th European Conference on Soil Mechanics and Foundation Engineering, Prague August (2003)

Kada-Benameur, H., Wirquin, E. and Duthoit, B., (2000), Determination of Apparent Activation Energy of Concrete by Isothermal Calorimetry, Cement and Concrete Research, 30: 301-305.

Khuri, A.I., Cornell, J.A., (1987), Response Surfaces: Designs and Analyses, Wiley

Komp ME. (1987), Atmospheric corrosion rating of weathering steels. Calculations and significance. Mater Performance 1987; 26(7).

Kraft D. (1988), A software package for sequential quadratic programming. Tech. Rep. DFVLR-FB 88-28, DLR German Aerospace Center – Institute for Flight Mechanics, Koln, Germany.

Kołakowski, P., Szelazek, J., Sekuła, K., Swiercz, A., Mizerski, K., Gutkiewicz, P., (2011) Structural health monitoring of a railway truss bridge using vibration-based and ultrasonic methods, Smart Materials and Structures, 20 (3).

Lindley, D.V., (1976),'Introduction to Probability and Statistics from a Bayesian Viewpoin', Vols. 1 and 2, Cambridge University Press, Cambridge.

Madsen, H.O., Krenk, S. and Lind, N.C., (1986), Methods of Structural Safety, Prentice-Hall.

MEDACHS (2005-2008), INTERREG IIIb Project No. 197, Marine environment damage to Atlantic coast historical and transport structures and buildings: methods of assessment and repair, maintenance.

Mehta, P.K. and Monteiro, P.J.M., (2006), Concrete – Microstructure, Properties, and Materials. McGraw-Hill, New York.

Melchers, R.E., (1999), Structural Reliability; Analysis and Prediction, John Wiley & Sons, 1999.

Minh N. Nguyen, Xiaoming Wang, Robert H. Leicester (2013), An Assessment of Climate Change Effects on Atmospheric Corrosion Rates of Steel Structures, Corrosion Engineering, Science and Technology, DOI: 10.1179/1743278213Y.0000000087, available online March 13, 2013, Maney Publishing.

Mirza, S.A., Hatzinikolas, M. & MacGregor, J.G., (1979). Statistical descriptions of strength of concrete, Jounral of Structural Division, Vol. 105, No. ST6, June, pp. 1021-1037.

Moser, T., Strauss, A., Bergmeister, K. ,(2011), Teilsicherheitsbeiwerte für bestehende Stahlbetonbauwerke – Nachweis der Schubtragfähigkeit. Beton- und Stahlbetonbau, 2011, pp 814-826

Neville, A. M. (2008). Properties of Concrete, 4th Edition. Pearson Education Limited, England.

Ng, C. W. W. and Shi, Q. (1998). A numerical investigation of the stability of unsaturated soil slopes subjected to transient seepage. Computer and Geotechnics, 22, 1-28.

NKB, (1978), Report No. 36, Guidelines for Loading and Safety regulations for Structural Design, Nordic Committee for Building.

Nocedal J., Wright S.U. (2006), Numerical Optimization. Springer New York.

O'Connor, A. and Enevoldsen, I. (2008), Probability based modelling and assessment of an existing post-tensioned concrete slab bridge, Engineering Structures, 30 (5), pp. 1408-1416.

O'Connor A., Pedersen C., Gustavsson L, Enevoldsen I., (2009), Probability based assessment and optimised maintenance planning for a large riveted truss railway bridge, Structural Engineering International. 19(4), 375 - 383.

Peng, J. and Stewart, M.G. (2008), Carbonation-Induced Corrosion Damage and Structural Safety for Concrete Under Enhanced Greenhouse Conditions, Research Report No. 270.11.2008, Centre for Infrastructure Performance and Reliability, The University of Newcastle, NSW, Australia.

PIARC, (2000), Reliability-Based Assessment of Highway Bridges. World Road Association, PIARC, Paris.

PIARC, (2000), Reliability-Based Assessment of Highway Bridges, World Road Association PIARC Report of Committee C11-Road Bridges.

Phoon, K. K. (2005), Reliability-based design incorporating model uncertainties, 3rd International Conference on Geotechnical Engineering combined with 9th Yearly Meeting of the Indonesian Society for Geotechnical Engineering, Samarang, Indonesia, August.

Proceedings of the JCSS Workshop on Reliability Based Code Calibration, Zürich, 2002. Available from: http://www.jcss.byg.dtu.dk

Rahardjo, H., Ong, T.H.,Rezaur, R.B., Leong, E.C. (2007), Factors controlling instability of homogeneous soil slopes under rainfall, Journal of Geotechnical and Geoenvironmental Engineering, 133(12): 1532-1543.

Rahmstorf, S., Cazenave, A., Church, J. A., Hansen, J. E., Keeling, R. F., Parker, D. E. and Somerville R. C. J., (2007), Recent Climate Observation Compared to Projections. Science, Vol 316, p.709.

Raiffa, H. & Schkaifer, R., (1961), Applied Statistical Decision Theory, Havard University Press, Cambridge, Mass.

Raupach, M., (2006), Models for the Propagation Phase of Reinforcement Corrosion - an Overview, Materials and Corrosion, 57(8): 605-613.

Reale, C. Xue, J.F, Gavin, K.G. (2014) Reliability analysis of slopes considering correlated variables, In preparation.

Ridley, A., McGinnity, B., Vaughan, P., (2004), Role of pore water pressures in embankment stability, Proceedings of the Institution of Civil Engineers-Geotechnical engineering, 157(4): 193-198.

Russell, D., Basheer, P.A.M., Rankin, G.I.B. and Long, E.A., (2001), Effect of Relative Humidity and Air Permeability on Prediction of the Rate of carbonation of Concrete, Proceedings of the Institution of Civil Engineers, 146(3): 319-326.

SAMARIS, (2005), State of the art report on assessment of structures in selected EEA and CE countries, Deliverable D19. Sustainable and Advanced Material for Road Infrastructure – 5th Framework Programme, Brussels. Available from: http://samaris.zag.si

SAMARIS, (2006), Guidance for the Optimal Assessment of Highway Structures, Deliverable D30. Sustainable and Advanced Material for Road Infrastructure – 5th Framework Programme, Brussels. Available from: http://samaris.zag.si

SAMCO, (2006), Final Report – F08a Guideline for the Assessment of Existing Structures, Structural Assessment Monitoring and Control, 2006. Available from: http://www.samco.org/

Sanjuan, M.A. & del Olmo, C., (2001), Carbonation Resistance of One Industrial Mortar Used as a Concrete Coating, Building and Environment, 36(8): 949-953.

SB-LRA, (2007), Guideline for Load and Resistance Assessment of Existing European Railway Bridges-Advices on the use of Advanced Methods, Deliverable D4.2, Sustainable Bridges - Assessment for

Future Traffic Demands and Longer Lives, 6th Framework Programme, Brussels,. Available from: http://www.sustainablebridges.net/

SB4.3.1, (2005), Summary code survey, Background document D4.3.1 to "Guideline for Load and Resistance Assessment of Railway Bridges". Prepared by Sustainable Bridges - a project within EU FP6. Available from: www.sustainablebridges.net

SB-D4.3.2, (2007), Assessment of Actual Traffic Loads Using B-WIM, Site Specific Characteristic Load from Collected Data & Statistical Evaluation of Dynamic Amplification Factors, Background Document D4.3.2, Sustainable Bridges - Assessment for Future Traffic Demands and Longer Lives, 6th Framework Programme, Brussels. Available from: http://www.sustainablebridges.net/

SB4.7, Masonry Arch Bridges, Background document D4.7 to "Guideline for Load and Resistance Assessment of Railway Bridges". Prepared by Sustainable Bridges - a project within EU FP6. Available from: www.sustainablebridges.net

Semih Yücemen, M. and Al-Homoud, A. S., (1990), Probabilistic three-dimensional stability analysis of slopes, Structural Safety, 9 (1), pp. 1-20.

Sørensen, J.D., Hansen, J.O., Nielsen, T.A., (2001), Partial Safety Factors and Target Reliability Level in Danish Structural Codes. Proceedings of IABSE International Conference on Safety, Risk and Reliability: Trends in Engineering, 2001.

Springman S, Jommi C,Teysseire P (2003) Instabilities on moraine slopes induced by loss of suction: a case history. Géotechnique 53(1): 3–10.

Stewart, M.G., Teply, B. and Kralova, H., (2002), The Effect of Temporal and Spatial Variability of Ambient Carbon Dioxide Concentrations on Carbonation of RC Structures, 9th International Conference on Durability of Building Materials and Components, CSIRO, Paper 246 (CD-ROM).

Stewart, M.G., Wang, X., Nguyen, M., (2011), 'Climate change impact and risks of concrete infrastructure deterioration', Engineering Structures, Volume 33, Issue 4, pp 1326-1337

UIC (2003). Draft Code 776-2; Design Requirements for rail bridges based on interaction phenomena between train, track, bridge and in particular speed. Internatioanl Union of Railways.

UIC 700, (2004), Classification of lines - Resulting load limits for wagons, International Union of Railways, Leaflet,.

UIC 776-1 (2006), Loads to be considered in Railway Bridge Design, International Union of Railways (UIC), 5th edition.

Vu, K.A.T. and Stewart, M.G., (2000), Structural Reliability of Concrete Bridges Including Improved Chloride-induced Corrosion Models. Structural Safety, 22(4): 313-333.

Val, D. and Stewart, M.G., (2009), Reliability Assessment of Ageing Reinforced Concrete Structures – Current Situation and Future Challenges, Structural Engineering International, 19(2): 211-219.

Val, D., Bljuger, F. & Yankelevsky, D. (1996). Optimization problem solution in reliability analysis of reinforced concrete structures. Computers and Structures, 60, 351-355.

WAVE, (2001), Weigh-in-Motion of Axles and Vehicles for Europe, Final Report pf RTD project, RO-96-SC, 403. Ed Jacob, B. Paris: LCPC, 103pp.

Wang, X., Nguyen, M., Stewart, M.G., Syme, M., Leitch, A., (2010), Analysis of Climate Change Impacts on the Deterioration of Concrete Infrastructure – Part 1: Mechanisms, Practices, Modelling and Simulations – A review. Published by CSIRO, Canberra

Wang, X., Nguyen, M., Stewart, M.G., Syme, M., Leitch, A., (2010), Analysis of Climate Change Impacts on the Deterioration of Concrete Infrastructure – Part 2: Modelling and Simulation of Deterioration and Adaptation Options. Published by CSIRO, Canberra

Wang, X., Nguyen, M., Stewart, M.G., Syme, M., Leitch, A., (2010), Analysis of Climate Change Impacts on the Deterioration of Concrete Infrastructure – Part 3: Case Studies of Concrete Deterioration and Adaptation. Published by CSIRO, Canberra

Wang, C-H. and Wang, X., (2009a), Hazard of Extreme Wind Gust in Australia and its Sensitivity to Climate Change. Technical Report of National Research Flagships – Climate Adaptation. CSIRO, Melbourne.

Wang, C-H. and Wang, X., (2009b), Hazard of extreme wind gusts to buildings in Australia and its sensitivity to climate change. 18th World IMACS / MODSIM Congress, Cairns, Australia 13-17, July, 2009.

Whitman, R. V. (1984). Evaluating calculated risk in geotechnical engineering. Journal of Geotechnical Engineering ASCE, 110, 143-188.

Xue, J. F. and Gavin, K. (2007). Simultaneous determination of critical slip surface and minimum reliability index for earth slopes. Journal of Geotechnical and Geoenvironmental (ASCE), Volume 133, No. 7, 878-886.

Yoon, I.S., Copuroglu, O., and Park, K.B., (2007), Effect of global climatic change on carbonation progress of concrete. Atmospheric Environment, 41: 7274-7285.

Zhu C.,Byrd R.H., Nocedal J (1997), L-BFGS-B: Algorithm 778: L-BFGS-B, FORTRAN routines for large scale bound constrained optimization. ACM Transactions on Mathematical Software 23 (4): 550-560.

Zhang, L. L., Zhang, J., Zhang L.M., Tang, W.H., (2011), Stability analysis of rainfall-induced slope failure: a review, Geotechnical Engineering, 164(5): 299-316.

Appendix A. Probabilistic Analysis of Nieporet Bridge, Poland

A.1. Introduction

A probabilistic based assessment similar to that described in chapter 3 was carried out on a steel railway bridge. The bridge is located in Nieporęt, near Warsaw. The steel truss bridge which was constructed in the 1970s is one of over one thousand similar bridges in Poland (Kolakowski et al., 2011). The bridge in question is a steel truss which spans 40 m and consists of five 8 m long bays. The height of the truss is also 8 m. Figure A1 shows an elevation (a) of the Nieporęt Bridge and a view from underneath the bridge (b).

a) ***b)***

Figure A1: Nieporęt Bridge: side view (left) and view from underneath (right)

The truss bridge is supported on four steel bearings, illustrated in Figure A2, two at each end. It carries a single unballasted railway track which runs along the centre. The main structure of the bridge consists of two main vertical trusses, one at either side, which can be seen clearly in Figure A1(a). The trusses are connected along the bottom chord by six cross beams which are located at the node points along the bottom of the truss (Figure A1(b)). At the top of the bridge the two main trusses are connected by minor elements at the node points; this is clearly illustrated in Figure A3(a).

The railway track is supported by timber sleepers which span onto two 'stringer' beams. These two stringer beams span longitudinally between the six cross beams. The loading on the track is transferred from the track into the sleepers and then onto the stringer beams. The stringer beams transfer the load into the cross beams which connect to the node points of the truss. There is diagonal wind bracing at the top and bottom of the structure.

a) ***b)***

Figure A2: Nieporęt Bridge: steel bearings

a) ***b)***

Figure A3: Nieporęt Bridge: (a) node point at the top of the truss and (b) stringer beam (on left)

A.2. Finite Element model

A Finite Element (FE) model was created using the Midas finite element software package. The bridge was modelled using linear elastic beam elements with full fixity at the node points. The design drawings for the bridge were used to set up the geometry and to calculate the section properties of each of the members. A Young's Modulus of 2.1×10^8 kN/m2 was assumed throughout and assigned to all steel members. Figure A4 shows an outline view of the Midas model with some of the main structural elements highlighted. The track and sleepers are omitted from the figure for clarity.

The model has four supports which are pinned at the left hand side and are on rollers at the right. The locations of these supports are illustrated at the four corners of the bridge shown in Figure A4. The supports are numbered 1 to 4. The following boundary conditions have been imposed at each of the four supports:

- Support 1 – Fixed against translation in all directions (x, y, z), free to rotate about all axes.
- Support 2 – Fixed against translation in x and z-directions, free to rotate about all axes.
- Support 3 – Fixed against translation in the z-direction, free to rotate about all axes.
- Support 4 – Fixed against translation in the y and z-directions, free to rotate about all axes.

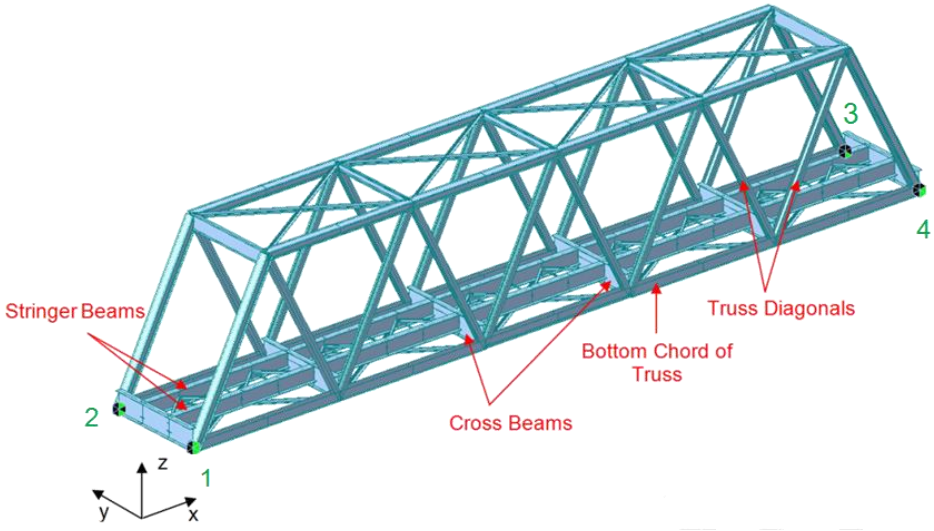

Figure A4: Midas finite element model of Nieporęt Bridge

A.3. Model validation

The Nieporęt Bridge has been the subject of investigation since mid-2007 as a result of interest from Polish Railways (PKP PLK S.A.) in the development of Structural Health Monitoring (SHM) systems for railway bridges (Kolakowski et al., 2011). The bridge has been instrumented with a number of sensors, with some readings from these sensors published by Kolakowski et al. (2011). Some of these published results were used in an effort to compare the accuracy of the static model to the measurements taken from the bridge.

Figure A5 illustrates the locations of the sensors which were used in the study which was carried out by Kolakowski et al. (2011).

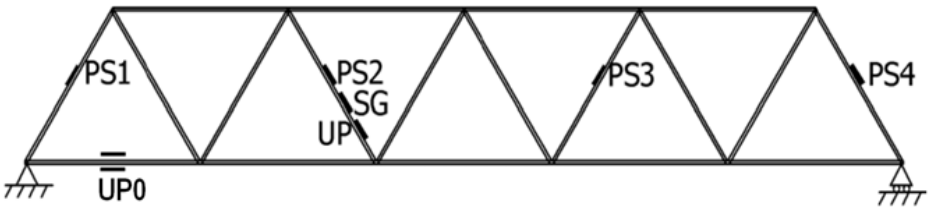

Figure A5: Measurement locations used by Kolakowski et al. (2011): PS – piezosensor, SG – strain gauge, UP – ultrasonic probehead

Three cases were examined to compare the measured results from the bridge to the theoretical signals generated from the model. Firstly, the measured response taken from the stringer beam at sensor location UPO due to the passage of an ET22 locomotive was examined. Kolakowski et al. (2011) presented the measurements for passages of the locomotive at three different speeds (Figure A6 (a)). The signal for the slowest speed (37 km/h) was deemed most appropriate to compare with

the static model as this signal contained the least dynamics. The black line in Figure A6(a) illustrates the measured voltage for the 37km/hr passage of the locomotive.

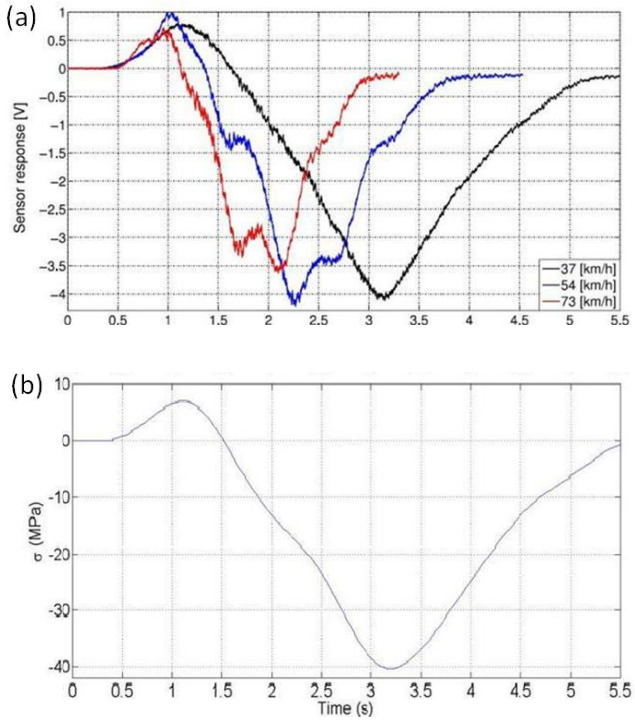

Figure A6: (a) Measured voltage and (b) theoretical stress from stringer at location UPO

As the conversion factor between voltage and stress or strain for the sensor at UPO was unknown, the only comparison that could be made was the shape of the signal and not the magnitude of the response. A theoretical signal was generated from the model by calculating the stress due to 6 No. 20 t axles traversing the influence lines which were generated from the model. These 6 No. axles were modelled as point forces in the standard configuration of an ET22 locomotive (Figure A7 shows the ET22 standard configuration). Figure A6(b) shows the theoretical stress response from the model.

A good match can be seen in the shape of the measured and theoretical responses. The theoretical signal does not contain any electrical noise which is evident in the measured voltage signal but overall the shape of the two signals is consistent.

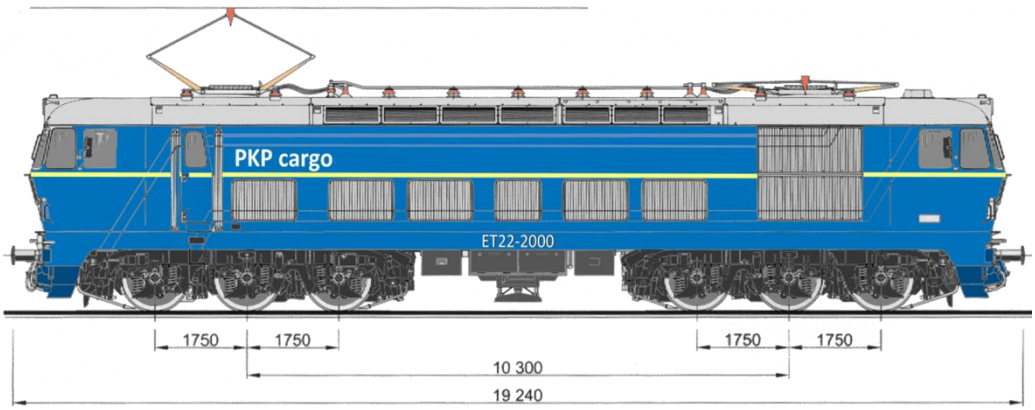

Figure A7: ET22 Locomotive configuration (www.locomotives.com.pl)

The second comparison was made between measurements taken from the truss diagonal at location PS2 and a theoretical signal generated at this location. Figure A8 shows five different signals. The first three signals show the measured response using different sensor types on the bridge for the passage of the ET22 locomotive at 40km/h. The fourth signal shows the theoretical stress generated by the model used by Kolakowski et al. (2011), while the final signal shows the theoretical stress generated by the static Midas model developed for the current assessment.

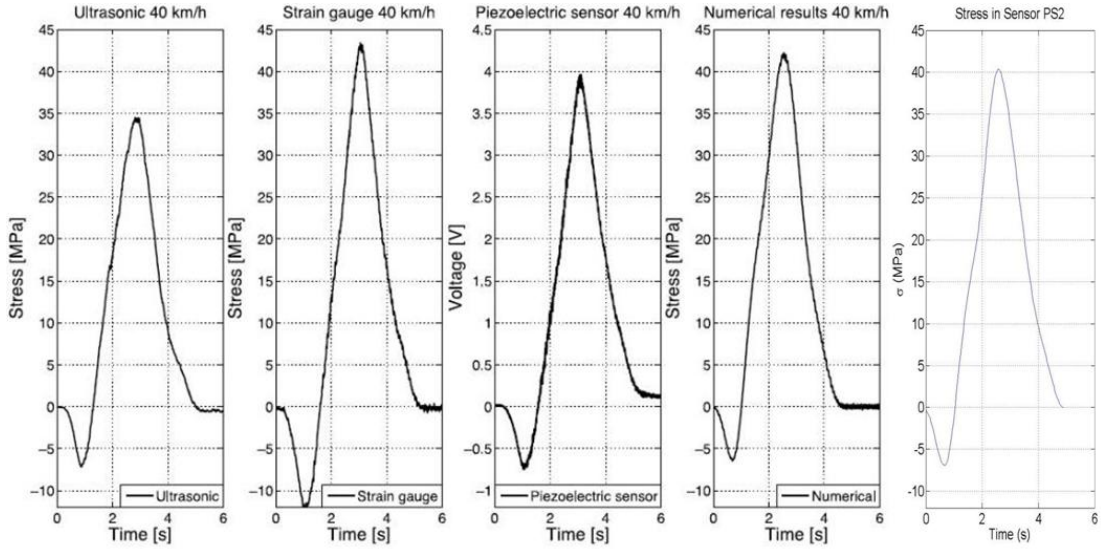

Figure A8: Measured vs. theoretical signals at location PS2

Comparing the signals shown in Figure A8, it can be seen that there is significant variation between the measurements recorded using the three different sensor types. Comparing the stress magnitude shown in the first signal (ultrasonic sensor) to that in the second (strain gauge), it can be seen that there is quite a difference. Comparing the theoretical stress generated by the Midas model shows very good conformity in both shape and magnitude to the measured signals.

The final comparison between the model and the measured response compared the measured stress at location UP0 to the signal generated by the model (this time the signal was measured at the underside of the top flange instead of the bottom flange). The measured response for the passage of an ET22 120t locomotive was recorded for passages at 20 km/h and 80 km/h. Figure A9(a) shows the measured signal for these passages of the locomotive. The signal for the slower speed was used to compare to the theoretical signal from the model as it was deemed to be closer to the static result. Figure A9 (b) illustrates the theoretical stress generated from the Midas model.

It can be seen that the shape of the two signals is slightly different. Both responses show troughs in the signal corresponding to the two axle groups of the locomotive. In the measured response the first trough is slightly greater than the second while the response from the model shows the second trough being slightly larger than the first. Apart from this difference there is good agreement between the model and the measured response, with both signals showing similar magnitudes and following a similar shape.

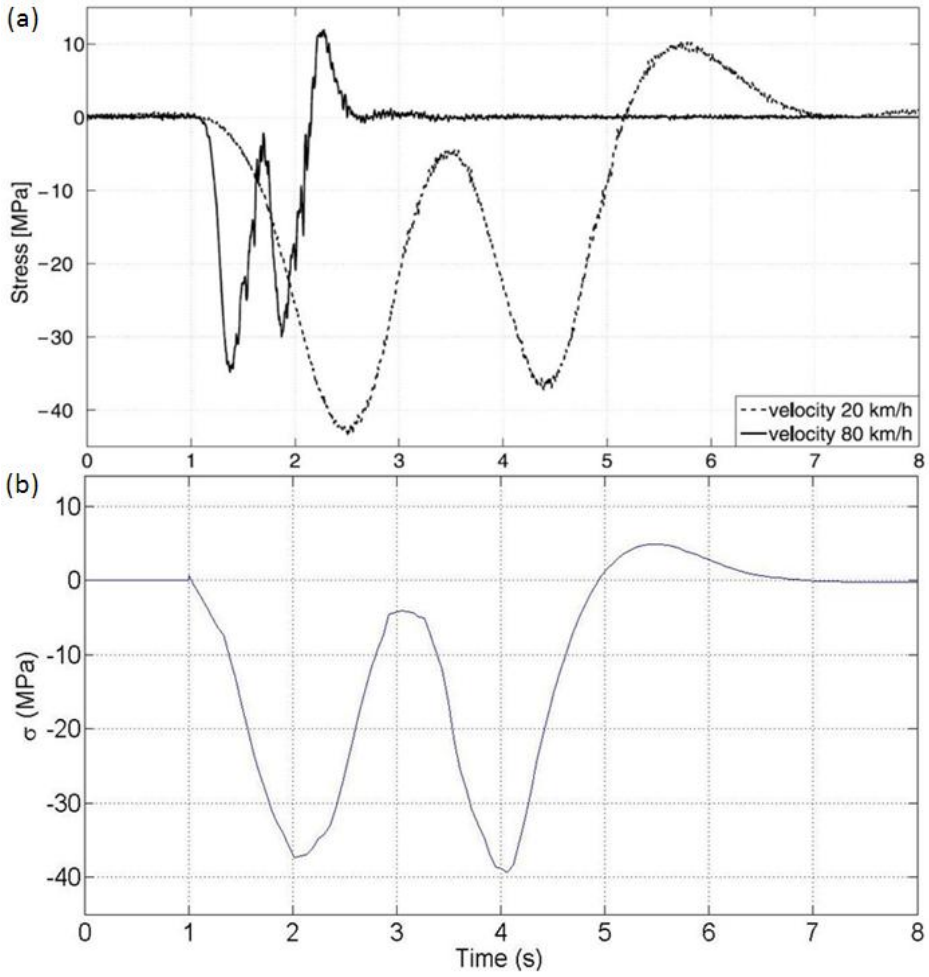

Figure A9: (a) Measured and (b) Midas Stress Signal at UP0 due to Passage of ET22 120t Locomotive

SHM and WIM data has been used herein to verify the FE model of the Nieporet bridge. In this case close agreement has been noted between the model and the measured response. In other cases, the results may be dissimilar. In these cases it may be prudent to alter the behaviour of the model in order to achieve a more accurate assessment.

A.4. Deterministic Assessment

Loading

The railway load model from Eurocode 1 (I.S. EN 1991-2:2003), Load Model 71, consists of 4 x 250 kN axles, spaced at 1.6m, with a UDL of 80 kN/m at a distance of 0.8m in front of and behind the axles as shown in Figure A10.

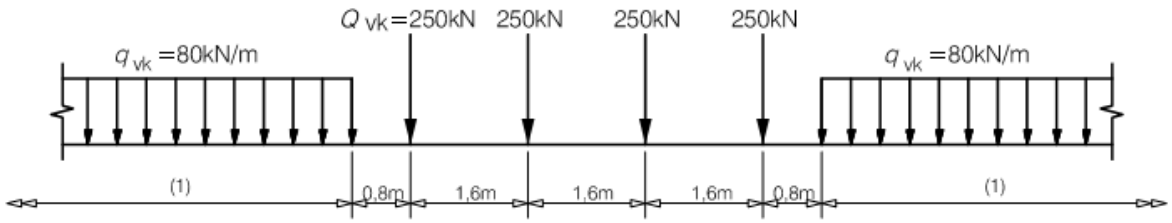

Key
(1) No limitation

Figure A10: Load Model 71 (I.S. EN 1991-2:2003)

These loads were multiplied by the following load factors in accordance with Eurocode 1:

- Adjustment factor α to account for rail traffic which is heavier or lighter than normal rail traffic. This factor was taken as 1.1 (recommended in IS EN 1991-2:2003 NA:2009).
- Dynamic factor ϕ to account for dynamic magnification of stresses and vibration effects in the structure.

The dynamic factor ϕ for a carefully maintained deck is given as:

$$\Phi = \frac{1.44}{\sqrt{L_\Phi} - 0.2} + 0.82 \qquad (A1)$$

The determinant length, $L_{\phi,}$ is given in EN 1991-2:2003, Table 6.2, for rail bearers (stringers) and cross beams as part of a steel grillage as:

- $L_{\phi\ (stringer)}$ = 3 times cross girder spacing = 24m.
- $L_{\phi\ (cross\ beam)}$ = Twice cross girder length = 10m.

Thus, the dynamic factors for the stringers and cross beams were calculated as:

- $\Phi_{stringer}$ = 1.13
- $\Phi_{cross\ beam}$ = 1.31

As no determinant length is specified in the code for members other than cross beams and stringers, the dynamic factor for all bridge members other than the stringers was conservatively assumed to be equal to the cross beam dynamic factor.

Analysis

The model created in Midas is a static model of the bridge, i.e. no vehicle or bridge dynamics are considered. It is not a simple task to generate signals due to moving loads traversing the bridge in Midas. Therefore, influence lines for total stress at different locations in the model were exported to Matlab. The Navier stress influence line ordinates are calculated in Midas as shown in equation A2.

$$\mathrm{i}_{\sigma t} = \frac{i_{mx} y}{I_x} + \frac{i_{my} x}{I_y} + \frac{i_{Pz}}{A} \qquad (A2)$$

Where:

- $i_{\sigma t}$ are the influence line ordinates for total stress.
- i_{mx} / i_{my} are the influence line ordinates for bending in each direction.
- i_{Pz} are the influence line ordinates for axial force.
- y / x are the distances to the maximum point of stress in the member.
- I_x / I_y are the moments of inertia about each axis of bending.
- A is the cross sectional area of the member.

Load Model 71 was run across the influence lines for the whole bridge length. The front UDL was first run across the influence line, followed by the axles and the back UDL. Therefore, the total distance for plotting the stress due to Load Model 71 is given as:

$$distance = 2(bridge\ length) + 3(axle\ spacing) + 2(gap)$$

$$= (2x40.32) + (3x1.6) + (2x0.8)$$

$$= 87.04m$$

Figure A11 shows a plot of the maximum stress in the second cross beam due to the axles and each UDL moving across the bridge, while Figure A12 shows the total stress in the same cross beam (i.e. the sum of the stresses in Figure A11). From these results, the absolute maximum stress was determined for each member type and the location of the load model to cause this maximum. For example, it can be seen in Figure A12 that the maximum stress in cross beam 2 is 300,991 kN/m2

and occurs when the front axle of the vehicle is 10.08m along the bridge. The stresses due to the live loading were added to the stresses due dead load and these were compared to a maximum allowable stress of 275,000 kN/m2 (assuming S275 steel). The results are shown in Table A1. The members included in table A1 are those which were at the highest level of stress. The column headed T/C indicates whether the maximum stress in the member was tensile or compressive.

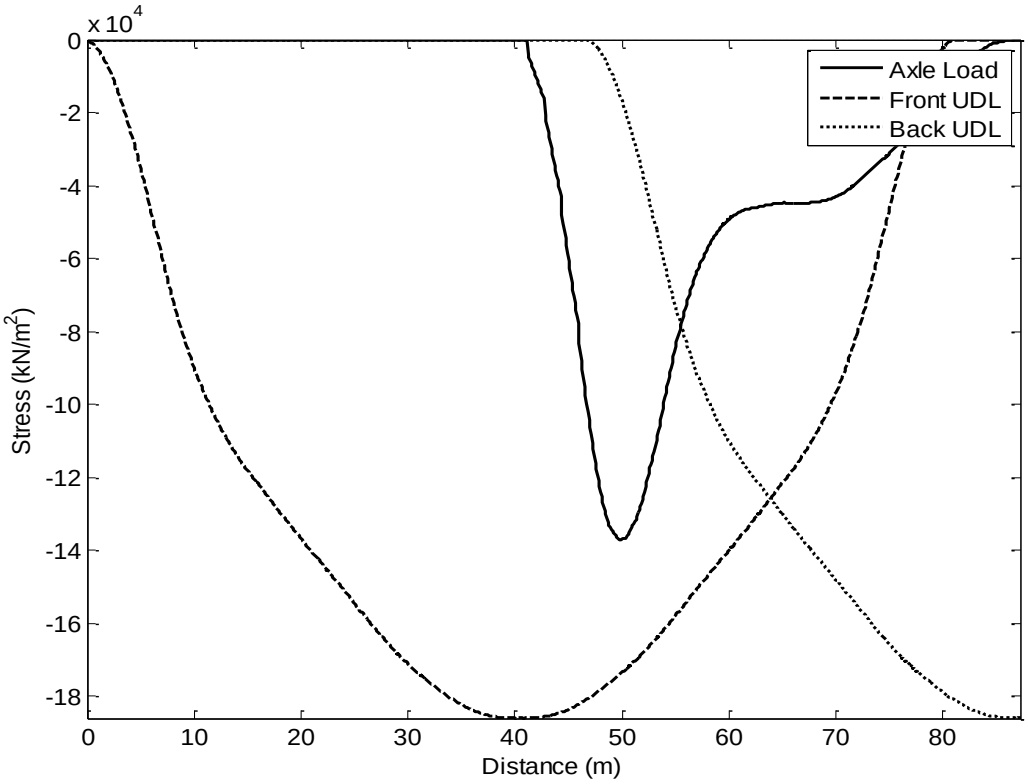

Figure A11: Stresses in cross beam 2 due to axles and UDLs

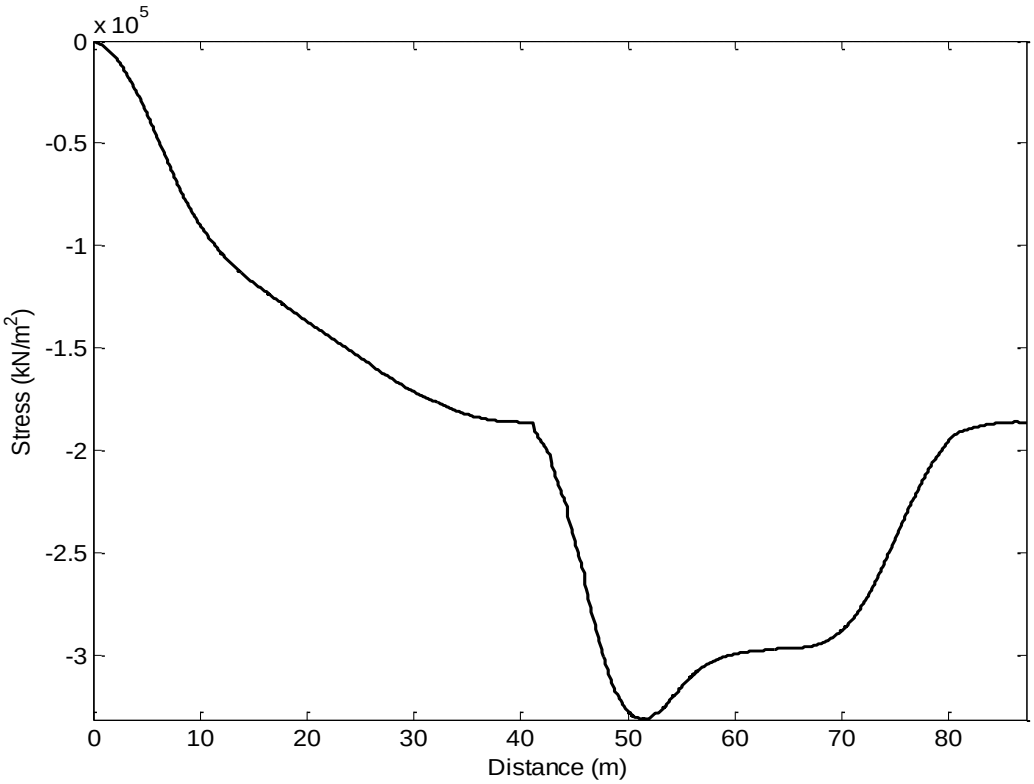

Figure A12: Total stresses in cross beam 2

Table A1: Maximum Stress and load factor for each member

ID	Element	Member	T/C	LL stress (kN/m2)	DL stress (kN/m2)	Total stress (kN/m2)	load ratio
1	100	Bottom cross beam 2	T	300991	20724	321715	1.17
2	99	Bottom cross beam 1	T	197390	19706	217096	0.79
3	103	Bottom cross beam 3	T	207273	8823	216096	0.79
4	48	Truss diagonal 2	C	176849	24962	201811	0.73
5	203	stringer 1-2 joint	T	159667	9230	168897	0.61
6	26	Truss diagonal 3	T	129496	16533	146029	0.53
7	3	Bottom boom 1-2 joint	C	115078	17684	132762	0.48
8	14	Top boom 2	T	111503	15467	126970	0.46
9	11	Top boom 1	T	108107	15415	123522	0.45
10	33	Bottom boom 3	C	95073	16009	111082	0.4
11	222	stringer 3	C	86737	6194	92931	0.34
12	177	Diag top bracing	T	64150	30530	94680	0.34
13	116	Top cross beam 2	C	47956	7691	55647	0.20
14	151	cross bottom bracing	C	27531	1598	29129	0.11
15	152	Diag bottom bracing	C	19617	2830	22447	0.08

Conclusions from Deterministic Assessment

It can be seen in Table A1 that the second cross beam on the Nieporet Bridge has failed due to the applied loading. It is noted that stresses due to wind, nosing and traction/braking forces were not

accounted for in Table A1. For cross beam 2, these were calculated as 3036 kN/m2, 15,923 kN/m2 and 22,227 kN/m2 for wind, nosing and traction/braking forces, respectively. Therefore, the Load ratio calculated for cross beam 2 may be recalculated by the following equation (I.S EN 1991-2:2003):

$$LR = 1.17 + \frac{[0.5x(nosing) + 1\ x\ (traction\ \&\ braking) + 0\ x\ (wind)]}{maximum\ allowable\ stress}$$

$$= 1.17 + \frac{[(0.5\ x\ 15{,}923) + (1\ x\ 22{,}227) + (0\ x\ 3036)]}{275{,}000}$$

$$= 1.17 + \frac{30{,}189}{275{,}000}$$

$$= 1.27$$

It is noted that the effects of these wind, nosing and traction/braking forces were not applied to all elements above. However, since the stresses in element 100 (cross beam 2) were substantially higher than those in all other members, and allowing for a conservative dynamic factor being applied to all other members, the other members are not considered to be critical. Therefore, a probabilistic model of the variables is required to determine whether the probability of failure of cross beam 2 is low enough for the structure to be considered safe.

A.5. Probabilistic Modelling of Variables

From the deterministic assessment, it was clear that the second cross beam, hereafter referred to as 'CB2', was the most critical element under consideration, with a load ratio of 1.27. The critical limit state function for the element was based on a check of Navier stresses, as for the deterministic assessment, described as:

$$g \leq 0\ where\ g = f_y - |\sigma| \qquad (A3)$$

Where f_y describes the yield strength of the structural steel and $|\sigma|$ is the induced Navier stress due to the applied loading ($\sigma_{F_x} + \sigma_{M_y} + \sigma_{M_z}$). The variables to be modelled stochastically include traffic load, dynamic amplification, dead load, superimposed dead load and steel yield strength. Therefore, the secondary effects of wind, side impact and traction/braking are incorporated deterministically.

Traffic load

In order to obtain a model for train wagon loads, data was gathered from a WIM system on the Nieporet bridge. At the time of inspection, 10-12 trains traversed the bridge per day. Based on this, the level of WIM data was enhanced to one month using statistical operations. Normal distributions were fitted to axle spacing data in order to obtain a standard wagon configuration. Figure A13 shows the derived wagon configuration

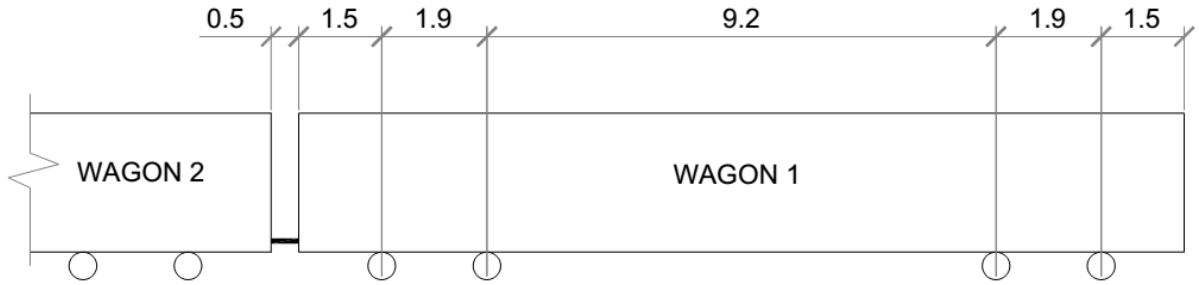

Figure A13: Wagon configuration

Extreme value modelling was used to derive train wagon weights. The parameters μ and σ of the Extreme Value Distribution (EVD) were required. The parameters are based on a Gumbel fit to the 30 maximum observations. The equation of the Cumulative Distribution Function (CDF) for the Gumbel EVD is:

$$F_x(x) = exp\left(-exp\left[\frac{-(x-\mu)}{\sigma}\right]\right) \qquad (A4)$$

The location, μ, and the scaling parameter, σ, of the Gumbel law, $F_x(x)$, are estimated by minimisation of the error between the empirical and modelled distribution. Figure A14 presents the CDF of the modelled Gumbel distribution fitted to the empirical data.

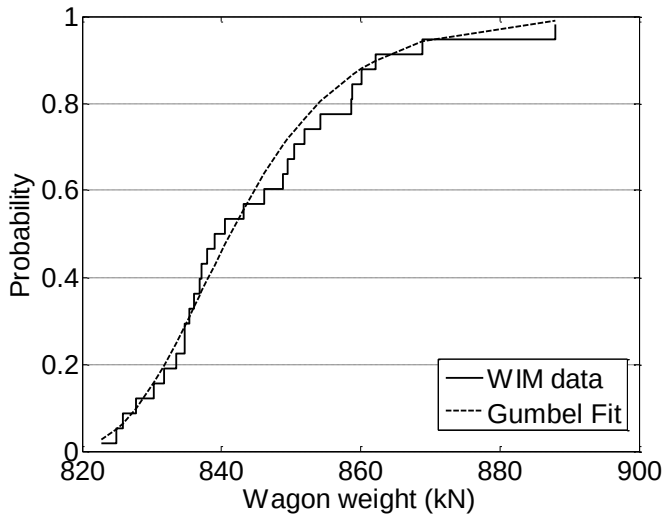

Figure A14: CDF of Gumbel EVD fitted to empirical data

Considering the stress influence line for CB2 (Figure A15) and the wagon configuration (Figure A13), it is clear that no more than 3 wagons would be positioned over the adverse portion of the influence line at any time. Therefore, it is appropriate that the Gumbel distribution is based on a fit to the maximum daily values of the total weight of 3 adjacent wagons. The distribution of 30 daily maximum observations $\mathrm{F_x(x)}$ (one month of simulated data) was converted to the yearly distribution of maxima, $\mathrm{F_{max}(x)}$, as:

$$F_{max}(x) = \exp\big(-N(1 - F_x(x))\big) \qquad (A5)$$

Where N is equal to 250 for 250 working days in a year. Figure A16 presents the daily and yearly CDF of the Gumbel distribution. The Gumbel parameters μ and σ, for 3 wagons were calculated as 2,688 kN and 32 kN, respectively. Therefore, the normalised values for 1 wagon are 896 kN and 10.7 kN, respectively.

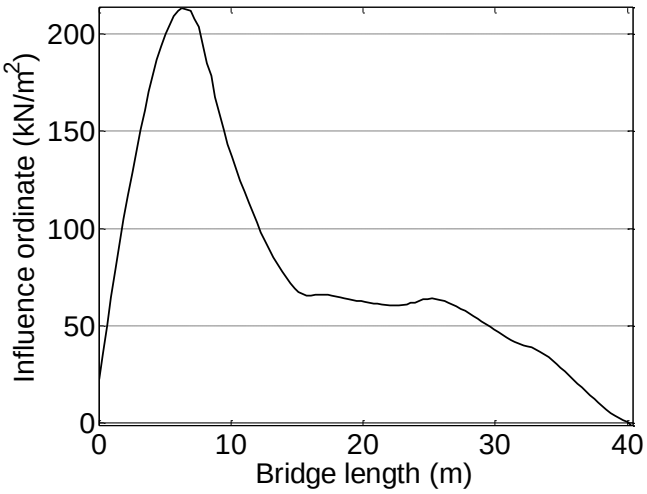

Figure A15: Influence line for CB2

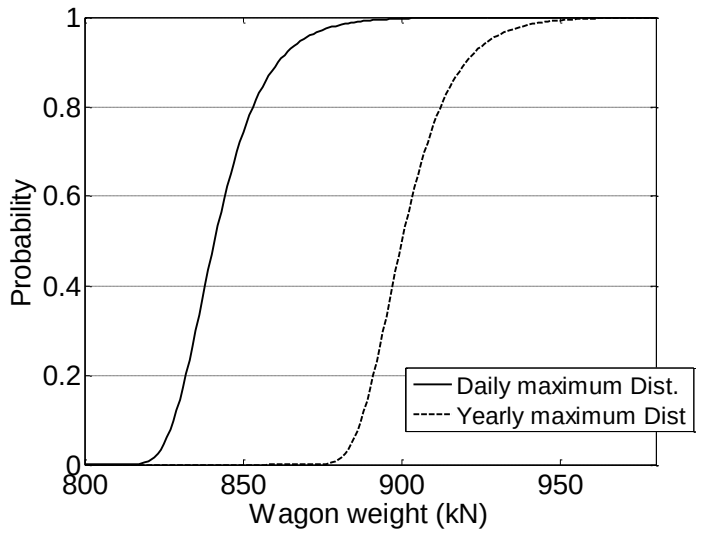

Figure A16: Yearly Gumbel CDF of wagon weights

The model uncertainty for wagon weight was considered as normally distributed with a mean of 1 and a Coefficient of Variation (CoV) of 10%, relating to a small level of uncertainty (DRD,2004). This is considered as conservative since the CoV in the data is quite low and considering the strict protocols used in the loading of train wagons.

Dynamic amplification of traffic load

The dynamic amplification factor in the probabilistic assessment is modelled as:

$$K_s = 1 + \varepsilon \qquad (A6)$$

Where ε is the dynamic increment which is modelled as normally distributed. The CoV of ε is given as 1 in DRD (2004). The dynamic increment represents the 98% fractile value of the deterministically calculated supplement, herein calculated as 0.31. Therefore, to ensure that a 98% fractile value of 0.31 is achieved, the mean and standard deviation are required to be 0.101 and 0.101, respectively.

Dead load

The stress due to dead load is modelled as normally distributed with a mean value, calculated for CB2 from the computer model, equal to 16,256 kN/m2. Note that this load is equal to the total dead load without considering the superimposed dead load (track and sleepers), which is modelled separately. The CoV for dead load (V_M) is taken as 5% with an additional 5% to model uncertainty (V_{IM}) (DRD, 2004). Since both CoVs are normally distributed, they can be combined as shown in Section 4.4 of this report to calculate the total CoV in stresses due to dead load (V):

$$V^2 = V_M^2 + V_{IM}^2 \qquad (A7)$$

Therefore, V is calculated as 7.1%.

Superimposed dead load

The stress due to superimposed dead load (composed solely of the track and sleepers) is also modelled as normally distributed with a mean value, calculated for CB2 from the computer model, equal to 4,468 kN/m2. The CoV for superimposed dead load is taken as 10% with an additional 5% to model uncertainty (DRD, 2004). Therefore, the overall CoV for superimposed dead load is calculated as 11.2%, using a formulation similar to equation A7.

Steel Yield Stress

The Yield stress (f_y) is modelled as logarithmic-normally distributed (DRD, 2004). In the absence of specific testing, St.37 steel is conservatively assumed (DRD, 2004). Therefore, with a minimum thickness (t) = 12mm the mean value of the yield stress is taken as 304 MPa with a standard deviation of 25 MPa (DRD, 2004). The model uncertainty for the yield strength must take account of:

- The accuracy of the calculation model;
- Uncertainty in determining material parameters from control specimens;
- Material Identity.

The accuracy of the calculation model is taken as good due to the verification of the model, as described in this appendix. The uncertainty in determining material parameters is classified as medium as this is assumed in the determination of f_y (DRD, 2004). The uncertainty associated with material identity is classified as normal due to the lack of test data. On the basis of these distinctions, the model uncertainty for the yield stress was modelled as logarithmic-normally distributed with a mean value of 1 and a standard deviation of 8.7%. Again, in accordance with Section 4.4 of this report, the contribution of the CoV of the yield stress and the associated model uncertainty can be combined in a formulation similar to equation A7 to give an overall CoV of 12%.

Incorporation of additional loads

In order to incorporate the effects of wind, nosing and braking/traction, the factored contribution of the stresses due to these loads were calculated deterministically as 30.2 MPa. This value was subtracted from the mean value of the yield stress. This stochastic-deterministic combination is only possible as the contribution of the deterministically calculated stresses is small in relation to the total stresses (<10%). This deterministic incorporation is conservative.
A summary of all variables modelled is given in table A2.

Table A2 . Modelled parameters and values for CB2

Variable	***Distribution***	***μ***	***σ***	***CoV***
Yield Strength	Lognormal	304 MPa	25 MPa	*(0.08)*
Model uncertainty for Yield Strength	Lognormal	1	*(0.09)*	0.09
Dead Load Stress	Normal	16.3 MPa	0.815 MPa	0.05
Model Uncertainty for Dead Load Stress	Normal	1	*(0.05)*	0.05
Superimposed Dead Load Stress	Normal	4.5 MPa	0.45 MPa	0.1
Model Uncertainty for Superimposed Dead Load Stress	Normal	1	*(0.05)*	0.05
Wagon Weight (based on 3 wagons)	Gumbel	2688 kN	32 kN	0.01
Model Uncertainty for Wagon Weight	Normal	1	*(0.1)*	0.1
Dynamic Amplification Factor (ε increment)	Normal	0.1	0.1	1
Wind, Nosing & Traction	Fixed	-	-	-

A.6. Results of Probabilistic Assessment

Evaluation of reliability index

A First Order Reliability Method (FORM) was used to estimate the reliability index, β, of the performance function presented in Eqn. A3, which can also be written as:

$$g(R,S) = R - S \qquad (A8)$$

where R is the steel yield strength (i.e. resistance) and S is the induced Navier stress due to applied loading (i.e. load effect). The distributions of the resistance and load effect are found through Monte Carlo Simulation. A lognormal distribution was found to be a good fit for both the yield strength and the induced Navier stress. The probability of failure is defined as:

$$P_f = P[g < 0] \qquad (A9)$$

where the notation $g < 0$ denotes the failure region. For this analysis, the Hasofer-Lind method was used to estimate β. The Hasofer-Lind method involves transforming the random variables from their

original space to standard normal space and finding the shortest distance from the origin to the limit state function in standard normal space as shown in Figure A17.

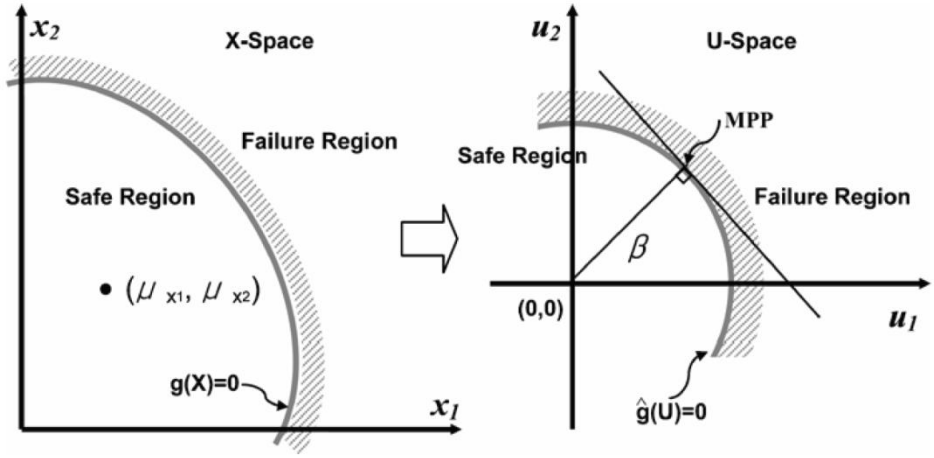

Figure A17: Mapping of failure surface from original (X-space) to standard normalised (U-space) space (Choi et al. 2007)

The resistance and load effect variables are transformed into their standardised forms as follows:

$$\hat{R} = \frac{R - \mu_R}{\sigma_R}, \hat{S} = \frac{S - \mu_S}{\sigma_S} \qquad (A10)$$

Where μR and μS are the mean values of the random variables R and S, respectively and σR and σS are the standard deviations of R and S, respectively. The limit state surface in the original space, as shown in Eqn. A8, is the transformed into the limit-state surface in the standard normalized space, $(\hat{\mathrm{R}}, \hat{\mathrm{S}})$, as:

$$g\left(R(\hat{R}), S(\hat{S})\right) = \hat{g}(\hat{R}, \hat{S}) = \hat{R}\sigma_R - \hat{S}\sigma_S + (\mu_R - \mu_S) \qquad (A11)$$

In standard normalised space, the shortest distance from the origin to the failure surface $\hat{\mathrm{g}}(\hat{\mathrm{R}}, \hat{\mathrm{S}}) = 0$ is equal to the reliability index as shown:

$$\beta = \frac{\mu_R - \mu_S}{\sqrt{{\sigma_R}^2 + {\sigma_S}^2}}$$

The point on the failure surface which corresponds to this shortest distance is often referred to as the most probable point, MPP. As mentioned previously, a requirement of FORM is that the variables in Eqn. A3 are normal and independent. Given the non normal nature of the load effect and resistance variables in this case, the Rackwitz Fiessler method is used, which involves the transformation of non-normal distributions into equivalent normal distributions. A more in depth description of the Hasofer-Lind Rackwitz-Fiessler method can be found in Choi et al. (2007).

Effect of number of runs

The input parameters for the FORM analysis include the mean and standard deviations of the load and resistance variables of the limit state function. The variation in these parameters is dependent on the number of runs of the static analysis. For the current analysis, the beta value was calculated for 10 – 100,000 runs of the static analysis. It is clear from Figure A18 that after 10,000 runs, a beta value of 3.9 was achieved, with a very low standard deviation. This value remained approximately constant after 100,000 runs. From Table 3.5 of this report (ISO/CD 2394:1998 target reliabilities), a minimum beta value of 3.8 is deemed appropriate for the element in question for a "great" consequence of failure and a "Medium" relative cost of repairs. That is, the beta value determined is sufficiently high for the bridge to be considered safe.

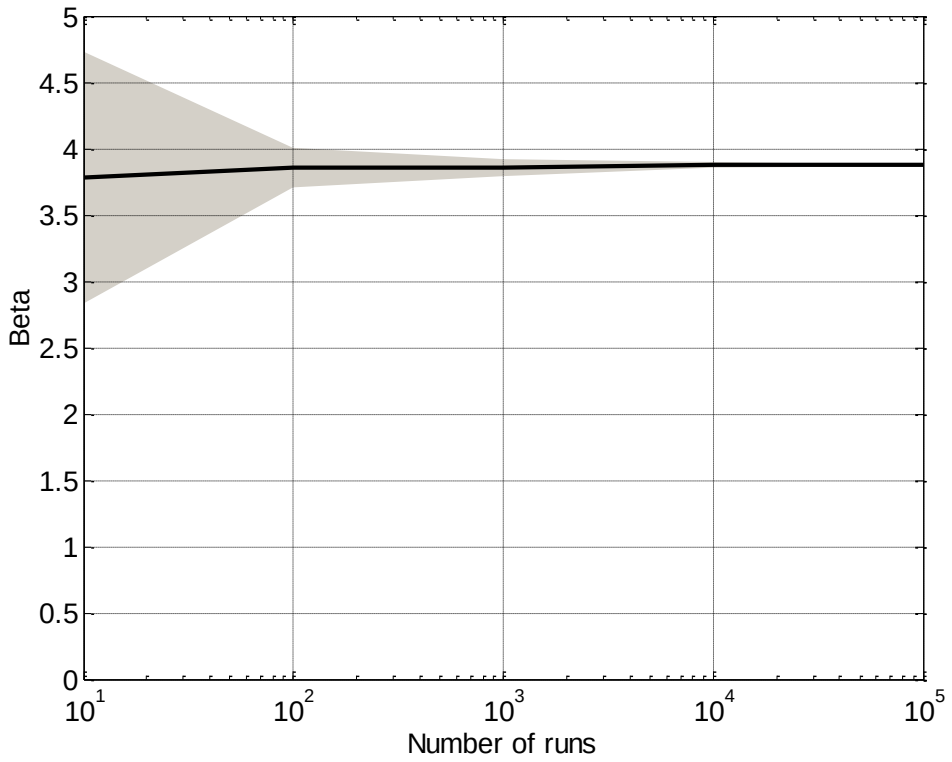

Figure A18: Reliability index and standard deviation for 10 – 10^5 runs of the static analysis

Sensitivity analysis

A reliability based classification should always be accompanied by a sensitivity analysis to evaluate the robustness of the result and to determine if the reliability index is overly sensitive to any of the modelled parameters (DRD, 2004). The sensitivity is measured by the ratio of the change in reliability index to the change in any particular parameter ($\delta\beta$ / δparameter). In the current analysis, the sensitivity of the analysis to each parameter is measured with respect to a 10% increase in the parameter value. The results are shown in Figure A.19. For example, it can be seen that the analysis

is most sensitive to the mean yield strength with a 17% increase in reliability index due to a 10% increase in the mean yield strength (i.e. δβ / δparameter = 1.7). As expected, the mean wagon weight is also an important parameter, with a 16% decrease in reliability index due to a 10% increase in weight. When reading Figure A.19, note that Fy is the yield stress of the steel, Unc_wag is the model uncertainty associated with the weight of a single wagon, 'DL' is the dead load, 'SDL' is the superimposed dead load, 'Wag' is the wagon weight, 'DAF' is the dynamic amplification factor. The 'mean' and 'sig' denote the mean and standard deviation respectively. Note that while the uncertainty associated with the wagon weight is the only uncertainty model analysed for sensitivity, the uncertainty models for each of the other parameters are accounted for in the standard deviation of that parameter.

It is clear from the sensitivity analysis that the incorporation of additional testing on the strength properties of the steel could result in higher levels of reliability. In the current analysis, the minimum yield strength was assumed from DRD (2004). Therefore, further analysis would not only reduce the uncertainty associated with the strength modelling, but may also lead to the allowance of higher mean yield strengths, increasing the reliability index.

Since the WIM database had to be artificially enhanced in the current analysis, and considering the high sensitivity to the mean wagon weight parameter, a full month of WIM data would be preferable to accurately model the distribution of train wagon weights. While this may result in either increased or decreased wagon weights, it would be accompanied by a reduction in the uncertainty associated with the mean wagon weights. It is clear from Figure A19 that this reduction in uncertainty would have a significant beneficial impact on the reliability index.

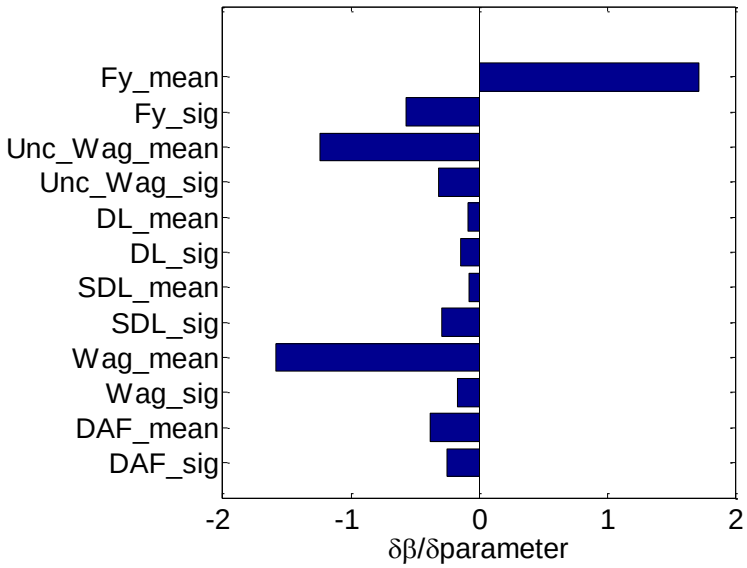

Figure A19: δβ for a 10% increase in mean and standard deviation for all parameters modelled

A.7. Conclusions

The Nieporet Bridge near Warsaw, Poland, is a 50-year old steel truss railway bridge. Increased traffic levels on the bridge required a deterministic assessment to be carried out. The deterministic analysis of the Nieporet Bridge showed that the cross beams of the structure did not have sufficient capacity to resist the live loading from LM1 of EN 1991-2:2003. A probabilistic approach showed the reliability index of the bridge element to be sufficiently high to provide adequate safety in accordance with ISO 2394:1998. The potential cost savings to the owner are clear as unnecessary repair/replacement can be avoided.

It should be noted that various codes have published target reliability indices, and not all are in agreement with one another. For example, EN 1990-(2002), ISO/CD 13822:1999, fib Bulletin 65:2012 and JCSS Model Code I:2000 have each published target levels of reliability for both the Ultimate and Serviceability limit states (see Section 3.5 of this report).

As outlined by the sensitivity analysis, the current assessment would benefit from additional bridge-specific information. Specifically, the provision of steel testing to obtain a more accurate model for the mean and standard deviation of the yield strength of the steel could prove to increase the reliability index. In addition, it is noted that a full month of WIM data for the bridge would be required to more accurately model the railway live load at the site.

Appendix B. Probabilistic Slope Stability Analysis, Ireland

B.1 Introduction

To investigate the effect of analysis type (deterministic versus probabilistic) on the predicted safety of an embankment slope, a study of the effect of rainfall on the stability of a Victorian era railway embankment was performed. The 7.5m high embankment is located in Co. Meath, Ireland (See Figure B1a and B1b). The embankment has a relatively steep slope angle of approximately 38^{o} which is typical of Irish Railway embankments (Jennings and Muldoon 2003). It is constructed from a glacial till, with low fines content (less than 20%). The natural moisture content of samples taken from within the embankment and measurements of in-situ water content measured over a five month period revealed moisture contents that ranged from 17.4% to 23.5%.

Figure B1: a) Location of embankment shown by red dot, b) photo of embankment preparation for instrumentation

The particle size distribution of a sample of the soil taken from the embankment is shown in Figure B2. A simple laboratory experiment was performed on the embankment fill to investigate the effect of increasing moisture content on suctions (Reale et al 2012). Samples of the soil were compacted into standard proctor moulds and were then ponded (i.e. a constant head of water was applied to the top surface). A tensiometer, placed at the base of the mould, allowed the variation in suction with time to be determined. The results of tests on two samples, which were compacted at initial moisture contents of 15% and 20% respectively, are shown in Figure B3. The initial suction varied from 20kPa for the sample with the highest moisture content to 40kPa for the drier sample. As water infiltrated into the samples the suction decreased rapidly. The sample with the lowest initial water content, and higher initial suction allowed water to infiltrate at a higher rate, and thus

suctions reduced faster in this sample initially. However, after approximately 12 hours of infiltration the suction in both samples was equal. The suctions continued to decrease over the period of the test (40 to 50 hours) and approached a residual value of between 3 and 4kPa. Tensiometers placed in the slope revealed that suctions monitored over a five-month period varied between 4kPa and 9kPa (September 2013 to January 2014), See Figure B4.

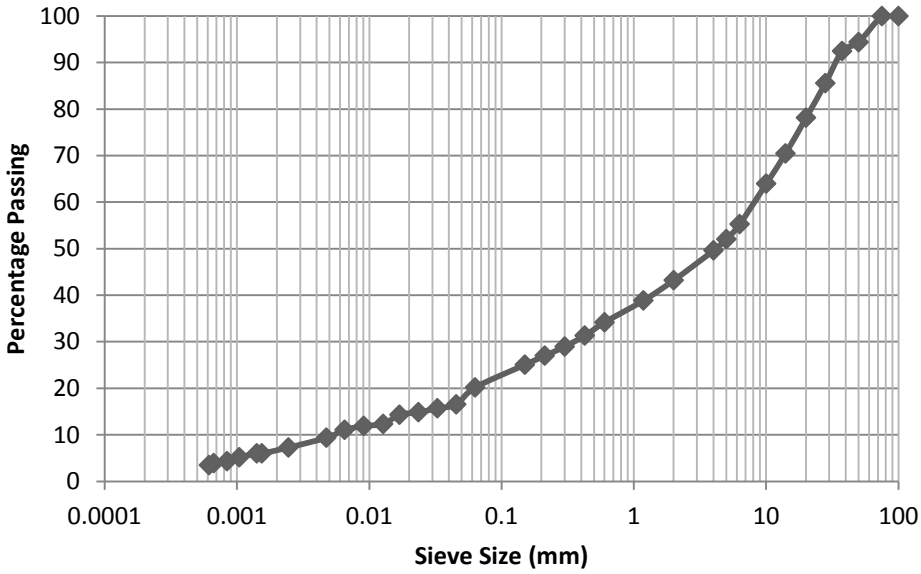

Figure B2: A particle size distribution combining sieving and sedimentation curves for a glacial till sample from Nobber Co. Meath.

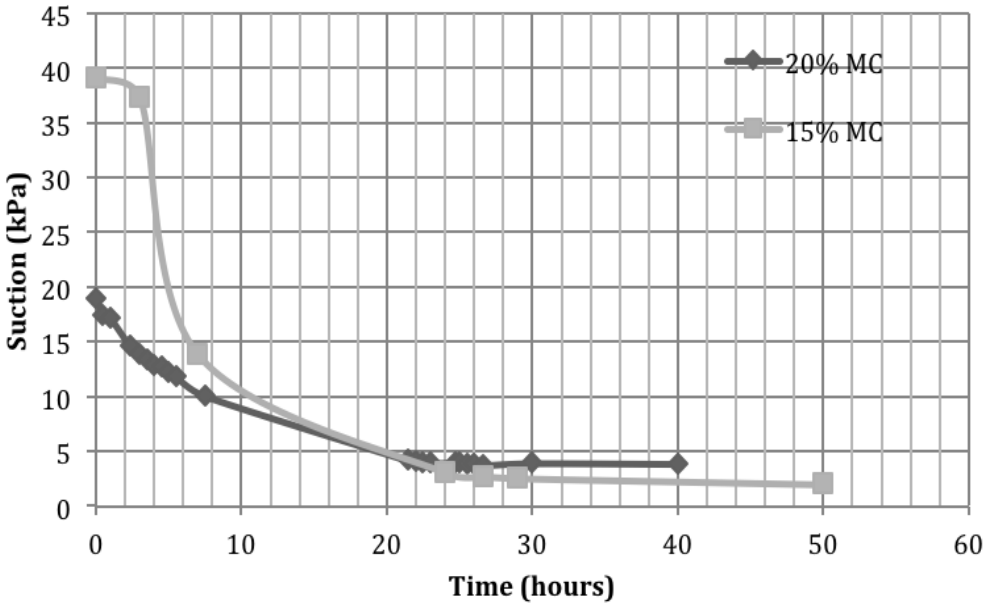

Figure B3: Suction drawdown of ponded soil sample over time due to infiltration. Reproduced with permission from (Reale et al., 2012)

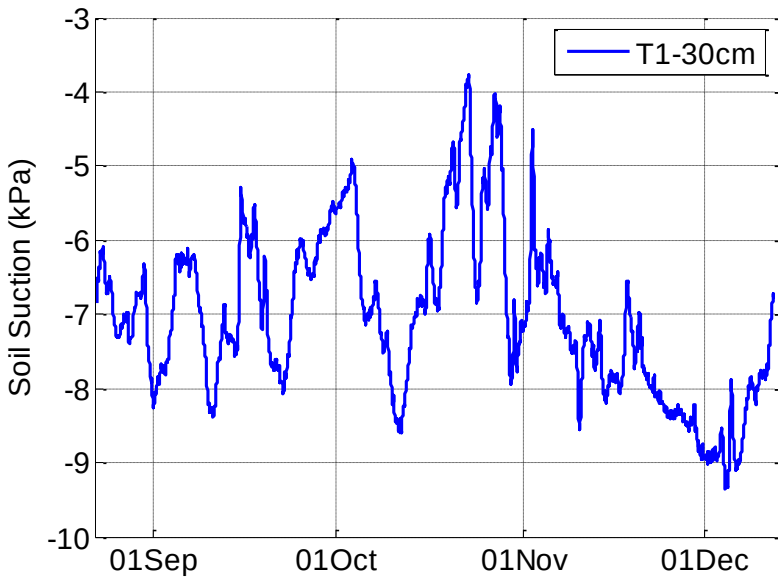

Figure B4: Tensiometer data from sensor embedded in the slopes face approximately 1.5m from the embankments crest at a depth of 30cm.

B.2 Deterministic Assessment

A deterministic analysis was performed in which the Factor of Safety (F) is given by:

$$F = \frac{c' + (u_a - u_w)\tan\varphi^b + \gamma h \cos^2\alpha \tan\varphi}{\gamma h \cos\alpha \sin\alpha}$$

in which γ is the unit weight of soil, h is the wetting front depth and α is the slope angle.

Since the model assumes a planar failure surface develops which is controlled by the wetting front depth (h), this parameter was varied in the analyses to quantify the effect of increasing wetting front depth during a rainfall event. All other parameters were assigned the constant values shown in Table B1. The soils unit weight and constant volume friction angle were measured in the laboratory. The average suction measured during the five month monitoring period was used as the suction value for design, whilst the ϕ^b value was chosen based on guidance in Gan et al. (1988).

Table B1: Deterministic parameter values

Parameter	Value
Cohesion (c')	0
Soil suction (u_a-u_w)	7 kPa
Internal Angle of Friction	34°
Rate of increase in shear strength due to matric suction ϕ^b	24°
Slope angle	38°
Unit weight	17 kN/m^3
Wetting front depth	Varied from 0.1 m to 2 m

By varying the wetting front depth from 0.1m to 2m the factor of safety reduced towards the critical value of one, but did not reach it suggesting some reserve of strength (see Figure B5). As the vast majority of shallow embankment failures in Ireland occur in the top 1.5m of the soil, this is a positive result.

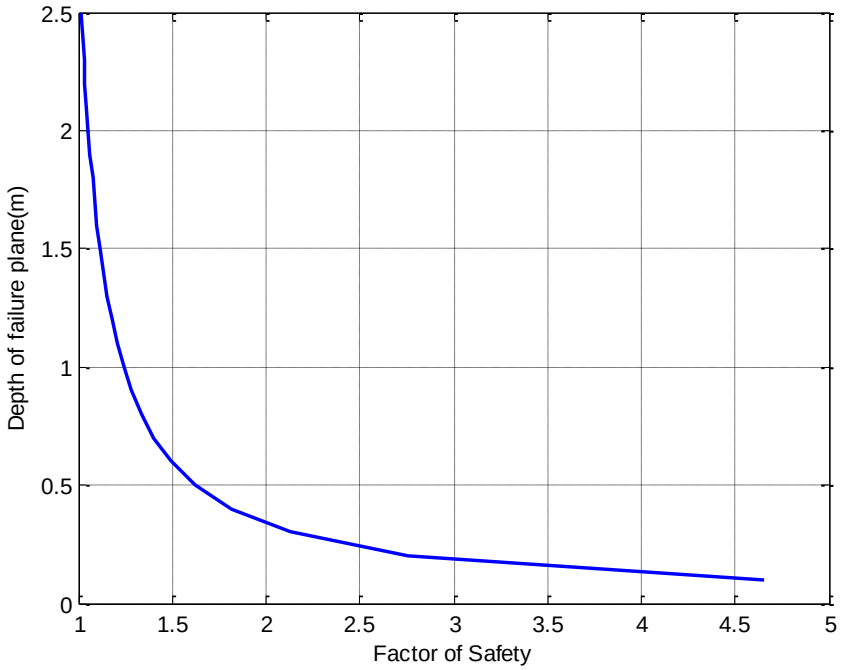

Figure B5: Effect of wetting front depth on factor of safety from deterministic analysis

It should be noted however that the use of average values might distort the analysis. Considering the histogram of suction values measured during the monitoring period (See Figure B6) it can be seen that whilst the mean suction value was 7kPa, there was substantial variation with a coefficient of variation of approximately 0.2. As a result the factor of safety derived from the mean suction value may be a poor indicator of actual stability. If the suction value used for the analysis is reduced to 3kPa (i.e. the residual value measured in the laboratory experiment), failure is predicted at a wetting front depth of 1m. The time required to achieve such a low suction over the entire wetting front depth of 1m would be substantially longer than that observed in the lab due to the much longer drainage path length. Given the rainfall patterns experienced in Ireland and evidenced from the suction measurements on site, such low values are unlikely in the near future.

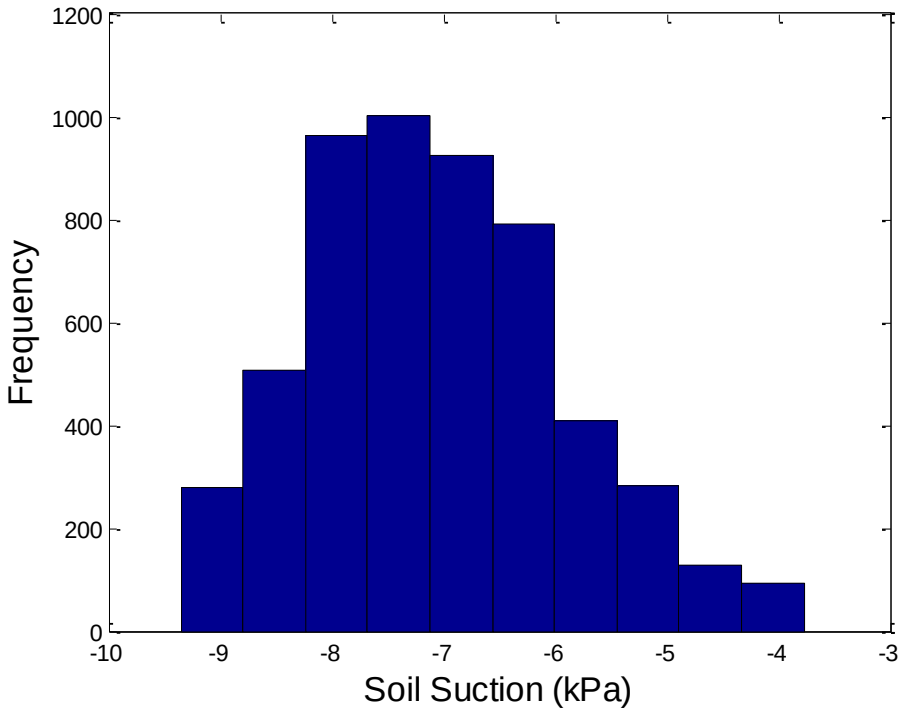

Figure B6: Histogram of suction measurements taken from embankment over five month monitoring period

B.3 Probabilistic Modelling

The UCD GASSA model was used to determine the reliability index, β with the performance function, g(x):

$$g(x) = \frac{c' + (u_a - u_w)\tan\phi^b + \gamma h \cos^2\alpha \tan\phi'}{\gamma h \sin\alpha \cos\alpha} - 1$$

The model requires all random variables to be transformed into a standard normal space before calculating the reliability index β. If the parameters are uncorrelated this can be easily accomplished by the following equation.

$$\overline{x_i} = \frac{x_i - \mu_i}{s_i} \text{ for i} = 1,2,...,n$$

Where x_i is a vector representing the entire set of random variables, $\overline{x_i}$ is the reduced set of random variables in the normal space, μ_i is a vector of the parameter means and σ_i is a vector of the parameter standard deviations. If the parameters are non-normal they must be transformed into equivalent normal distributions first, using the Rackwitz-Fiessler (1978) two parameter equivalent normal transformation. Once equivalent normal distributions are obtained the parameters can then be transformed into the standard normal space using the equation outlined above. A normal distribution was assumed for the angle of internal friction and the rate of increase of shear strength due to matric suction. Lognormal distributions were assumed for soil suction and soil unit weight. The glacial till soils used to form the majority of earthworks in Ireland have no natural cohesion so a deterministic value of zero for c' was assumed.

After transforming the variables to the standardised normal space the limit state function can be rewritten as:

$$g(X) = g(\overline{x_1}, \overline{x_2}, ..., \overline{x_n})$$

In this reduced variable space, the limit state surface (g(X) = 0) separates safe and unsafe states (see Figure B7) and the reliability index (β) can be defined as the distance from the origin to the most probable failure or design point. This distance can be described as:

$$\beta = \min \sqrt{X^T X} \quad for\ X \in \Psi$$

Where X is a vector representing the set of reduced random variables and Ψ is the failure region defined by (g(X) = 0). The probability of failure P_f can then be calculated by integrating the failure region.

$$P_f = P[g(X) < 0]$$

where the notation $g < 0$ denotes the failure region.

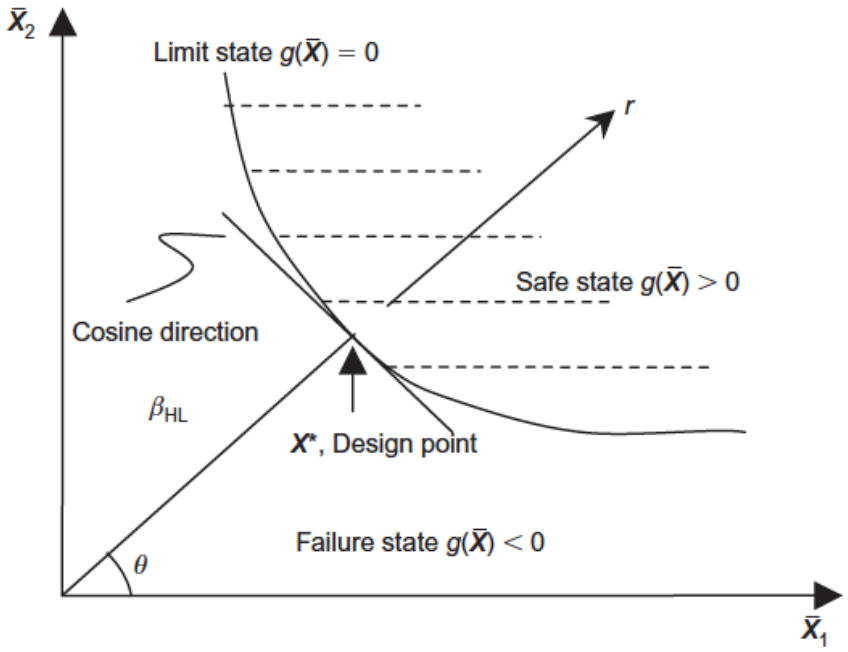

Figure B7: Definition of failure surface in polar coordinates

The design values assumed in the analysis are shown in Table B2. The variation in reliability index as the wetting front depth increased from 0.1m to 2m is shown in Figure B8. Comparing results of the reliability index with the deterministic analysis, it is clear that the reliability index decreases at a much slower rate as the wetting front develops than the decrease in sharp safety predicted by the FOS. This is a result of the relatively low variability of many of the input parameters. As a result we can see that at a wetting front depth of 1m we have a reliability index of 2.75, which is substantially higher than the minimum β value of 2.2 required by most infrastructure owners.

Table B2: Summary table of probabilistic inputs

Parameter	Mean Value	Distribution
Cohesion (c')	0	-
Soil suction (u_a-u_w)	7 kPa	Lognormal
Internal Angle of Friction	34°	Normal
Rate of increase in shear strength due to matric suction ϕ^b	24°	Normal
Slope angle	38°	-
Unit weight	17 kN/m^3	Lognormal
Wetting front depth	Varied from 0.1 m to 2 m	-

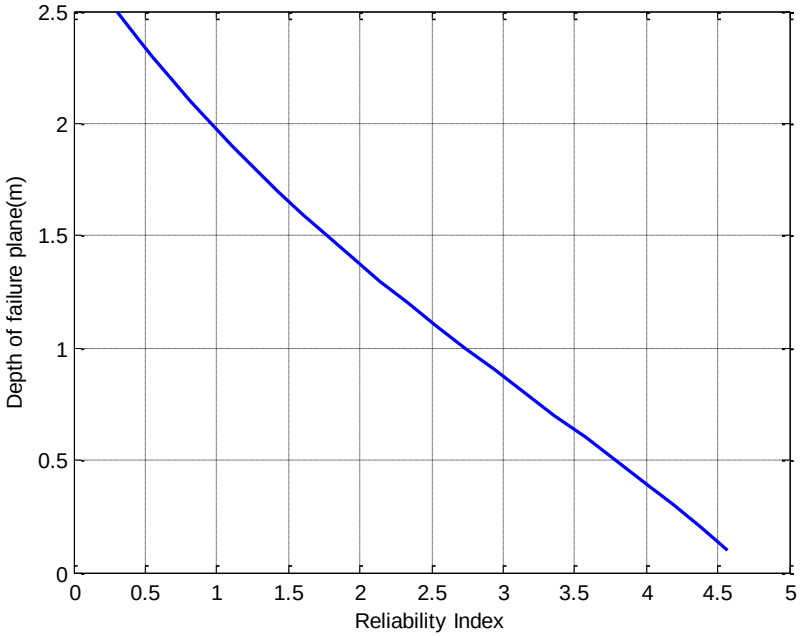

Figure B8: Results of probabilistic analysis

It is worth noting that the suction measurements shown in the histogram in Figure B6 are not truly random variables. Rather, the suction varies in response to applied rainfall. The next stage of the model development is to derive a method for predicting the wetting front depth during given rainfall events, and the variation of wetting front depth due to the variation of soil permeability. This will allow the designer to choose rational values of suction (or water content) in the slope for a given climate condition. It is expected that fragility curves will be developed to describe the slope response to a range of possible climate scenarios.

B.4 Sensitivity Analysis

A sensitivity study was carried out to analyse the effect each parameter had on the reliability index. The sensitivity is defined as the ratio of the change in reliability index to the change in any particular parameter ($\delta\beta$ / δparameter). In the current analysis, the sensitivity related to each parameter is measured with respect to a 10% increase in the parameter value. As shown in Figure B9 the analysis is particularly sensitive to any change in the friction angle of the material. This is expected as most glacial tills found in Ireland have low cohesion and relatively low soil suctions, in comparison to finer grained material. Therefore they derive most of their strength from their constant volume friction angle. These friction angles are generally quite high due to the large percentage of cobbles and boulders usually present in the material.

From Figure B9 it can be seen that soil suction is the second most important parameter. This is also the parameter that is most susceptible to climate change, as increased rainfall reduces suction. If rainfall amounts increase in a given area, this could result in a large increase in the number of shallow slope failures. Similarly, increased rainfall will mean increased soil unit weights as the soil imbibes more rainwater. From figure B9 it can be seen that a 10% increase in soil unit weight results in a significant reduction of the reliability index.

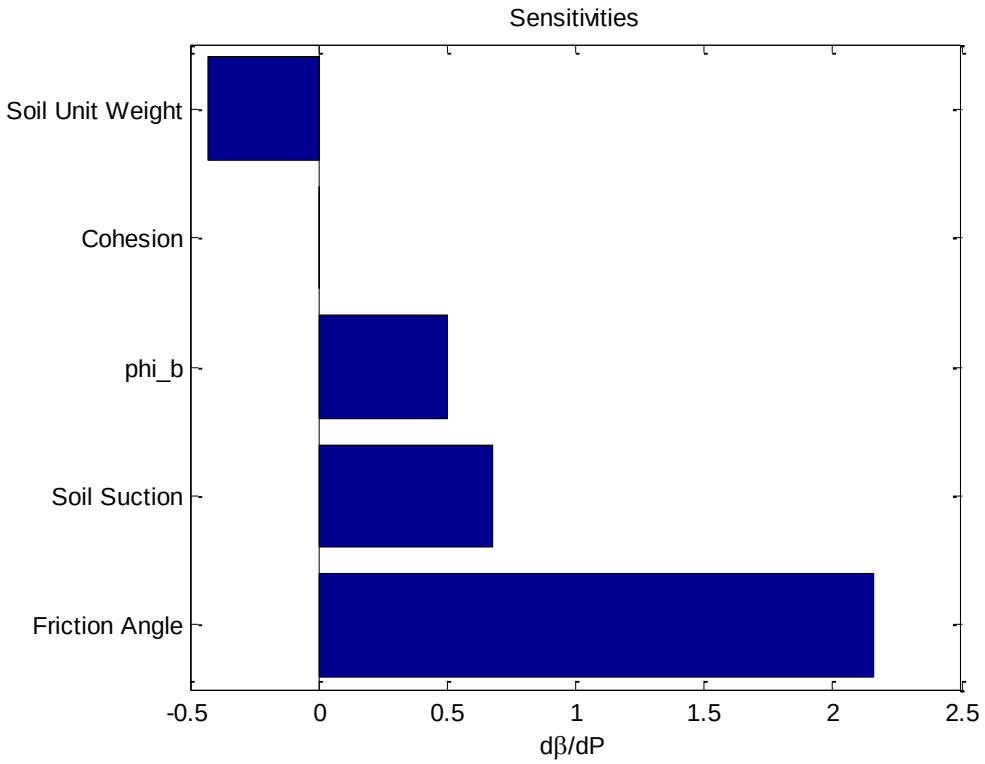

Figure B9: A sensitivity analysis evaluated at a depth of 1m for the design values given in Table B2.

B.5 Conclusion

Probabilistic tools are extremely useful for extending the service life of existing infrastructure as they give a more accurate representation of performance. Deterministic approaches which assume constant values for parameters which vary temporally cannot provide an adequate description of the performance of an asset. A mathematically rigorous approach for analysing slopes is presented. The important soil parameters can be determined using simple laboratory tests. Consideration of the performance of a 150 year old railway slope showed that despite having very steep sided slopes, the embankment is relatively stable and a very extreme rainfall event would be required to trigger failure. A sensitivity analysis revealed that the reliability index reduced significantly as weather (or climate) sensitive parameters (soil suction and unit weight) were varied. Increased monitoring

should give further insight into the variability of the structure and could be accomplished at a far lower cost than repair works.

Appendix C. Simplified Probabilistic Bridge Analysis, Austria

C.1. Introduction

This appendix shows an example of the application of the recalibration process of partial safety factors as described in Chapter 9 – Simplified Approach. The example deals with a single span steel railway bridge, located in lower Austria. The bridge has a span of 15.4m and consists of 7 longitudinal girders. Figure C1 shows a photograph of the bridge and Figure C2 shows a sketch of the cross section.

Figure C1: Photograph of steel bridge

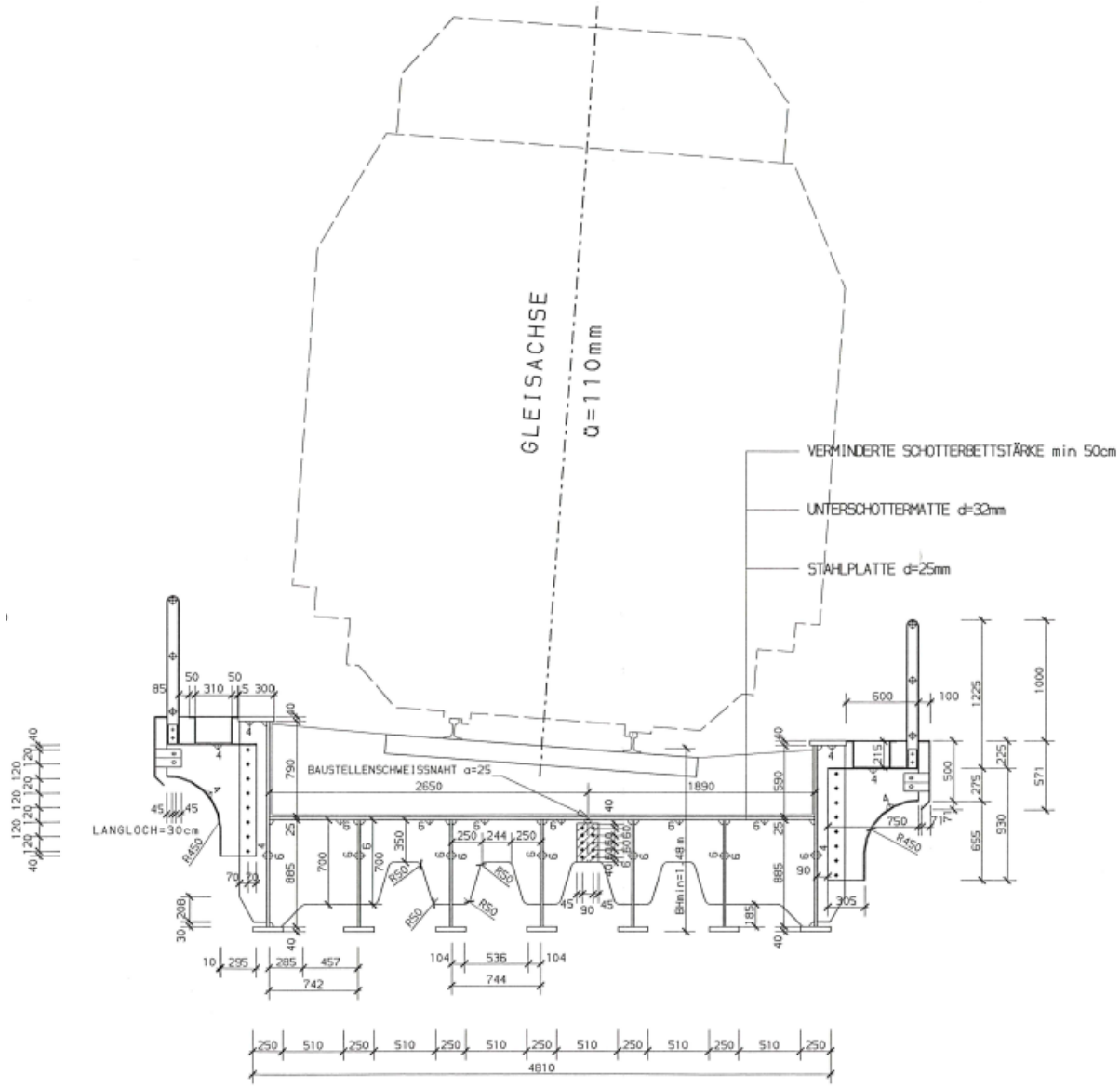

Figure C2: Cross-Section of analyzed steel bridge

Measurements have been conducted on the bridge for one week using accelerometers, strain gauges and laser displacement transducers. The results of the measurements were used to calibrate the finite element model of the bridge and to obtain bridge specific loading information which could be used for fatigue assessment of a critical detail (cross girder weld). Prior to the calibration process of the partial safety factors a full probabilistic analysis of the bridge was conducted.

C.2. Finite Element Model

Firstly, a finite element (FE) model of the bridge was developed. The bridge was modelled using shell elements and the model was calibrated to fit the measured distribution of the loads on the bridge. Figure C3 shows an outline of the model and the first two extracted mode shapes obtained from the modal analysis.

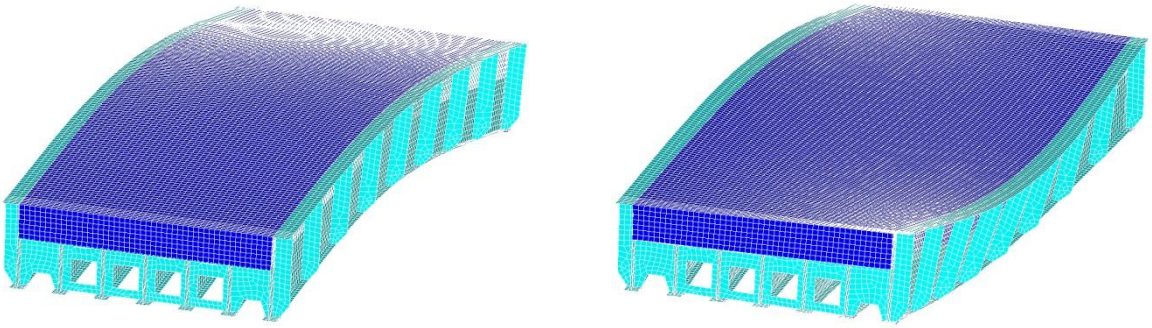

Figure C3: FE Model of the bridge showing the first (left) and second (right) mode shape

The following load cases have been calculated:

- LC1 – Selfweight
- LC2 – Permanent loads (Ballast)
- LC3 – Train according to LM71 from EN 1991-2, 2003; Locomotive in the middle of the bridge
- LC4 - Train according to LM71 from EN 1991-2, 2003; Locomotive over support
- LC5 – Train according to LM71 from EN 1991-2, 2003; Eccentricity with locomotive in the middle of the bridge
- LC6 – Train according to LM71 from EN 1991-2, 2003; Eccentricity with locomotive over support

The resulting actions from a linear analysis, for each of the seven longitudinal girders, have been extracted at six different sections. The sections range from the support (section 1) to the middle of the bridge (section six). The stress in the mid-span cross girder and the mid-span deflection have also been extracted.

C.3. Probabilistic Analysis

The probabilistic Framework was programmed within the open source programming language PYTHON. The resistance values were modelled for each of the longitudinal girders.

Input Parameters

An attempt was made to model all input parameters for load, resistance and model uncertainties with stochastic distributions. The distributions were taken from publications (mainly JCSS, 2000) or from reasonable estimations. Table C1 shows the chosen distributions for the material parameters, Table C2 shows the geometric parameters and Table C3 shows the model uncertainties.

Table C1: Material distributions

Name	Description	Distribution	Mean	COV
f_y	Yield strength	LN	1	0.07
E	Modulus of elasticity	LN	1	0.03
v	Poisson´s ratio	LN	1	0.03

LN Lognormal Distribution

Table C2: Geometric distributions

Name	Description	Distribution	Mean	COV
H1	Total height girder 1	N	1	0.004
H2	Height below deck	N	1	0.004
H3	Total height girder 7	N	1	0.004
B11	Top flange width girder 1	N	1.01	0.01
B12	Top flange width girder 7	N	1.01	0.01
B31	Bottom flange width girder 1	N	1.01	0.01
B32	Bottom flange width girder 2	N	1.01	0.01
B33	Bottom flange width girder 3	N	1.01	0.01
B34	Bottom flange width girder 4	N	1.01	0.01
B35	Bottom flange width girder 5	N	1.01	0.01
B36	Bottom flange width girder 6	N	1.01	0.01
B37	Bottom flange width girder 7	N	1.01	0.01
T11	Top flange thickness girder 1	N	1	0.04
T12	Top flange thickness girder 7	N	1	0.04

T2	Deck thickness	N	1	0.04
T31	Bottom flange thickness girder 1	N	1	0.04
T32	Bottom flange thickness girder 2	N	1	0.04
T33	Bottom flange thickness girder 3	N	1	0.04
T34	Bottom flange thickness girder 4	N	1	0.04
T35	Bottom flange thickness girder 5	N	1	0.04
T36	Bottom flange thickness girder 6	N	1	0.04
T37	Bottom flange thickness girder 7	N	1	0.04
TW1	Web thickness girder 1	N	1	0.04
TW2	Web thickness girder 2	N	1	0.04
TW3	Web thickness girder 3	N	1	0.05
TW4	Web thickness girder 4	N	1	0.04
TW5	Web thickness girder 5	N	1	0.04
TW6	Web thickness girder 6	N	1	0.04
TW7	Web thickness girder 7	N	1	0.04
Tquer	Central cross girder thickness	N	1	0.04

N Normal Distribution

Table C3: Model Uncertainty distributions

Name	Description	Distribution	Mean	COV
Θ_S	Actions	LN	1	0.1
Θ_M	Moment resistance	LN	1	0.05
Θ_V	Shear resistance	LN	1	0.05
Θ_N	Tension resistance	LN	1	0.05

As no WIM data is available for the site, the deterministic load model LM71 from EN 1991-2:2003 is used for the train loads. According to Chapter 5.4.2 of this deliverable, appropriate distributions and coefficients of variations have been chosen. As these parameters have a large influence on the results of the probabilistic analysis and the calibration process of the partial safety factors, they should be chosen with caution, in order to ensure that they are appropriate. A Gumbel distribution with a coefficient of variation of 20% was chosen for the train load. The load, given in EN 1991-2:2003, was taken as the 98% fractile value. For the given example, which aims to demonstrate the techniques of the calibration process, the chosen parameters should be adequate. Table C4 shows the distributions for the load parameters. All distributed parameters were modelled using Latin Hypercube Sampling technique (LHS).

Table C4: Load distributions

Name	Description	Distribution	Mean	COV
Selfweight	Selfweight of bridge	N	1	0.01
Permanent	Permanent loads (ballast)	N	1	0.1
Train	Train loads	Gumb	0.65856	0.2
Train eccentricity	Train eccentricity	N	0	-
DAF	Dynamic amplification factor	LN	1.23	0.2

Gumb Gumbel Distribution

Sample Size

In order to determine the required number of samples, test calculations with the given distributions for one limit state function (shear failure on girder 5) were conducted. For the n=10 to n=1000 sample sizes, 15 calculations were carried out and for the n=1e4 to n=1e7 sample sizes, 10 calculations were carried out. From the results of the calculations the mean and standard deviation of the reliability index was calculated. Figure C4 shows the influence of the number of samples on the reliability index β and its standard deviation. It can be seen that the mean of the reliability index β quickly converges to its "final" value of 8.96, but the results show a large scatter for sample sizes up to n=1e3. For the probabilistic analysis and for the calibration process of the γ-factors a sample size of n=1e5 was chosen.

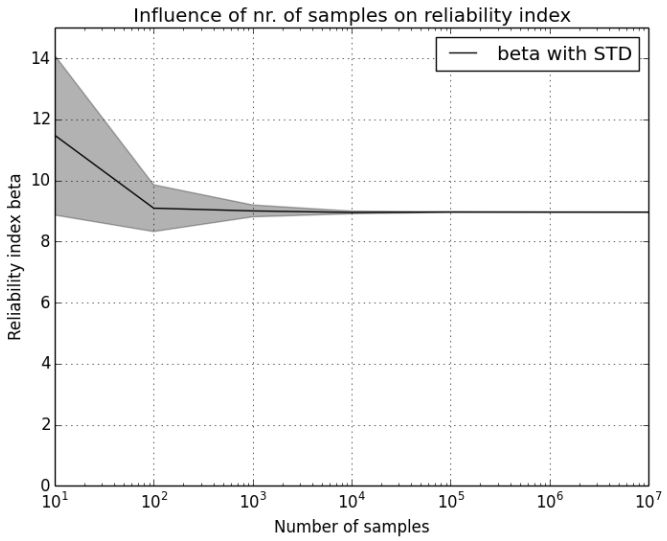

Figure C4: Influence of number of samples on reliability index beta incl. standard deviation

Corrosion Degradation Model

It was assumed that the bridge will show degradation due to corrosion over its lifetime. Therefore a simple exponential corrosion model, as shown in Eq. C1, according to Komp (1987), was used.

$$C = A.t^B \qquad (C1)$$

Where C is the average corrosion penetration (in µm) and t is the number of years. The parameters A and B of the corrosion model can be taken from Table C5.

Table C5: Parameters for the corrosion model (taken from Komp (1987))

Environment	A	B
Rural	34.0	0.65
Urban	80.2	0.59
Marine	70.6	0.79

For the implementation of the corrosion model some basic assumptions were made:

- Corrosion starts at the time of erection of the bridge (t = 0 years)
- Corrosion rate for urban environment according to Table C5.
- The whole bridge corrodes uniformly

The calculations were conducted for a time span of 100 years which should represent the service life of the bridge. Results were evaluated at time steps of T = [0,6,12,20,30,40,50,60,70,80,90,100] years and for a reference period of one year.

Evaluation of Reliability Index β

For the evaluation of the sampled results, a distribution fit was carried out and the failure probability p_f was evaluated with the use of the corresponding cumulative distribution function (CDF). The reliability index β was calculated according to Eq. C2, where – Φ^{-1} is the inverse of the standardised normal distribution function.

$$\beta = -\Phi^{-1}(p_f) \qquad (C2)$$

Results: Ultimate Limit States

Each of the seven longitudinal girders was examined at six sections (from the support to the middle of the bridge). Two different load combinations (locomotive in the middle of the bridge and over support) were used for the following ultimate limit states (ULS):

- Plastic Moment resistance
- Shear resistance
- Elastic Moment/Shear Interaction resistance

An additional analysis was carried out for the maximum cross girder stress in the middle of the bridge for the first load combination (locomotive in the middle of the bridge).

Figure C5 shows the results of the probabilistic analysis. The diagram shows the lowest β-indexes for the given ULS. It can be seen that the bridge shows a sufficient reliability over its whole service life with the lowest β-index for the stress in the cross girder after a time of 100 years with $\beta_{CG,100} = 5.23$. The evaluation for the plastic moment showed a β-index of $\beta_{Mpl,100} = 8.90$, for shear $\beta_V = 9.08$ and for the elastic moment/shear interaction a β-index of $\beta_{MV} = 8.25$.

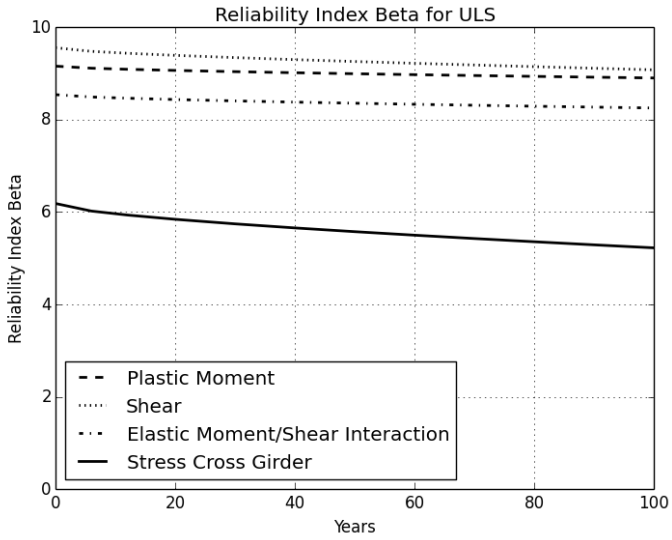

Figure C5: Results of the probabilistic analysis for ultimate limit states

Results: Serviceability Limit States (SLS)

For the serviceability limit state the vertical deflection in the middle of the bridge was analysed. According to EN 1990(2002) Annex A2, the vertical deflection should not exceed 1/600 of the of the bridge span.

Figure C6 shows the results of the probabilistic analysis. The analysis showed a very high reliability level for SLS over the whole service life of the bridge resulting in a β-index of $\beta_{SLS} = 10.53$ after a reference period of 100 years.

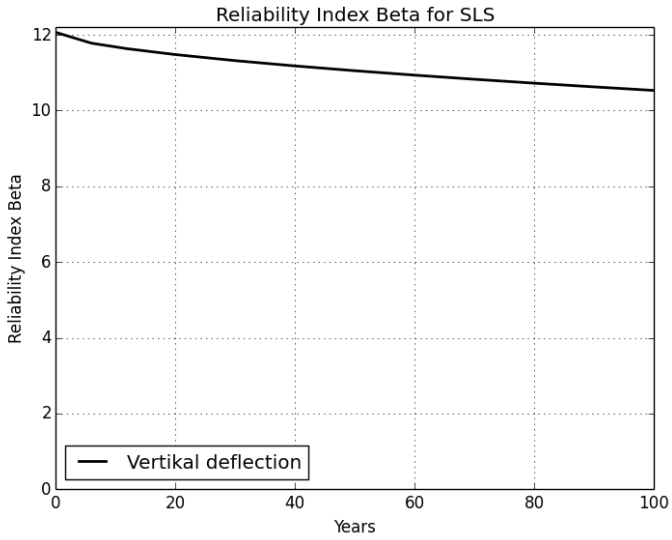

Figure C6: Results of the probabilistic analysis for serviceability limit state

Results: Fatigue

Calculations for fatigue failure of the cross girder weld in the middle of the bridge were conducted with two different calculations.

The first calculation compared the stress from load model LM71, taken from the finite element analysis, with the decisive notch case, as suggested by EN 1993-2 (2010). This analysis demonstrated a rapidly degrading β-index with a final value of $\beta_{Fat,LM71}$ = -2.55. This would mean that there is a strong likelihood that the bridge will show damage due to fatigue over its lifetime. The degradation of $\beta_{Fat,LM71}$ can be seen in Figure C7. It should be noted, however, that it is unlikely that the extreme values from the LM71 will occur with such a high frequency as that which has been conservatively assumed for the fatigue calculation according to EN 1993-2 (2010).

The second calculation used the collected data from the measurements with strain gauges at the point of the highest cross girder stress in the middle of the bridge. The data from the full week of measurements was evaluated using a rainflow counting algorithm and the frequency of occurrence of the resulting stress-histogram was extrapolated to give a full year stress collective. The stress collective was evaluated for each year, using the damage accumulation law of Palmgren-Miner (see EN 1993-9, 2005). Taking the degradation due to corrosion into account, each single year had to be evaluated separately. The results of this calculation can also be seen in Figure C7. The final value for the reliability index for a one year reference period after 100 years of service life resulted in $\beta_{Fat,SG}$ = 1.86. According to EN 1990(2002) (see Section 3.5.5) the target reliability level for a 50 year reference period should be between 1.5 and 3.8 (depending on inspectability, reparability and

damage tolerance). These values translate into target reliability levels for a one year reference period between 2.9 and 4.7. That means that the calculated reliability for fatigue of the cross girder weld will be below the target reliability level given in EN 1990(2002) after about 70 years of service.

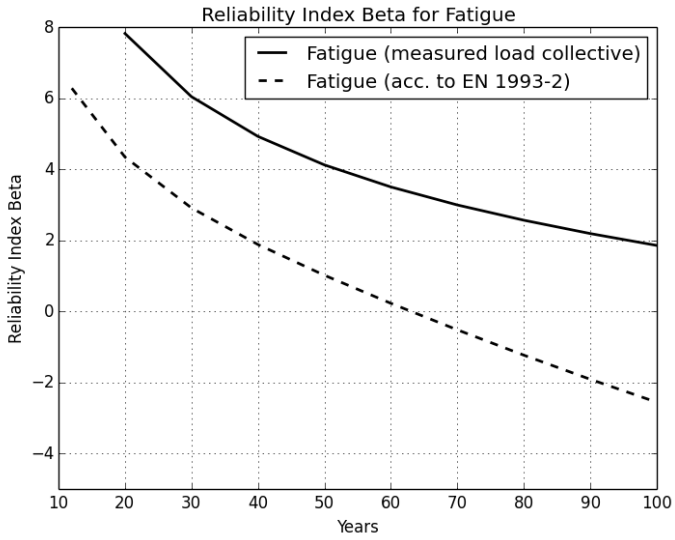

Figure C7: Results of the probabilistic analysis for fatigue

Results: Summary

The probabilistic analysis showed that the steel bridge in question shows high reliability levels for ULS, SLS and a low reliability level for fatigue when considering the assumptions used in the analysis. The highest failure probability for the ULS occurred due to the stresses in the cross girder in the middle of the bridge with $\beta_{CG,100}$ = 5.23. The corresponding value for fatigue of the cross girder weld was calculated to be $\beta_{Fat,SG}$ = 1.86. The results from the fatigue calculation according to EN 1993-2, 2010 are based on a very conservative assumption and are not taken into account as the use of real data is deemed to lead to more accurate results.

C.4. Recalibration of partial safety factors

The recalibration process of the partial safety factors followed the simplified approach as described in Chapter 9 of this deliverable. The process is shown in the flow-chart diagram in Figure 9.1. The distributions of the input parameters, the degradation model (corrosion) as well as the basic assumptions for the analysis are the same as described above for the probabilistic analysis.

Scope of Calibration

The calibration was done for the same single span steel bridge as described in the probabilistic analysis. The bridge was built in 1996 and a number of similar bridges exist on the same railway line.
The scope of the recalibration process was for the recalibration of the partial safety factors (γ-factors) for ultimate limit state. Based on the results from the probabilistic analysis the following three design criteria have been chosen for the calibration process:

- Plastic Moment in Section 5, Girder 7 of the bridge (design equation G1, limit state function g1)
- Shear in Section 1, Girder 4 of the bridge (design equation G2, limit state function g2)
- Tension in the Cross Girder in the middle of the bridge (design equation G3,limit state function g3)

According to EC0 all γ-factors for SLS should equal to 1. It is not recommended to adjust partial safety factors to values below 1. So no calibration for SLS was conducted within this example.
The chosen code format for the recalibration process is based on the current Eurocodes (EN 1990, 2002; EN 1993-2, 2010). For the given example with only one variable load (i.e. vertical train loading), the basic design criteria for ULS could be written according to Eq. C3.

$$\frac{R_k}{\gamma_{M,0}} \geq \sum_{j=1}^{n} \gamma_G \cdot G_{k,j} + \gamma_{Q,1} \cdot Q_{k,1} \qquad (C3)$$

With:

$\gamma_{M,0}$	γ-factor for the material
γ_G	γ-factor for permanent loads
$\gamma_{Q,1}$	γ-factor for the single variable load
R_k	Characteristic value of resistance
$G_{k,j}$	characteristic value of the effect of permanent loads
$Q_{k,1}$	characteristic value of the effect of variable loads

Eurocode 3 (EN 1993-2, 2010) gives the following values for the γ-factors on the load side:

$$\gamma_G = 1.35; \quad \gamma_{Q,1} = 1.5$$

The value for the γ-factor on the material side was chosen with $\gamma_{M,0}$ = 1.1. This value was used for the original code calibration and implemented in early codes like the DIN 18800-1 (1990) or early ENV versions of the Eurocode 3 but was reduced because of expert judgement to $\gamma_{M,0}$ = 1.0 within the current Eurocode 3 (EN 1993-2, 2010). As the γ-factors for load and resistance are dependent on

each other, the value $\gamma_{M,0}$ = 1.0, as given in the Eurocode would lead to high resulting γ-factors on the load side after calibration. Therefore the original value of $\gamma_{M,0}$ = 1.1 was used and kept constant during the calibration process.

For the calibrated γ-factors $\gamma_{G,cal}$ and $\gamma_{Q,1,cal}$ on the load side the calibration was constrained to values between 1 and 3 (Eq. C4).

$$1 \leq \gamma_{G,cal};\ \gamma_{Q,1,cal} \leq 3 \qquad (C4)$$

Target reliability level

The target reliability index β_T for a one year reference period at the end of a 100 year service life was chosen as the optimisation objective for the calibration process.
Chapter 3.5 of this deliverable gives information on recommended values for the target reliability index β_T. For the calibration process the γ-factors have been calibrated for target reliability indexes ranging from 1.5 to 5 (Eq. C5).

$$1.5 \leq \beta_T \leq 5 \qquad (C5)$$

Design situations and input parameters

Three different design situations $G_j(\boldsymbol{x}_c, \mathbf{p}_j, \mathbf{z}, \boldsymbol{\gamma})$=0, j=1, 2, 3 and associated limit state functions $g_j(\mathbf{X}, \mathbf{p}_j, \mathbf{z})$=0, j=1, 2, 3 have been chosen, as described under *"Scope of calibration"* above.

As all the design variables have been modelled as distributed variables, an additional design variable C_{xx} = 1 was added to the resistance side of the equations for the design situations and limit state functions. C_{xx} is expressed in dependence of the γ-factors.

G1, g1: Plastic Moment M_{pl} for Section 5, Girder 7

The design situation for the plastic moment in Section 5/Girder 7 of the bridge, with the additional design variable C_{Pl}=1 is given in Eq. C6 for the optimal design point.

$$\mathbf{G_1} = W_{Pl,G7} \cdot \frac{f_y}{\gamma_{M,0}} \cdot C_{Pl} - [\gamma_G \cdot (M_{k,LC1,S5,G7} + M_{k,LC2,S5,G7}) + \cdots$$

$$\ldots \gamma_Q \cdot (M_{k,LC3,S5,G7} + M_{k,LC5,S5,G7})] = 0 \qquad (C6)$$

With:

$W_{Pl,G7}$ *yield strength of the steel*

f_y	yield strength of the steel
$M_{k,LC*,S5,G7}$	characteristic moment load effects for the single load cases LC* (see Section C2)

The deterministic variable C_{Pl} can be expressed according to Eq. C7. This variable was used to evaluate the limit state function at the optimal design point for the given γ-factors.

$$C_{Pl} = \frac{\gamma_{M,0} \cdot [\gamma_G \cdot (M_{k,LC1,S5,G7} + M_{k,LC2,S5,G7}) + \gamma_Q \cdot (M_{k,LC3,S5,G7} + M_{k,LC5,S5,G7})]}{W_{Pl,G7} \cdot f_y} \quad (C7)$$

The limit state function g_1 then results in Eq. C8.

$$g_1 = \theta_M \cdot W_{Pl,G7} \cdot f_y \cdot C_{Pl} - \theta_S \cdot (M_{LC1,S5,G7} + M_{LC2,S5,G7} + M_{LC3,S5,G7} + M_{LC5,S5,G7}) \quad (C8)$$

G2, g2: Shear V for Section 1, Girder 4

The design situation for the shear in Section 1/Girder 4 of the bridge, with the additional design variable C_V=1 is given in Eq. C9 for the optimal design point.

$$G_2 = \frac{f_y}{\sqrt{3} \cdot \gamma_{M,0}} \cdot A_{Web,G4} \cdot C_V - [\gamma_G \cdot (V_{k,LC1,S1,G4} + V_{k,LC2,S1,G4}) + \cdots$$

$$\cdots \gamma_Q \cdot (V_{k,LC4,S1,G4} + V_{k,LC6,S1,G4})] = 0 \quad (C9)$$

With:

$A_{Web,G4}$	area of the web from girder 4
$V_{k,LC*,S1,G4}$	characteristic shear load effects for the single load cases LC* (see Section C2)

The deterministic variable C_V can be expressed according to Eq. C10. This variable was used to evaluate the limit state function at the optimal design point for the given γ-factors.

$$C_V = \frac{\gamma_{M,0} \cdot \sqrt{3} \cdot [\gamma_G \cdot (V_{k,LC1,S1,G4} + V_{k,LC2,S1,G4}) + \gamma_Q \cdot (V_{k,LC4,S1,G4} + V_{k,LC6,S1,G4})]}{f_y \cdot A_{Web,G4}} \quad (C10)$$

The limit state function g_2 then results in Eq. C11.

$$g_2 = \theta_V \cdot \frac{f_y}{\sqrt{3}} \cdot A_{Web,G4} \cdot C_V - \theta_S\left(V_{c,LC1,S1,G4} + V_{c,LC2,S1,G4} + V_{c,LC4,S1,G4} + V_{c,LC6,S1,G46}\right) \quad (C11)$$

G3, g3: Tension σ_{CG} in cross girder

The design situation for the tension stress in the cross girder at the middle of the bridge, with the additional design variable C_{CG}=1 given in Eq. C12 for the optimal design point.

$$G_3 = \frac{f_y}{\gamma_{M,0}} \cdot C_{CG} - [\gamma_G \cdot (\sigma_{k,LC1,CG} + \sigma_{k,LC2,CG}) + \cdots$$

$$\cdots \gamma_Q \cdot (\sigma_{k,LC3,CG} + \sigma_{k,LC5,CG})] = 0 \quad (C12)$$

With:

$\sigma_{k,LC*,CG}$ characteristic tension stress in the cross girder at the middle of the bridge for the single load cases LC* (see Section C2)

The deterministic variable C_{CG} can be expressed according to Eq. C13. This variable was used to evaluate the limit state function at the optimal design point for the given γ-factors.

$$C_{CG} = \frac{\gamma_{M,0} \cdot [\gamma_G \cdot (\sigma_{k,LC1,CG} + \sigma_{k,LC2,CG}) + \gamma_Q \cdot (\sigma_{k,LC3,CG} + \sigma_{k,LC5,CG})]}{f_y} \quad (C13)$$

The limit state function g_3 then results in Eq. C14.

$$g_3 = \theta_N \cdot f_y \cdot C_{CG} - \theta_S \cdot (\sigma_{LC1,CG} + \sigma_{LC2,CG} + \sigma_{LC3,CG} + \sigma_{LC5,CG}) \quad (C14)$$

The probabilistic calculation (Section C3) showed the following reliability levels β for the three failure modes:

$$\beta_{Mpl,100} = 8.90;\ \beta_{V,100} = 9.08;\ \beta_{CG,100} = 5.23$$

All of the three limit state functions have been weighted equally with weighting factors w_j as shown in Eq. C15.

$$w_1 = w_2 = w3 = \frac{1}{3}; \sum_{j=1}^{3} w_j = 1 \qquad (C15)$$

Optimisation of γ-factors

For the calibration process the simple least squares function was used, as shown in the minimization function (Eq. C16)

$$\min_{\gamma}(W_j) = \sum_{j=1}^{3} w_j\left(\beta_j(\gamma) - \beta_T\right)^2 \qquad (C16)$$

With:

β_j resulting β-index for limit state function 'j'

This function is easy to implement and gives good results, however the downside of weighting symmetrically means that it can result in reliabilities below the optimisation objective for single failure modes.

An iterative minimization process for Eq. C16 was carried out using a solver that allows for consideration of constraints (Eq. C4).

For each iteration step a probabilistic analysis of the three limit state functions g_j was conducted and the reliability indices β_j have been evaluated. The first calculations using multivariate optimisation for $\gamma_{G,cal}$ and $\gamma_{Q,1,cal}$ showed that the two γ-factors are dependent on each other. The multivariate optimisation was carried out using three different solvers for bound constraint optimisation:

- Solver 1 uses the L-BFGS-B algorithm for bound constraint optimisation (see Zhu et.al., 1997)
- Solver 2 uses the TNC algorithm which is a truncated Newton (see Nocedal & Wright 2006)
- Solver 3 uses the SLSQP algorithm which is a sequential least squares minimization (see Kraft, 1988)

Figure C8 shows a comparison of the results of the three different solvers. It can be seen that the results for a multivariate optimisation of the two γ-factors depend strongly on the chosen solver. Due to the dependence of the two γ-factors an infinite number of valid results exist.

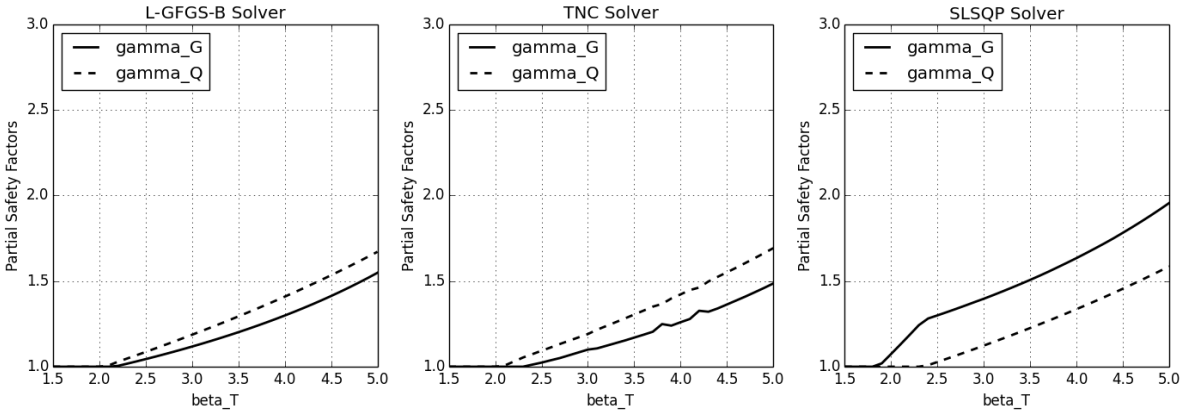

Figure C8: Partial safety factors vs. target reliability level for a constant $\gamma_{M,0}$=1.1; Comparison of the calibration results with three different solvers

Because the two partial safety factors for permanent and variable loads are dependent on each other the final calibration process was conducted with only one independent variable for the optimisation process. The calibration process was carried out three times with different preconditions:

- Calibration 1: Ratio γG,cal/γQ,1,cal = 1.35/1.5 =constant
- Calibration 2: γG,cal =1.35 = constant
- Calibration 3: γQ,1,cal =1.5 = constant

Figure C9 shows the results of the three calculations for the end of the bridges service life at T=100 years. The calibration process has been carried out every 10 years from T=0 to T=100 years. Figure C10 shows the development of the partial safety factors for a target reliability index of βT=4.2 over the 100 year period. It can be seen that the γ-factors stay on a constant level during the deterioration process due to corrosion of the bridge. This is because every limit state function is evaluated at its optimal design point for every single calibration.

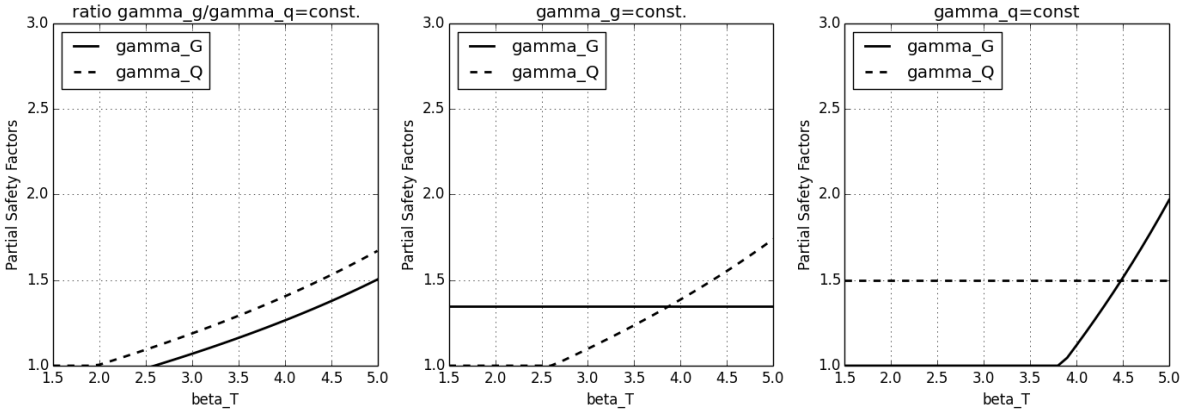

Figure C9: Partial safety factors vs. target reliability level after 100 year service life of the bridge for a constant $\gamma_{M,0}$=1.1; Ratio $\gamma_{G,cal}/\gamma_{Q,1,cal}$=const. (left); $\gamma_{G,cal}$=const. (middle); $\gamma_{Q,1,cal}$=const. (right)

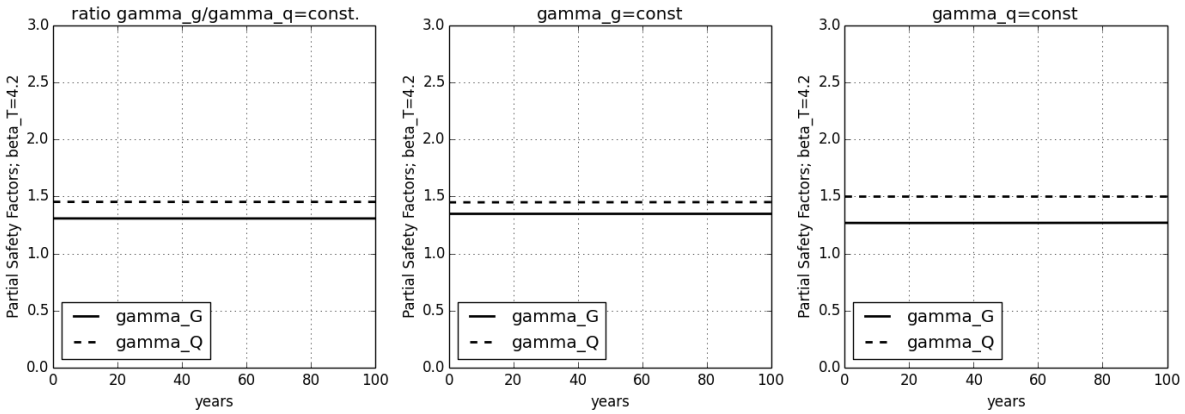

Figure C10: Partial safety factors for a constant $\gamma_{M,0}$ = 1.1; Development over the years (dependent on the corrosion rate) for a target reliability index β_T = 4.2

Verification of γ-factors (Discussion of results)

The results of the calibration showed that the calibrated β-factors for a target reliability level of β_T=4.2, for a reference period of one year, result in γ-factors below the values given in Eurocode 3. This means that the values given in Eurocode 3 are "on the safe side" and the calibrated γ-factors are judged as reasonable values. But it has to be kept in mind, that some of the input distributions, especially for the load variables, are chosen based on assumptions.

As mentioned under the "Scope of calibration" section in this appendix, the γ-factor on the material side was kept constant at $\gamma_{M,0}$ = 1.1 during the calibration process. This factor, resulting from the original code calibration, was reduced to $\gamma_{M,0}$ = 1.0 due to expert judgement in the final version of Eurocode 3. A γ-factor calibration with the assumption of $\gamma_{M,0}$ = 1.0 leads to higher factors on the load side than those given in the codes, as shown in Figure C11.

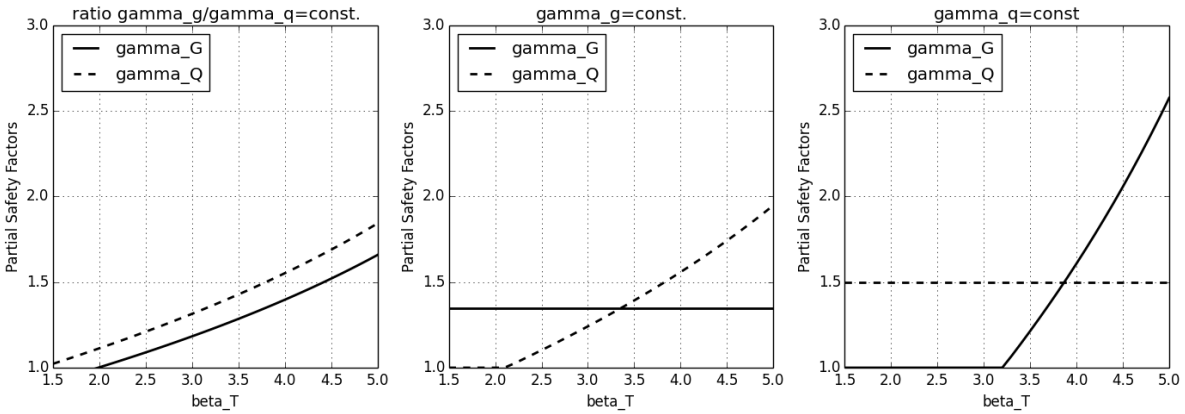

Figure C11: Partial safety factors vs. target reliability level after 100 year service life of the bridge for a constant $\gamma_{M,0}$ = 1.0; Ratio $\gamma_{G,cal}/\gamma_{Q,1,cal}$ = const. (left); $\gamma_{G,cal}$ = const. (middle); $\gamma_{Q,1,cal}$ = const. (right)